THE FLUOROSULPHURIC ACID

SOLVENT SYSTEM

by

ROBERT C. THOMPSON, B.Sc.

A Thesis

Submitted to the Faculty of Graduate Studies

in Partial Fulfillment of the Requirements

for the degree

Doctor of Philosophy

McMaster University

August 1962

DOCTOR OF PHILOSOPHY (1962)   McMASTER UNIVERSITY
(Chemistry)   Hamilton, Ontario.

TITLE: The Fluorosulphuric Acid Solvent System

AUTHOR: ˙Robert Clayton Thompson, B.Sc. (University of Western Ontario)

SUPERVISOR: Dr. R. J. Gillespie

NUMBER OF PAGES: xii, 196

SCOPE AND CONTENTS:

A cryoscopic technique for the investigation of solutions in
fluorosulphuric acid has been developed, and the cryoscopic constant for
the solvent has been determined.

Conductimetric measurements, cryoscopic measurements and n.m.r.
spectroscopic studies have been used to determine the mode and extent of
ionization of antimony pentafluoride in fluorosulphuric acid. The
reactions in fluorosulphuric acid of antimony pentafluoride with sulphur
trioxide, and of boron trifluoride with sulphur trioxide have also been
investigated.

Solutions of arsenic trifluoride in fluorosulphuric acid have
been investigated by conductimetric measurements. Conductimetric and
cryoscopic studies have been made on solutions of the supposed compound
"$2AsF_3 \cdot 3SO_3$".

Conductimetric and transport number measurements on solutions of
barium fluorosulphate in fluorosulphuric acid have been used to calculate
the mobility of the fluorosulphate ion. The mobility of the fluoro-
sulphuric acidium ion has also been determined, and the autoprotolysis

ii

constant of fluorosulphuric acid calculated.

In order to obtain information on self-dissociation reactions of fluorosulphuric acid, cryoscopic studies were made on solutions of water, sulphur trioxide, and potassium fluoride.

ACKNOWLEDGEMENTS

The author wishes to express gratitude to Dr. R. J. Gillespie
who first suggested the problem, and under whose supervision the work
was done.

Thanks are due to Mr. R. Palme who constructed the glass
apparatus, and to Mr. J. Bacon who assisted in the operation of the
n.m.r. spectrometer.

Finally, the author would like to thank the Ontario Research
Foundation for financial support.

TABLE OF CONTENTS

LIST OF TABLES

LIST OF FIGURES

ix

CHAPTER I

INTRODUCTION

(a) HISTORICAL

Fluorosulphuric acid was first described by Thorpe and Kirmann in 1892[1]. They prepared it by the reaction of hydrogen fluoride with sulphur trioxide. No further studies were reported on this acid for almost twenty years. In 1913 Traube[2] described the preparation of the anhydrous acid by distillation from a mixture of ammonium fluoride and fuming sulphuric acid. Later, Ruff[3] prepared fluorosulphuric acid from calcium fluoride and fuming sulphuric acid, and Meyer and Schram[4] prepared it from potassium hydrogen fluoride and fuming sulphuric acid.

Since 1919 fluorosulphuric acid has been used in a variety of organic and inorganic reactions. It has been used as an acid catalyst in alkylation reactions[5,6,7,8,9], acylation reactions[10,11], polymerization of olefins[12], hydrofluorination of olefins[13], and isomerization of saturated hydrocarbons[4]. It has also been used as a condensing agent, for example, in the production of D.D.T.[15,16]. Many organic derivatives of fluorosulphuric acid have been prepared, for example: aromatic fluorosulphates[17], diazonium fluorosulphates[18], esters of fluorosulphuric acid[4], and aromatic sulphonyl fluorides[19]. Various refining processes involve the use of fluorosulphuric acid, such as the removal of organic fluorine compounds from hydrocarbons[20], the refining of lubricating oil[21], and the removal of metals from crude petroleum[22]. Fluorosulphuric acid has been used to effect ring

1

closure[23] and to prepare fluorides of organic acids[24]. The action

of fluorosulphuric acid on cellulose[25] has also been studied.

In the field of inorganic chemistry, hydrogen fluoride has been

prepared by the hydrolysis of fluorosulphuric acid[26], boron trifluoride

has been prepared by the reaction of boric acid with fluorosulphuric

acid[27], and silicon tetrafluoride by the interaction of hydrated silica

and fluorosulphuric acid[28]. Fluorosulphuric acid has been electrolyzed

in hydrogen fluoride solution with the production of SO_2F_2 and F_2O[29].

A study of the usefulness of fluorosulphuric acid as an electro-

polishing agent has been described by Young and Hesse[30].

Traube, Hoerenz, and Wunderlich[31] describe the preparation of

NH_4^+, Li^+, K^+, Rb^+, Na^+, Ca^{++}, Ba^{++}, Cu^{++}, and Zn^{++} fluorosulphates either

from oleum, ammonium fluoride, and the oxide or hydroxide or the metal,

or by direct reaction between fluorosulphuric acid and the metal oxide,

hydroxide or fluoride. Traube[32] and Lehmann and Kolditz[33] describe

the preparation of ammonium and sodium fluorosulphates from the fluorides

and sulphur trioxide. Nitrosyl fluorosulphate was prepared by Woolf[34]

from nitrosyl chloride and fluorosulphuric acid in bromine trifluoride.

Woolf also describes the preparation of potassium fluorosulphate from

potassium hydrogen fluoride and fluorosulphuric acid in anhydrous hydrogen

fluoride[35], and also by the reaction of bromine trifluoride with potas-

sium persulphate[36]. Hayek, Puschmann, and Czaloun[37] prepared metal hal-

ide fluorosulphates by the reaction of metal chlorides with fluorosul-

phuric acid. Traube and Brehmer describe the preparation of a series of

sulphamido salts with the aid of fluorosulphates[38]. Hayek, Czaloun

and Krismer describe the preparation of the fluorosulphates of some metals,

such as Si, Ti, Sn, and As by the reaction of the metal chlorides with silver fluorosulphate in acetonitrile solution[39]. They also prepared thallium fluorosulphate from thallium fluoride and sulphur trioxide, and aluminum trifluorosulphate from the chloride and fluorosulphuric acid using sulphuryl chloride as solvent. Muetterties and Coffman[40] prepared the alkaline earth fluorosulphates from the fluorides and sulphur trioxide. They also prepared $Sb(SO_3F)_3$ from SbF_3 and SO_3, and the supposed compound $2AsF_3 \cdot 3SO_3$ from AsF_3 and SO_3.

Structural investigations of fluorosulphuric acid and its salts have been reported by several workers. Fluorosulphuric acid presumably has a structure (I) analogous to that of H_2SO_4 (II) with an approximately tetrahedral arrangement of groups about sulphur.
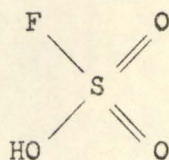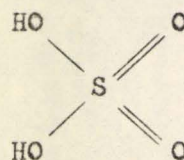
I   II

The Raman spectrum of the pure acid has been described by Gillespie and Robinson[41] and the lines obtained have been satisfactorily assigned to the fundamental vibrations of the tetrahedral molecule (I).

It seems reasonable to assume that there will be intermolecular hydrogen bonding in liquid HSO_3F, analogous to that found in other protonic solvents. However, since there is only one proton per molecule, the opportunities for such bonding are fewer than in the case of H_2SO_4 for example. In fact, HSO_3F is less viscous than H_2SO_4[42] ; this is in agreement with a smaller extent of association. A line in the Raman spectrum of

liquid HSO_3F at $1178cm.^{-1}$, which Gillespie and Robinson[41] assigned to an OH wag, is absent in a 50 mole % solution of HSO_3F in AsF_3. They suggest the change in the nature and extent of hydrogen bonding caused by diluting HSO_3F with AsF_3 shifts this band to a region of the spectrum where it is obscured by another line.

HSO_3F has an abnormally high boiling point for a compound of its molecular weight and this may be considered as further evidence for hydrogen bonding in this system. N-heptane, for example, which has a molecular weight of 100.2 compared to a molecular weight of 100.1 for HSO_3F, boils at $98\cdot43^{o}C$ while the boiling point of HSO_3F is $163^{o}C$.

The Raman spectrum of SO_3F^- has been obtained by Gillespie and Robinson[41] from solutions of sodium fluorosulphate in water and solutions of the same solute in fluorosulphuric acid. They assigned the Raman lines to the six normal modes of vibration for an ion XSO_3^- with a tetrahedral structure. The assignments of these workers compared favourably with those of Siebert[43] and Sharp[44]. Siebert obtained the Raman spectrum of a solution of $NaSO_3F$ in water and Sharp obtained the infrared spectra of solid alkali metal, ammonium, silver, and triphenyl carbonium fluorosulphates.

Lange[45] has shown that fluorosulphates resemble perchlorates and permanganates in their chemical and crystallographic properties. He was able to prepare mixed crystals of Li, K, Cs, tetramethylammonium, and Cu-4-pyridine complex perchlorates and fluorosulphates. Wilke - Doerfurt[46] prepared mixed crystals of the permanganates, perchlorates, fluoroborates, and fluorosulphates of the chromium III hexaurea complex, thus demonstrating the isomorphism of these salts.

Because of the violent reaction of fluorosulphuric acid with water, Thorpe and Kirmann[1] thought that the acid is instantaneously and completely hydrolyzed. Traube, however, discovered that the acid is not hydrolyzed completely when it is dropped into water, but instead undergoes slow hydrolysis of HF and H_2SO_4. The equilibrium

$$HSO_3F + H_2O \rightleftharpoons HF + H_2SO_4$$
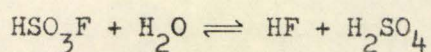
was studied by Traube and Reubke[47], by Lange[48] and later by Woolf[49]. The latter suggested that initially part of the fluorosulphuric acid is hydrolyzed rapidly to HF and H_2SO_4 while the remainder forms the hydronium salt $H_3O^+SO_3F^-$, and the fluorosulphate ion then undergoes slow hydrolysis.

In spite of its wide applications the properties of the pure acid, especially with respect to its possibilities as a non-aqueous solvent, were not investigated, except for the study of its hydrolysis, until the work reported by Woolf in 1955[36].

Woolf prepared anhydrous fluorosulphuric acid by passing sulphur trioxide into excess HF. The acid was purified by two distillations at atmospheric pressure. The fraction boiling at 163 ± 0.5^oC was collected and the middle fraction (range 0.1^oC) was transferred to a tapless vacuum apparatus where it could be fractionated by trap to trap distillation, each trap being sealed in turn. The specific conductance of this acid was 2.20×10^{-4} ohm^{-1} cm.$^{-1}$ at 25^oC. Woolf suggests the existence of three possible self-ionization equilibria to explain this conductivity.

$$HSO_3F \rightleftharpoons H^+ + SO_3F^- \qquad \qquad 1.1$$

$$HSO_3F \rightleftharpoons HSO_3^+ + F^- \qquad \qquad 1.2$$

$$2HSO_3F \rightleftharpoons H_2F^+ + S_2O_6F^- \qquad \qquad 1.3$$
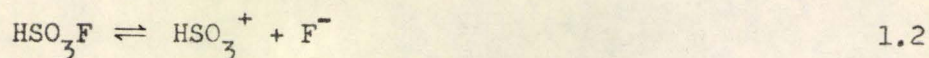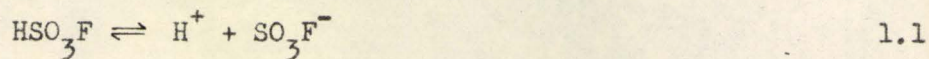
The only gas liberated on electrolysis of fluorosulphuric acid is hydrogen at the cathode. This is incompatible with 1.2 since the fluoride ion would need to discharge as fluorine. Woolf also suggests that the transport of fluorine to the anode renders 1.3 improbable since the relative mobilities of the ions would tend to transport fluorine in the opposite direction. It should be noted here, however, that Woolf merely assumes that the mobility of H_2F^+ would be greater than the mobility of $S_2O_6F^-$ without any experimental evidence.

Woolf considers 1.1 to be the most important mode of self-ionization and he cites as evidence in support of this, the observation that the molecular conductivity of KSO_3F solutions is practically independent of dilution when the solvent conductivity is deducted. However, this cannot, in fact, be regarded as evidence for 1.1. Since the self-dissociation 1.1 would be repressed by added SO_3F^- it is not correct merely to deduct the solvent conductivity from the observed conductivity of KSO_3F solutions. An appropriate correction can be made if the equilibrium constant for 1.1 is known. Moreover, the molecular conductivity is not expected to be independent of concentration and, in fact, Barr[42] found that the molecular conductivity of KSO_3F solutions increases with dilution.

Woolf found that the solvent becomes oxidizing at the anode during electrolysis. This observation, he suggests, is in accord with the formation of an oxidizing peroxydifluorosulphate ion

$$2SO_3F^- - e^- \longrightarrow S_2O_6F^-$$
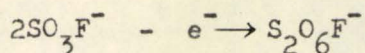
He cites this as evidence for the existence of 1.1. However, as it is not possible to suggest a reasonable structure for $S_2O_6F^-$, it is doubtful that it exists. It is possible, on the other hand, that the oxidizing

behaviour at the anode is due to the formation of peroxydisulphuryl-
difluoride.

$$2SO_3F^- - 2e^- \longrightarrow S_2O_6F_2$$
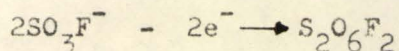
$S_2O_6F_2$ has, in fact, been prepared by Dudley and Cady[50] by the reaction
of fluorine with sulphur trioxide. However, this cannot be regarded as
evidence for the existence of SO_3F^- in the pure acid since the reaction
could be

$$2HSO_3F - 2e^- \longrightarrow S_2O_6F_2 + 2H^+$$

Woolf considers that 1.2 might occur to a small extent and suggests
that the presence of HSO_3^+ would explain the sulphonation of benzene in
fluorosulphuric acid. Brand and Horning[51] postulated such an ion to
explain sulphonation in oleum. However, Ingold[52] pointed out that mono-
meric SO_3 or a solvate of it, is likely to be the active species in sul-
phonation.

In conclusion it may be stated that none of Woolf's arguments
for any of the above three modes of self-ionization can be regarded as
conclusive.

Woolf studied solutions of some fluorides in fluorosulphuric acid
and he divided them into the following three groups: (i) soluble, KF,
AgF, AuF, SbF_5, TaF_5, BrF_3, and IF_5, (ii) sparingly soluble, BF_3, SnF_4,
SbF_3, and PF_4, (iii) insoluble, BiF_3 and TlF_3.

Woolf concluded that potassium fluorosulphate is a strong electro-
lyte and acts as a base in fluorosulphuric acid. He found, on the other
hand, that antimony pentafluoride solutions could be conductimetrically
titrated with base and thus he concluded that SbF_5 behaves as an acid in
this system, and suggested the following possible modes of ionization for

SbF_5.

$$SbF_5 + HSO_3F \rightleftharpoons H^+ + SbF_5SO_3F^- \qquad 1.4$$

or $\qquad SbF_5 + HSO_3F \rightleftharpoons H^+ + SbF_6^- + SO_3 \qquad 1.5$
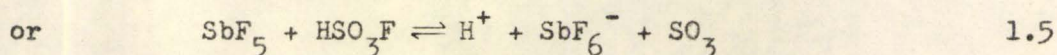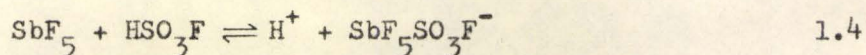
Woolf identified acids and bases in this system by conductimetric titration with KSO_3F and SbF_5. If KSO_3F increases the conductivity when added to a solution while SbF_5 added to the same solution decrease the conductivity, then the initial solution must contain a substance behaving as a base in fluorosulphuric acid. Similarly if a solution contains a substance behaving as an acid in fluorosulphuric acid, then the conductivity will be increased upon addition of SbF_5 and decreased upon addition of KSO_3F. Thus Woolf found SbF_5, AuF_3 and PtF_4 act as acids while SbF_3, AsF_3, BrF_3 and IF_5 act as bases in the HSO_3F system.

In 1959 Barr[42] reported further investigations on solutions in fluorosulphuric acid. He obtained acid of lower conductivity than that obtained by Woolf, by double distillation of the commercial product at atmospheric pressure. The specific conductance that Barr obtained for anhydrous fluorosulphuric acid was $1\cdot085 \times 10^{-4}$ ohm^{-1} cm.$^{-1}$. It will be shown in this work that trap to trap distillation at reduced pressures as carried out by Woolf may concentrate HF in the product. This could account for the high conductivity of Woolf's acid.

Barr measured the conductivities of solutions of the alkali metal fluorosulphates and found that they all have very similar specific conductances. This indicates that the major part of the current is carried by the ion which is common to all these salts, the fluorosulphate ion. He confirmed this conclusion in the case of KSO_3F by a direct measurement of the transport numbers of K^+ and SO_3F^-, which he found to be 0·11 and

0·89 respectively. The fluorosulphate ion thus clearly has an abnormal mobility which very probably results from a proton transfer mechanism of conduction. Woolf had previously suggested such a mechanism although he had very little evidence for it.

The conductivities of solutions of several incompletely ionized bases were also investigated by Barr. He showed that sulphuric acid behaves as a weak base in fluorosulphuric acid, contrary to the results of Woolf who stated that sulphuric acid forms solutions as conducting as potassium fluorosulphate.

Barr studied the titration curve obtained for SbF_5 titrated conductimetrically with KSO_3F, and showed that the minimum in the curve occurs at a mole ratio of KSO_3F to SbF_5 less than 1·0 and not at the mole ratio 1·0 as previously reported by Woolf. Barr attempted to determine the acid dissociation constant for SbF_5 from the position of the minimum and from these calculations estimated the mobility of the acidium ion $H_2SO_3F^+$ to be between 40 and 60. From transport number and conductivity measurements on KSO_3F he estimated the mobility of the fluorosulphate ion to be approximately 142 and that of K^+ to be approximately 18. From these results and assuming that the only self-dissociation process was 1·1, Barr estimated the autoprotolysis constant of fluorosulphuric acid to be $1 \pm 0.3 \times 10^{-7}$ $mole^2$ $kg.^{-2}$.

Barr also determined the density and viscosity of the pure acid; $d_4^{25} = 1·7264$, $\eta = 1·56$ cp.

(b) PURPOSE OF THIS WORK

The purpose of this work was to continue the investigation of
the chemistry of solutions in fluorosulphuric acid by

(i)   the application of the experimental techniques of cryoscopy

and nuclear magnetic resonance spectroscopy,which had not pre-

viously been used in the study of this solvent.

(ii)   extending the study of acid behaviour in fluorosulphuric

acid.

(iii)   investigating further the self-dissociation of fluorosulphuric

acid.

(iv)   obtaining new data on the mobilities of the fluorosulphate and

fluorosulphuric acidium ions.

PREPARATION AND PURIFICATION OF MATERIALS

(a) FLUOROSULPHURIC ACID

Commercial fluorosulphuric acid obtained from the "Allied Chem-
ical Company" was purified by double distillation at atmospheric pressure
in the apparatus shown in Fig. 1. The procedure was as follows. Crude
fluorosulphuric acid was poured into bulb A. Air, dried by passing first
over calcium chloride and then over magnesium perchlorate, was allowed to
enter the apparatus via tap H and exit via outlet I through a tube of
calcium chloride. The air was allowed to flow through the apparatus for
at least two hours and the apparatus was flamed periodically during that
time. The acid was then distilled into tube C until a constant boiling
point was reached, at which time the distillate was directed into flask B
by the fraction collector E. E is shown in more detail in Fig. 2. The
second distillation was carried out in a similar manner; however, the air
was now allowed to exit via outlet J. In practice it was not necessary
to continue passing dry air through the apparatus throughout the second
distillation and, therefore, tap H was usually closed once a steady dis-
tillation was obtained. G is a standard taper B19 outer ground glass
joint. Conductivity cells were attached by means of a B19 inner ground
glass joint directly to the distillation apparatus at G and flushed with
dry air. Fluorosulphuric acid was then distilled directly into the cell.
Acid obtained this way usually had a conductivity between $1 \cdot 1 \times 10^{-4}$ and
1.3×10^{-4} ohm^{-1} cm^{-1}. For cryoscopy, acid was transferred to the

cryoscope by means of a weight burette which was filled by attaching

the burette to the distillation apparatus at G. The freezing point of

the acid obtained in this manner was usually between -88.995 and

-89.010°C.

Fig. 1 FLUOROSULPHURIC ACID DISTILLATION APPARATUS
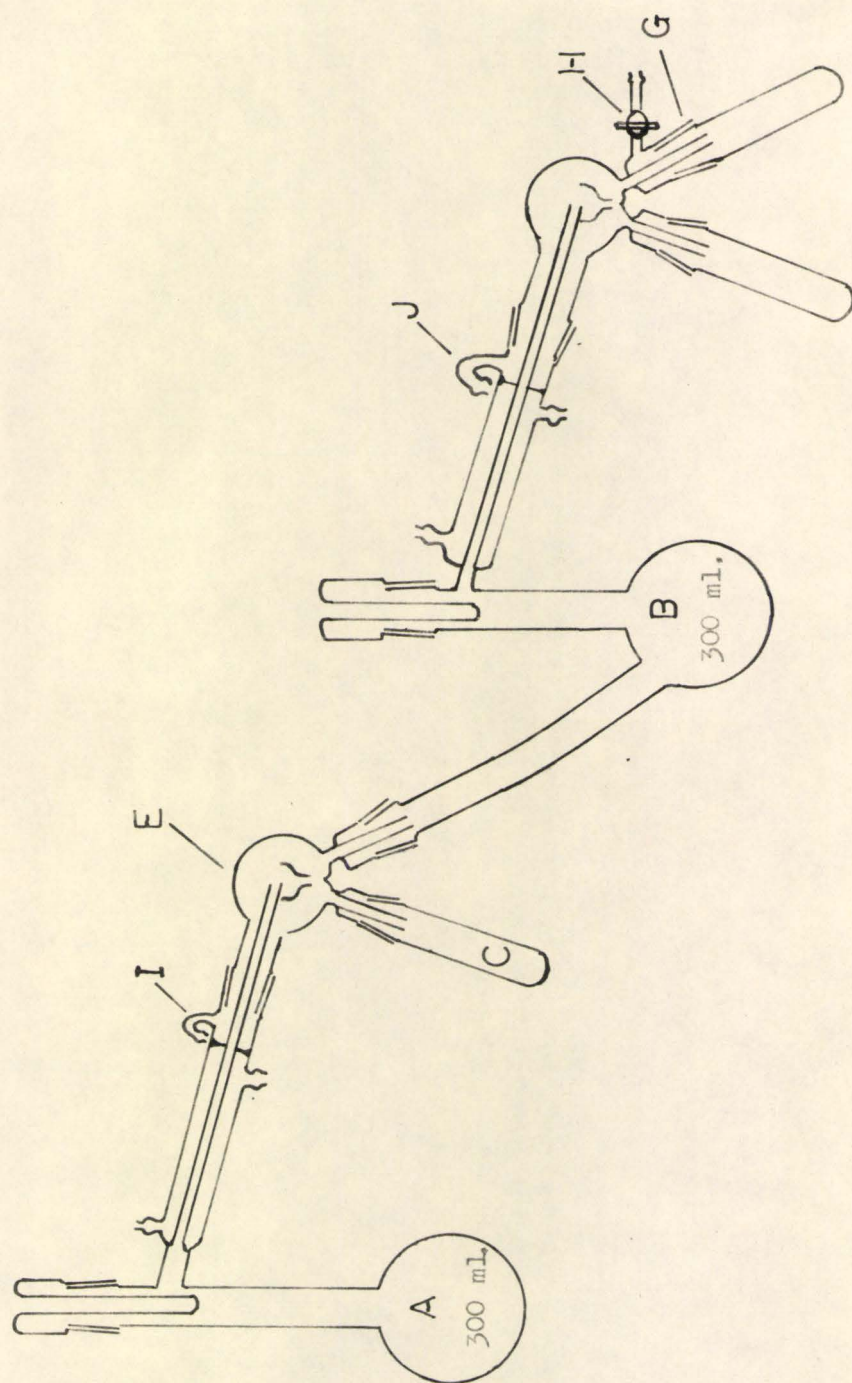
Fig. 2 FRACTION COLLECTOR USED ON DISTILLATION APPARATUS
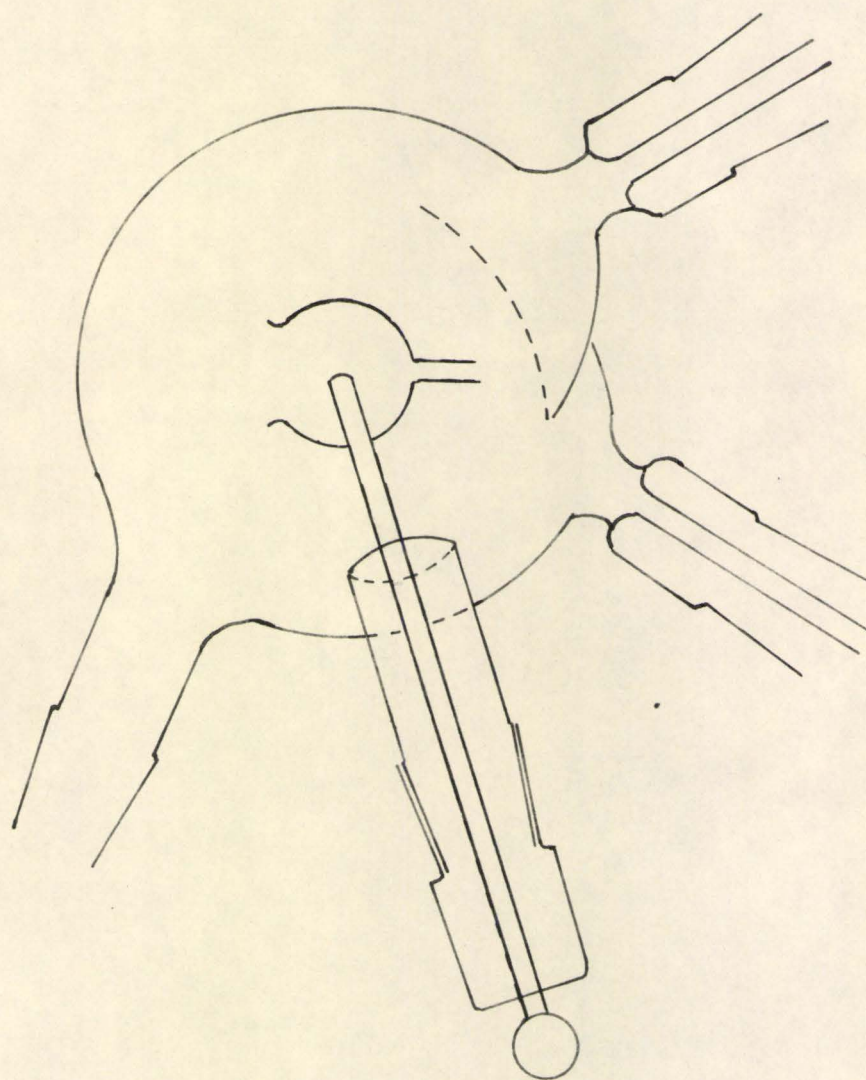
(b) FLUOROSULPHATES

Potassium, rubidium and cesium fluorosulphates were prepared by the reaction

$$MCl \ + \ HSO_3F \longrightarrow MSO_3F \ + \ HCl \ .$$
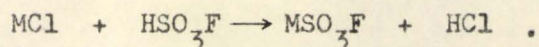
Fig. 3 shows the apparatus used. The dry metal chloride was put into A. The reaction vessel was then attached to the acid distillation apparatus at G (Fig. 1) via B (Fig. 3) and thoroughly dried by passing dry air through the vessel in the normal manner. Fluorosulphuric acid was then distilled onto the chloride which reacted with the acid resulting in immediate evolution of HCl. When enough acid had been added to dissolve all of the solid present in the vessel, it was removed from the distillation apparatus and a ground glass B19 cap was placed on B (Fig. 3). Tube C was then removed and the reaction vessel was attached via D (Fig. 3) to a vacuum pump through two liquid air traps. The excess fluorosulphuric acid was thus removed at a pressure of about 0.1 mm. of mercury, with occasional warming of the vessel A with a bunsen flame. After all the acid had been removed the product was recrystallized from water, washed with acetone and dry ether, and stored in a vacuum desiccator, over phosphoric oxide.

The salts, when dissolved in water showed no precipitation on addition of silver nitrate solution (negative test for chloride) and no precipitation on addition of barium chloride solution (negative test for sulphate) but copious precipitation on addition of nitron solution (positive test for fluorosulphate).

Potassium fluorosulphate was analyzed by conversion to sulphate

15

which was determined by precipitation as barium sulphate according to Vogel[53]. The conversion to sulphate was done as follows. A solution of known concentration of KSO_3F in water was prepared in a volumetric flask; 10 ml. aliquots were then heated to $121^{\circ}C$ in a stream of air for several hours. The residue was then dissolved in water and the percentage sulphate was determined.

Three sample analyses are given:

Theoretical %S for KSO_3F: 23.21

found: 23.38

23.12

23.08

Barium fluorosulphate is more easily hydrolyzed than the alkali metal fluorosulphates and, thus, cannot be recrystallized from water. It was, therefore, prepared under extremely anhydrous conditions. The apparatus used is shown in Fig. 4. Barium chloride dihydrate was dried in an oven at $150^{\circ}C$ for fourteen hours, and then placed in the reaction vessel A. A B19 cap was placed on C and the vessel was joined via B to a vacuum pump through two liquid air traps. The vessel was pumped out and flamed to dry both the vessel and the salt. The reaction vessel was then attached to the fluorosulphuric acid distillation apparatus at G (Fig. 1) via C (Fig. 4) and sufficient acid was distilled onto the chloride to dissolve all the solid. The vessel was removed from the distillation apparatus by the "flame-seal" D and again attached to the vacuum line via B. The excess fluorosulphuric acid was removed at a pressure of 0.005 mm. of mercury, warming A to $100^{\circ}C$ during the later stages. The product obtained was very granular and so was transferred in a dry-box to a mortar and ground to a fine powder. It was then

returned to the reaction vessel which was again placed on the vacuum line. The last traces of fluorosulphuric acid were thus removed. The product was handled at all times in a dry-box and stored in sealed glass ampules. The barium fluorosulphate was analyzed for barium by precipitation as barium sulphate according to Vogel[54]. In order to minimize hydrolysis of the fluorosulphate ion it was necessary to precipitate barium sulphate in the cold. This resulted in a very fine precipitate. It was, therefore, necessary to filter the solution twice before obtaining a clear filtrate.

Three sample analyses are given:

Theoretical % Ba for $Ba(SO_3F)_2$: 40·9

found: 40·9

40·4

40·7

Fig. 3 APPARATUS USED FOR THE PREPARATION
OF ALKALI METAL FLUOROSULPHATES
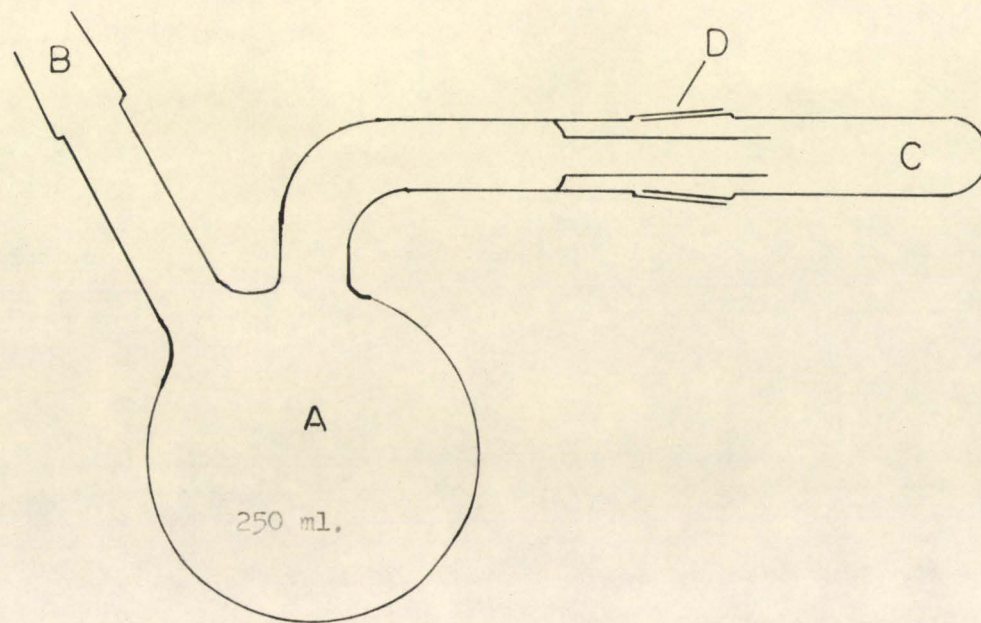
Fig. 4   APPARATUS USED FOR THE PREPARATION
OF BARIUM FLUOROSULPHATE
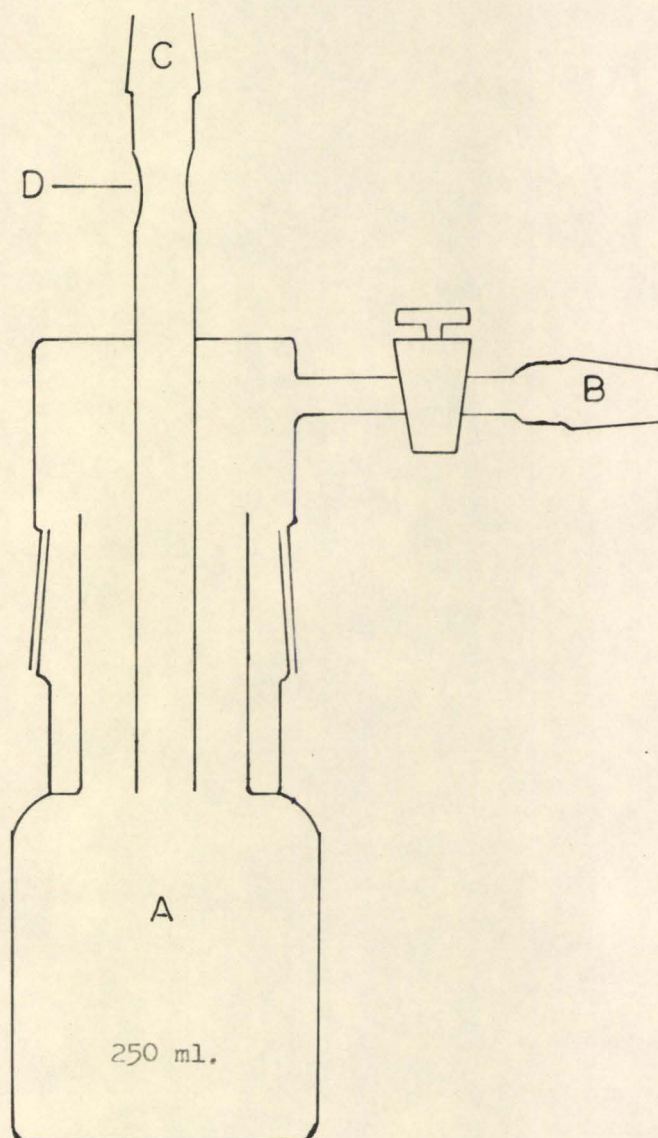
(c) OTHER MATERIALS

<u>Sulphur trioxide</u>: SO_3 was distilled from 30% or 65% oleum to which potassium persulphate had been added to oxidize any sulphur dioxide impurity.

<u>Antimony pentafluoride</u>: Commercial SbF_5 was double (sometimes triple) distilled in the all glass apparatus shown in Fig. 5, in an atmosphere of dry air. The boiling point of the triple distilled material was $142 - 143^{o}C$.

<u>Boron trifluoride</u>: Commercial BF_3 was used directly from the cylinder. In some experiments the BF_3 was passed through a cold trap of dry ice and acetone to remove any condensable impurities.

<u>Trinitrobenzene</u>: 8·6 grams of trinitrobenzoic acid were put into a beaker and 200 ml. of water added. The water was then brought to a boil and boiling was maintained until frothing ceased (2 hours and 40 minutes). The product was recrystallized from glacial acetic acid, washed with water, dried on an unglazed porcelain plate and stored over phosphoric oxide in a vacuum desiccator. The melting point of the product was $119 - 121^{o}C$.

<u>Arsenic trifluoride</u>: 100 grams of arsenic trioxide and 120 grams of calcium fluoride were dried in an oven at $130^{o}C$ for a few hours and then mixed well in a mortar. This mixture was then placed in the distilling flask shown in Fig. 5 and 250 ml. of concentrated sulphuric acid were added. The mixture was warmed and the AsF_3 distilled at $57^{o}C$ into a flask immersed in ice water.

<u>Benzoic acid</u>: Analar benzoic acid was recrystallized from water, dried

at 80°C for one and one-half hours, and stored in a vacuum desiccator, over phosphoric oxide.

Dry Air: Compressed air was passed first through a tube of anhydrous calcium chloride and then through a tube of anhydrous magnesium perchlorate. Air, dried in this manner, was always tested for traces of water before use by means of the "drying-train tester" shown in Fig. 6 . The air was allowed to enter the tester at A, pass over 30% oleum contained in B and exit via C. If the air caused no fuming in the vessel it was considered to be dry enough for use.

Some compounds were handled in a dry-box. Air or nitrogen, dried in the manner outlined above, was passed through the box for several hours before use. Metal dishes containing phosphoric oxide were also placed at several locations in the box to ensure as dry an atmosphere as possible.

Potassium fluoroborate: Commercial KBF_4, obtained from the Harshaw Chemical Company, was used without further purification.

Potassium fluoride: Purified grade KF was dried in an oven at 120°C for two days.

Fig. 5 GENERAL PURPOSE DISTILLATION APPARATUS

dry air

250 ml.
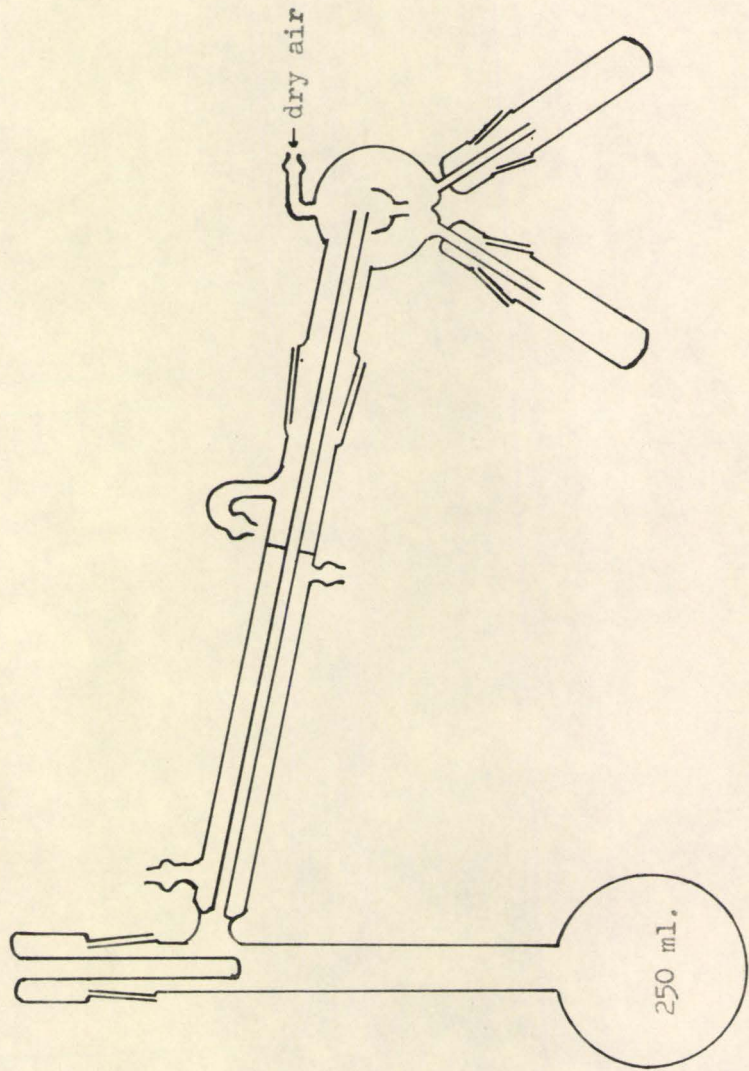
Fig. 6 DRYING-TRAIN TESTER

A —

C

B

100 ml.
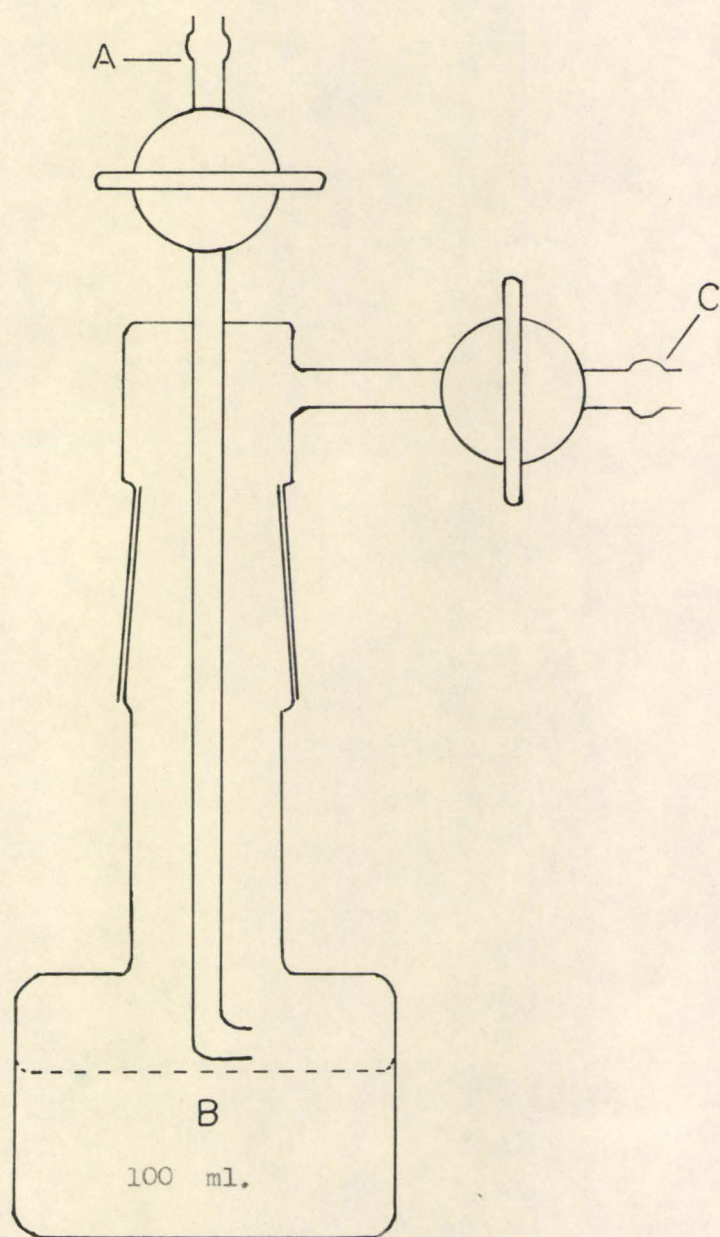
EXPERIMENTAL TECHNIQUES

(a) CONDUCTIVITY

The design of the cell used in measuring the conductivities of
solutions in fluorosulphuric acid is shown in Fig. 7. The cell contained
three electrodes and was designed so that the cell constant, when using
electrodes A and B, was approximately 2 while the constant, when using
electrodes B and C, was approximately 40. Thus, accurate conductivity
measurements on weakly conducting solutions were made using electrodes
A and B, while measurements on strongly conducting solutions were made
using electrodes B and C. The insert in Fig. 7 is a detailed diagram of
an electrode. The capacity of the cell was about 200 ml.

The cell shown in Fig. 8 was designed for conductivity measure-
ments on solutions of gases in fluorosulphuric acid. It was small enough
to be weighed on an analytical balance. Fluorosulphuric acid was distilled
into the cell through B, the cell being weighed before and after distil-
lation to determine the amount of acid used. Stopcock C was then opened
to the air via a tube of anhydrous calcium chloride,and the gas was bubbled
into the cell through A. The cell was again weighed to determine the
amount of gas added. The solution was then drawn into the electrode com-
partment F for measurement of its conductivity,by opening stopcock E and
applying suction at D.

The cells were cleaned with aquaregia. The electrodes were plated
with platinum black by electrolyzing a chloroplatinic acid solution pre-

pared according to Jones and Bollinger[55]. The solution consisted of a 0.3% solution of chloroplatinic acid in 0.025N hydrochloric acid with 0.025% lead acetate added. A current of 10 milliamps was passed for 20 minutes, with reversal of current every 50 seconds.

In the early stages of this work the cells were calibrated using aqueous potassium chloride solution, according to the method of Lind, Zwolenik and Fuoss[56]. Although this method is very accurate it was found more convenient to calibrate the cells by measuring the resistance of minimum conducting sulphuric acid. This was accomplished by adding dilute oleum or aqueous acid to approximately 100% H_2SO_4 in the cell, until a minimum conductivity was reached. Minimum conducting sulphuric acid has a specific conductance of 1.0432×10^{-2} ohm^{-1} cm.$^{-1}$ at $25^{\circ}C$ [57]. Thus the conductimetric studies, described later in this work, on arsenic trifluoride solutions in fluorosulphuric acid, and on the reaction of boron trifluoride with sulphur trioxide in fluorosulphuric acid, were done in cells calibrated using aqueous KCl solution. All other experiments were done in cells calibrated using minimum conducting H_2SO_4. The cells were replated and recalibrated after 5 or 6 experiments.

All measurements were made with the cells immersed in an oil thermostat regulated by means of a mercury-toluene regulator at $25 \pm 0.002^{\circ}C$. The temperature of the thermostat was measured to $\pm 0.001^{\circ}C$ with a platinum resistance thermometer. Thermometer resistance readings were made on a Mueller resistance bridge (see III(b)).

Solutions for conductivity measurements were prepared in the following manner. Fluorosulphuric acid was distilled directly into the cell which was weighed before and after addition of acid. Solid solutes

were added by means of the weight dropper shown in Fig. 9(a). If the solute was very hygroscopic it was usually added to the cell as a con- centrated solution in HSO_3F. In this case, and for liquid solutes, the weight dropper shown in Fig. 9(b) was used.

After each addition of solute the cell was shaken well to ensure good mixing, and placed in the thermostat. After sufficient time had elapsed to allow for temperature equilibrium (10 to 15 minutes) the resistance measurement was made. The cell was then removed from the ther- mostat, again shaken, and the resistance measurement repeated. In this manner errors due to insufficient mixing were eliminated.

Resistances of solutions were measured using a Leeds and Northrup, Jones conductivity bridge (No. 1513578). For two experiments (Numbers 96 and 97), however, a Wayne Kerr Universal bridge was used.

Throughout this work specific conductance will be referred to by the symbol $\mathcal{K}$.

Fig. 7 FLUOROSULPHURIC ACID CONDUCTIVITY CELL
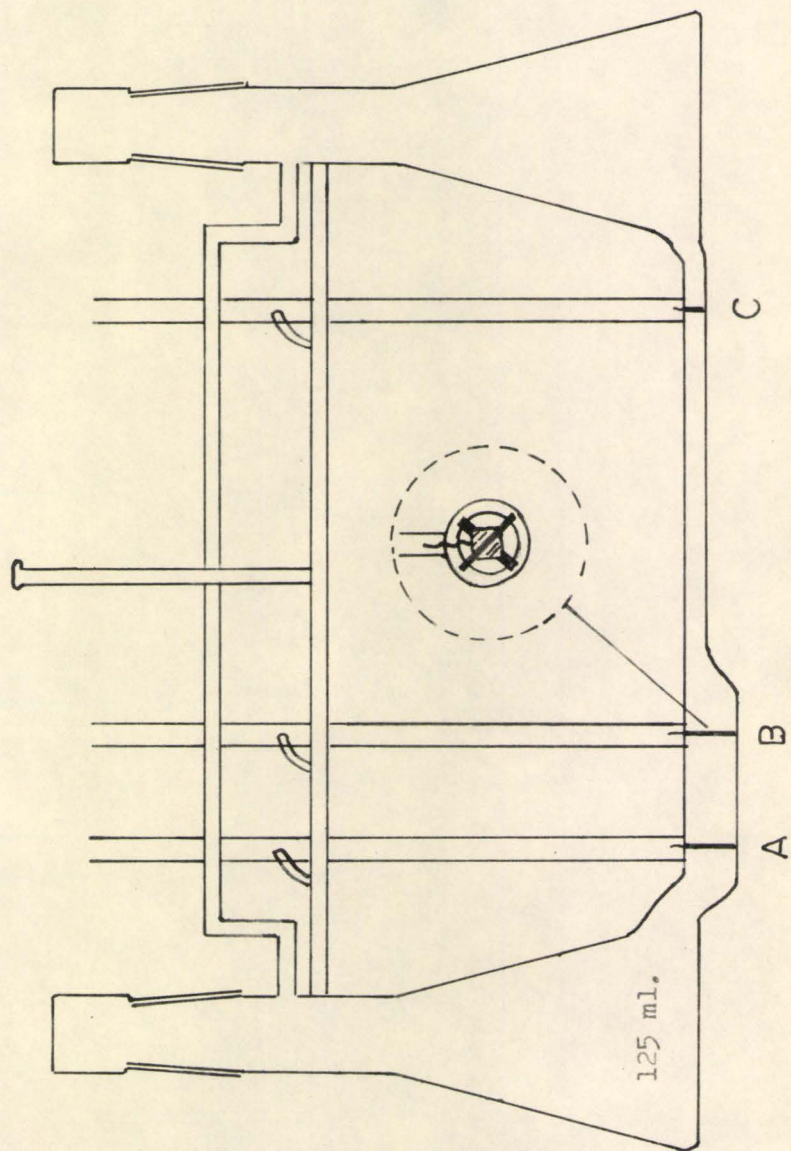
Fig. 8 CONDUCTIVITY CELL FOR USE WITH GASES

Side View   Front View
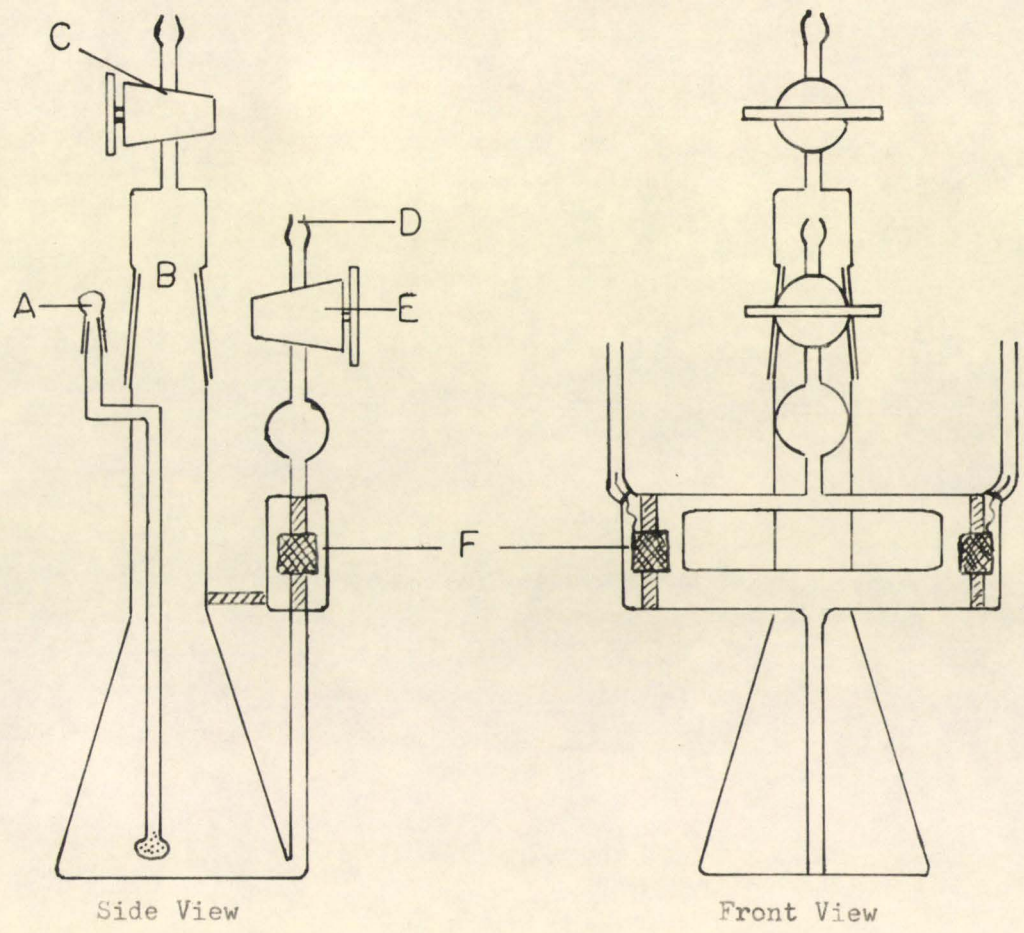
Fig. 9 WEIGHT DROPPERS USED FOR
SOLUTE ADDITIONS
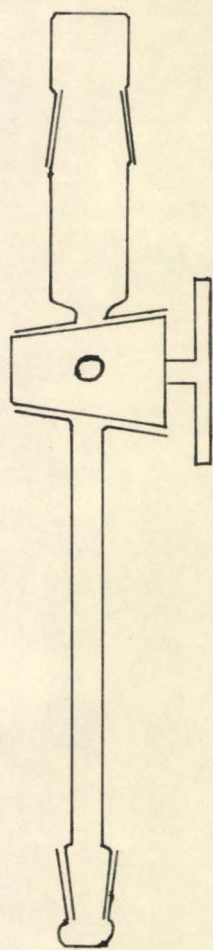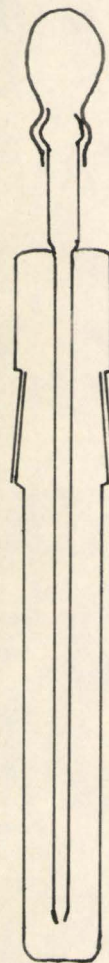
(a)   (b)

(b) CRYOSCOPY

A cryoscopic method of investigation has been developed utilizing
the cooling curve method of Mair, Glasgow and Rossini[58] for determining
freezing points. The cryoscope (Fig. 10) was a double walled vessel con-
structed so that the space between the walls could be evacuated to any
pressure required, from atmospheric to 10^{-4} mm. of mercury. The walls
surrounding space A were silvered. Temperatures were measured with a
platinum resistance thermometer B. A teflon sleeve fitted around the
thermometer at C allowed a tight fit of the thermometer into a length of
glass tubing to which a standard B14 inner ground glass joint was attached.
This joint was fitted into a B14 outer ground glass joint in the cryoscope
cap and the whole unit was made air tight by a paraffin wax seal at E.
The thermometer was a Leeds and Northrup platinum resistance thermometer
(No. 1331405) calibrated by Leeds and Northrup. The thermometer cali-
bration was checked periodically by determining its resistance at the
triple point of water using a Trans-Sonics Inc. "Equiphase cell". The
resistance of the thermometer was measured on a Mueller resistance bridge
(Leeds and Northrup No. 1338840).

Before fluorosulphuric acid was added to the cryoscope, dry air was
passed through it for about two hours, entering through K and leaving
through L and H, thus ensuring a dry atmosphere in the vessel. The acid
was then distilled into the weight dropper shown in Fig. 11. The dropper
was fitted to L via P and dry air was passed through the cryoscope for
an additional 15 minutes, the air leaving the vessel through outlet Q on

the dropper. The acid was then allowed to run into the cryoscope. The dropper was weighed before and after the addition to determine the weight of acid used. In a typical experiment the level of the solvent in the cryoscope was close to M (Fig. 10). Additions of solute to the cryoscope were made through L, using the weight droppers described in III(a).

Stirring was maintained throughout an experiment by means of the Nichrome metal stirrer F shown in detail in Fig. 10(b). This was a reciprocal motion stirrer driven by a 6-volt automobile windshield wiper motor. The stirrer had a 3 cm. stroke and a frequency of approximately 45 strokes per minute. The connection between the motor and the stirrer was made by the metal rod G which entered the cryoscope through a teflon plug H. The stirrer remained inert to fluorosulphuric acid itself and to all the fluorosulphuric acid solutions studied except antimony penta-fluoride solutions which attacked the stirrer. It was necessary to use the spiral glass stirrer shown in Fig. 10(c) for the SbF_5 solutions. The stem of this stirrer was nicrome wire, and it was joined to the glass spiral at the coupling R (Fig. 10(c)).

During a freezing-point determination dry air was passed into J and left the apparatus through the space between the metal rod G and the teflon plug H, and also through a small groove cut into H. This stream of dry air prevented moist atmospheric air from entering the cryoscope through H.

Freezing points were determined as follows. A dewar of liquid air was placed around the cryoscope so that the portion of the vessel from the level N (Fig. 10) to the bottom was completely immersed in liquid air. The temperature was allowed to drop rapidly until it reached approx-

imately -70°C. At this point stopcock O was opened and the pressure was reduced to approximately 1.0 mm. of mercury so that the rate of cooling was reduced to approximately 1.0 degrees per minute. When the temperature reached -80°C stopcock O was again opened and the pressure reduced to approximately 0.01 mm. of mercury. The rate of cooling was thus adjusted to between 0.2 degrees and 0.4 degrees per minute. After the temperature reached the expected freezing point, temperature readings were recorded every minute. When the solution had supercooled by approximately 2 degrees the solution was seeded. This was accomplished by dropping a small piece of platinum wire, previously cooled in liquid air, into the solution via the opening L. The temperature rose as solid solvent separated out and readings of temperature were recorded every minute for an additional 20 to 30 minutes.

During the development of the above described procedure for measuring the freezing points of solutions in fluorosulphuric acid, several techniques were tried and found to be inadequate. Initially the cryoscope was not silvered and the vacuum was obtained by a mechanical rotary pump. Under these conditions it was possible to obtain a vacuum of 0.15 mm. of mercury, which gave a rate of cooling of 2 degrees per minute at -80°C. This rate was much too fast to obtain an accurate cooling curve. When the cryoscope was silvered the rate of cooling was slowed to approximately 1 degree per minute, which was still too fast. In order to obtain an ideal rate of cooling (0.2 to 0.4 degrees per minute) it was necessary to incorporate a diffusion pump into the apparatus. Attempts were originally made to obtain adequate stirring with an electro-magnetic stirrer. However, at temperatures close to the freezing point the stirring became

very sluggish and, in fact, stopped as soon as the acid began to freeze.
A more powerful method of stirring was, therefore, required and the mech-
anical stirrer described above was found to be adequate.

Freezing points were determined from the time-temperature cooling
curves (Fig. 12). Mair, Glasgow and Rossini interpret these curves in some
detail in their paper[58]. The freezing point of a solution is defined
as the temperature at which crystals of the major component (solvent)
are in thermodynamic equilibrium with a liquid phase having the original
composition of the solution. Mair, Glasgow and Rossini state that the
freezing point can be determined by extrapolation of the equilibrium
portion of the cooling curve FG (Fig. 12) to its intersection at B with
the line ABC. These authors also point out that this method yields the
correct freezing point, provided the temperature head (i.e. the difference
in temperature between the solution and the cooling bath) is large com-
pared to the amount of supercooling. They show that this method can be
used with a 50° temperature head and 5° supercooling. In this work the
temperature head was approximately 60° and the amount of supercooling was
never greater than 4°. The extrapolation described above was done vis-
ually and the accuracy of this procedure was estimated to be $\pm$ 0.005°C.
Taylor and Rossini[59] describe a geometrical method of extrapolation.
This method was used on several of the cooling curves obtained in this
work and yielded freezing points which agreed with those obtained by
visual extrapolation, to within $\pm$ 0.005°C.

Fig. 13 gives the cooling curves obtained for five solutions of
KSO_3F in HSO_3F. The concentrations of these solutions are listed in
Table I (the first five solutions studied in experiment 141). The scale

of the ordinates gives the resistance in ohms of the platinum resistance
thermometer. The part of these curves corresponding to the region CDE
of Fig. 12 has been omitted in order to simplify the graph.

It was found that a minimum amount of supercooling is needed in
order to obtain reproducible freezing points. Fig. 14 is a graph of
freezing point versus amount of supercooling (S) for a single solution
of $RbSO_3F$. It can be seen that the freezing point is independent of S
for S greater than $1 \cdot 8^{\circ}$ but the apparent freezing point is lower if S
is less than $1 \cdot 8^{\circ}$. This arises from the fact that when S is small,
insufficient solid is formed on seeding to establish true thermodynamic
equilibrium.

When the freezing point was determined several times for the same
solution, using different initial rates of cooling (varying from $0 \cdot 2$ to
$0 \cdot 6$ degrees per minute), the freezing point was found to be independent
of the rate of cooling, but, extreme rates of cooling (beyond the limits
given above) resulted in cooling curves which were difficult to extra-
polate.

Fig. 10 FLUOROSULPHURIC ACID CRYOSCOPE

(a)

(b)

(c)
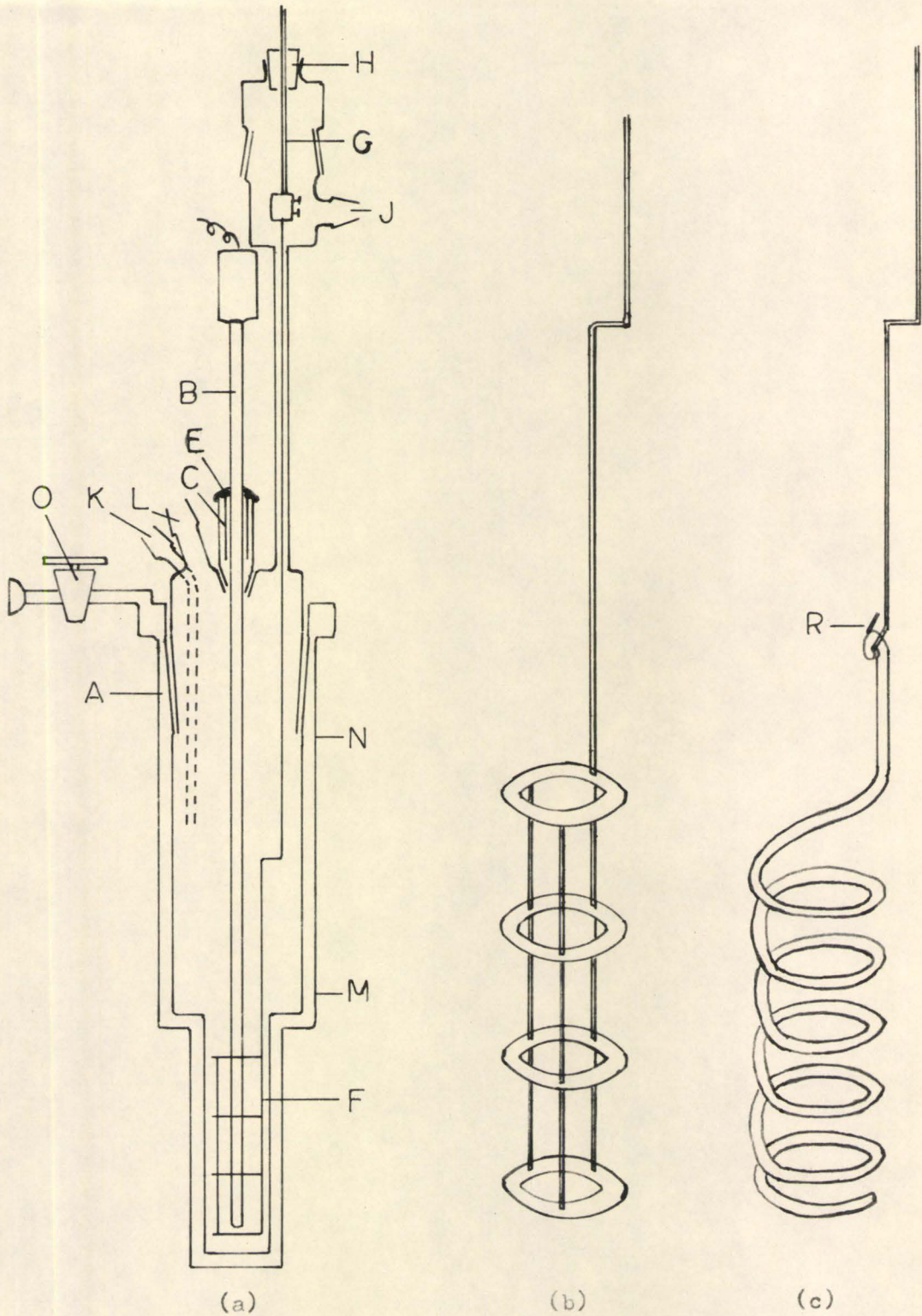
Fig. 11 WEIGHT DROPPER USED FOR ADDITION OF FLUOROSULPHURIC ACID TO CRYOSCOPE

100 ml.

teflon stopcock

Q

P

Fig. 12 SCHEMATIC DIAGRAM OF A TIME-TEMPERATURE
COOLING CURVE
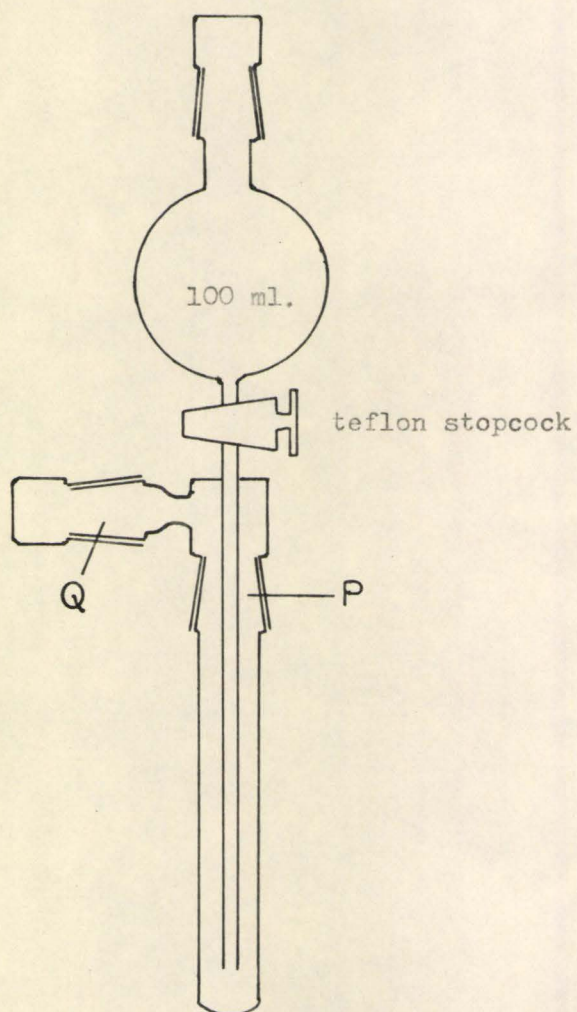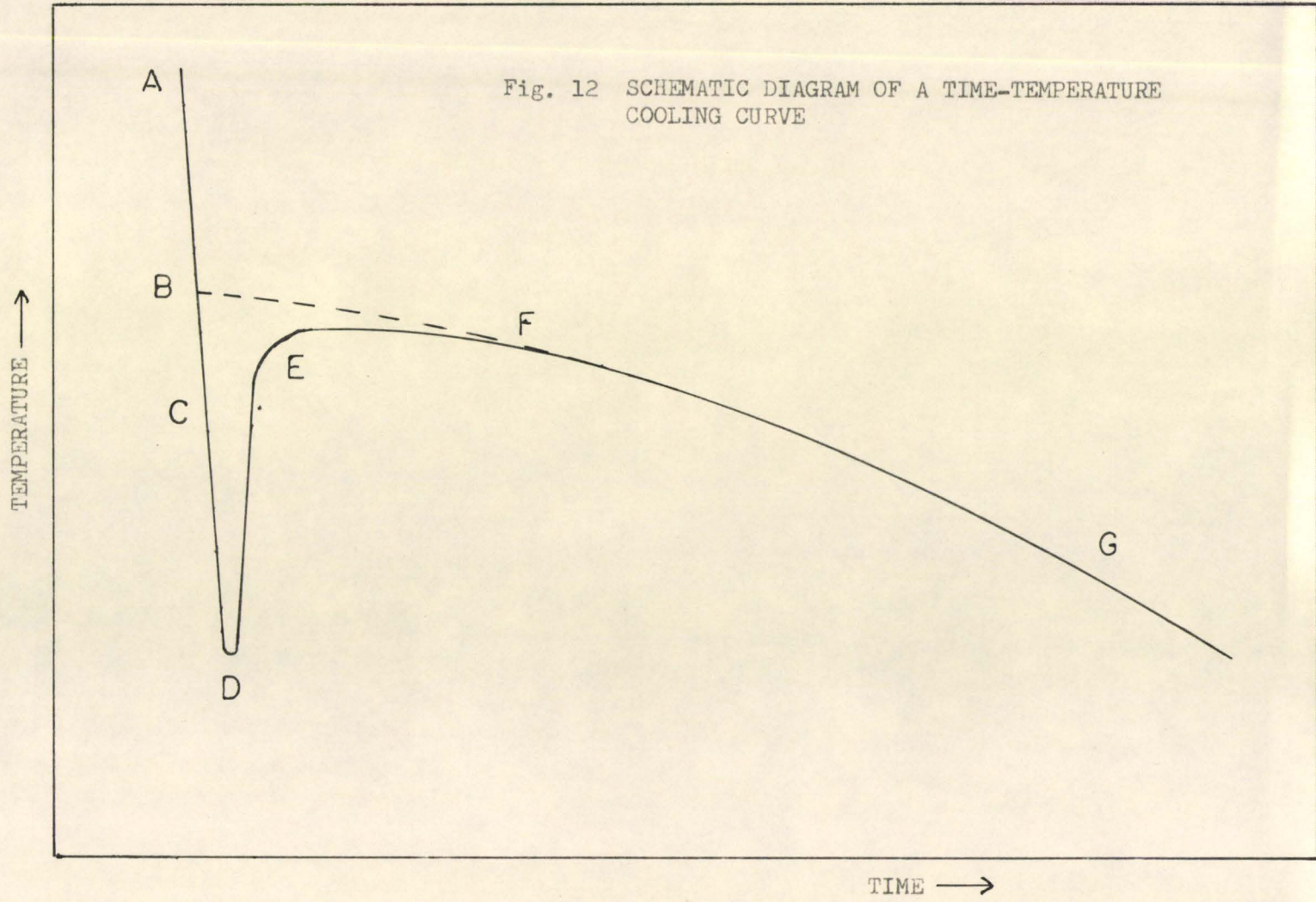
TEMPERATURE

TIME

Fig. 13 SOLUTIONS OF KSO$_3$F : TIME-TEMPERATURE COOLING CURVES

Resistance (ohms)

16·32

16·31

16·30

Time (minutes)

0   5   10   15   20

38
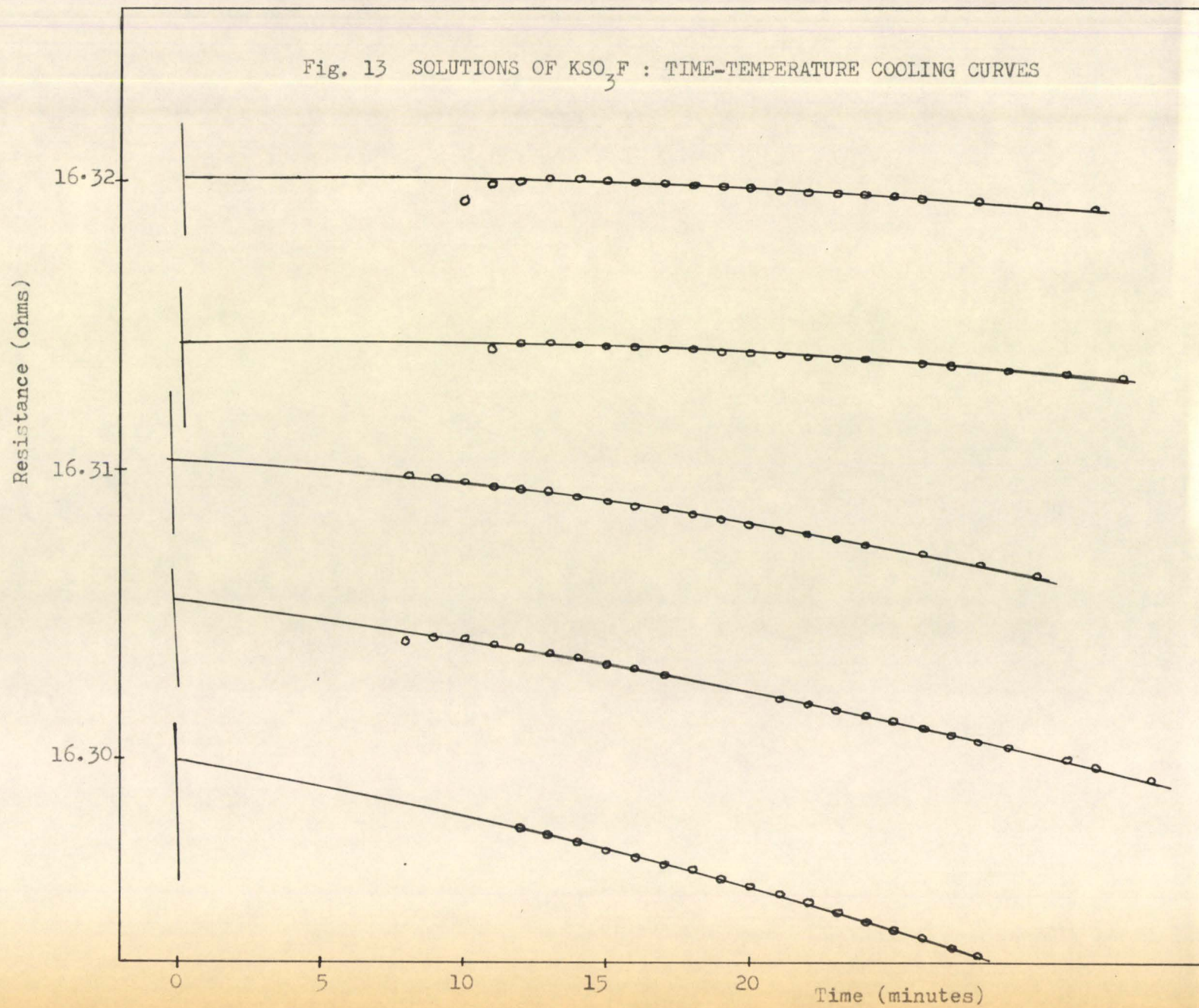
Fig. 14 A SOLUTION OF $RbSO_3F$: EFFECT OF AMOUNT OF
SUPERCOOLING ON THE FREEZING POINT

Freezing Point (°C)

- 89.7

- 89.8

- 89.9

1.0   2.0   3.0

Amount of Supercooling (°C)
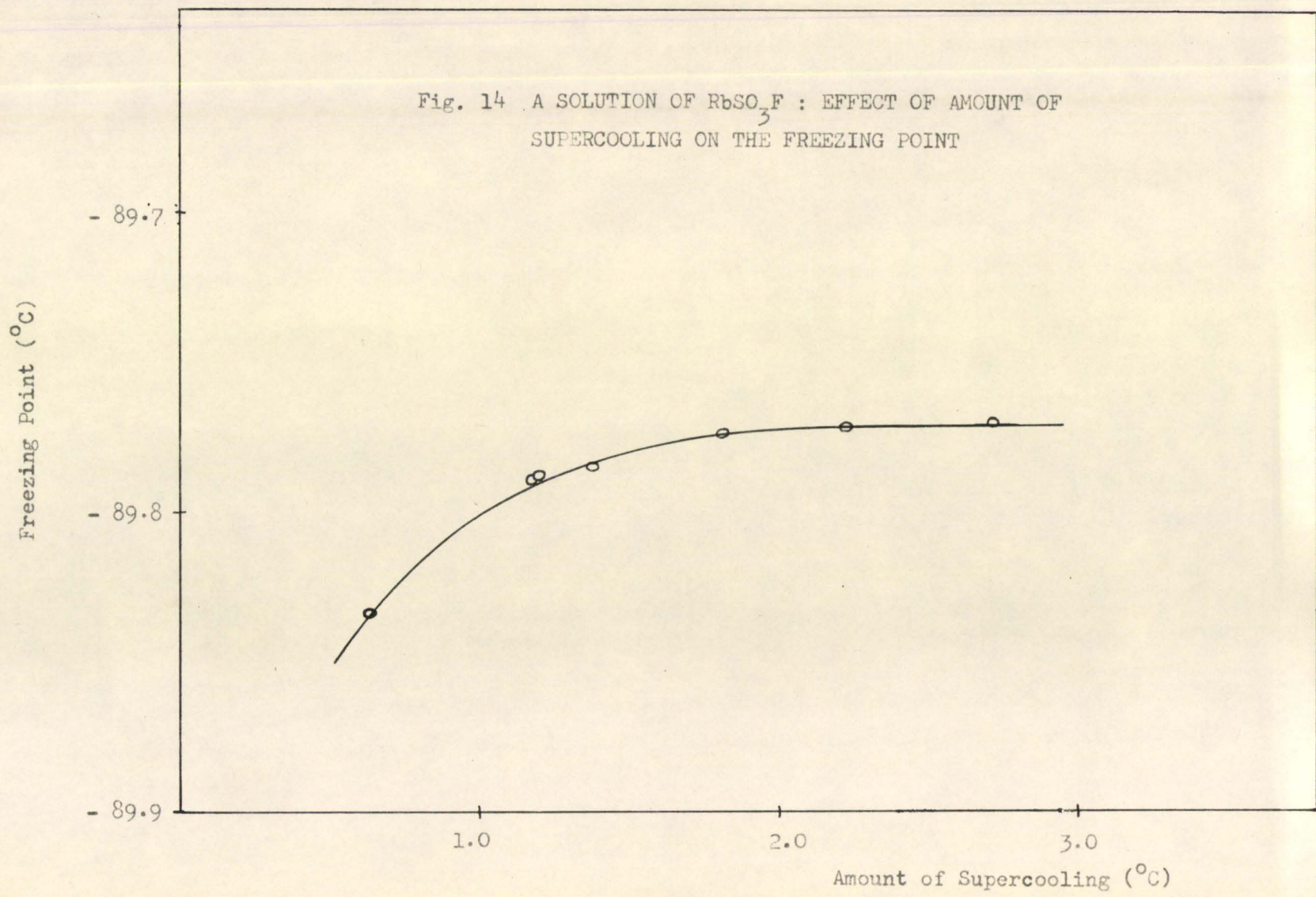
(c) TRANSPORT NUMBER MEASUREMENTS

The transport number cell, similar in design to the one used by Gillespie and Wasif[60] is shown in Fig. 15. It was designed so that the volume of liquid in sections A and C could be measured by means of the side arms D and E. The cell was calibrated for this purpose by the following procedure. A known volume of fluorosulphuric acid was added to C from a pipette. The level of the liquid in the arm connecting sections B and C was made to coincide with I by applying pressure at H or K. The level of the liquid in E was then recorded. This was repeated for several known volumes of fluorosulphuric acid and a graph of volume against side arm reading was plotted for both compartments A and C. From this graph it was possible to determine the volume of solution in each compartment from the level of the liquid in the capillary side arm.

The transport number of barium ion was determined by the Hittorf method using this cell. Barium fluorosulphate was weighed from an ordinary weight dropper (Fig. 9(a)) into section A of the dropper shown in Fig. 16. Fluorosulphuric acid was distilled into the dropper which was weighed before and after distillation. When the $Ba(SO_3F)_2$ had dissolved, the solution was added to the transport number cell via B (Fig. 15). The dropper was again weighed in order to determine the amount of solution added. All three compartments of the cell were thus approximately half filled and connected with each other via an unbroken column of solution in the connecting arms.

The electrical contact was made by means of the dipping mercury electrodes L and M. A current of about 20 m.a. from a sargent coulo-

metric current source was passed through the cell for two to three hours.
The cell was immersed in a $25^{\circ}C$ thermostat throughout the electrolysis.
After this time the current was turned off and the three compartments were
separated by forcing the columns of solution to break in the connecting
arms by applying pressure at G and H. The volumes of solution in com-
partments A and C were then determined by observing the level of the liquid
in the capillary side arms. After allowing approximately one hour for
mixing, two 10 ml. aliquots were taken from each of the compartments A and
C and placed into tubes on the apparatus shown in Fig. 17. The fluoro-
sulphuric acid was removed through A (Fig. 17) under vacuum and the amounts
of $Ba(SO_3F)_2$ remaining in each tube were determined according to the pro-
cedure given in Chapter II.

The results of two experiments are given in a later chapter.

Fig. 15 TRANSPORT NUMBER CELL
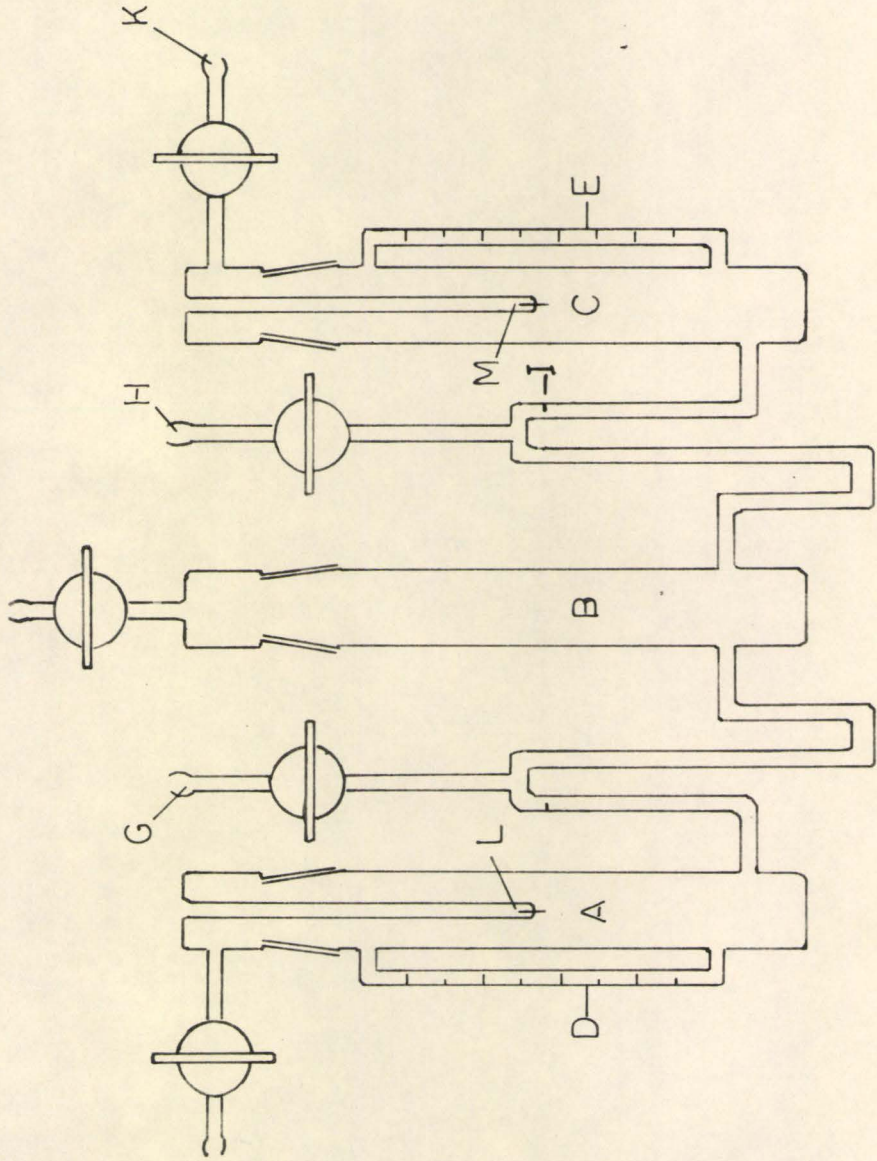
Fig. 16   WEIGHT DROPPER USED FOR
          ADDITION OF SOLUTION TO
          TRANSPORT NUMBER CELL

A

Teflon stopcock
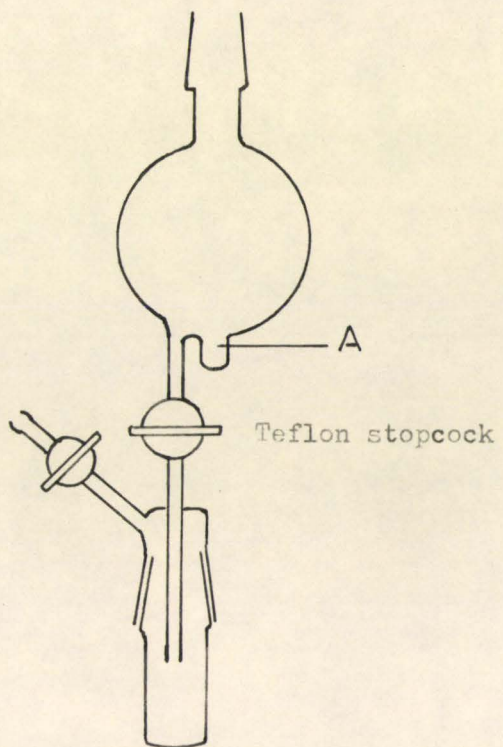
Fig. 17   APPARATUS USED FOR REMOVAL
          OF HSO_3F FROM SAMPLES TAKEN
          FROM TRANSPORT NUMBER CELL

A
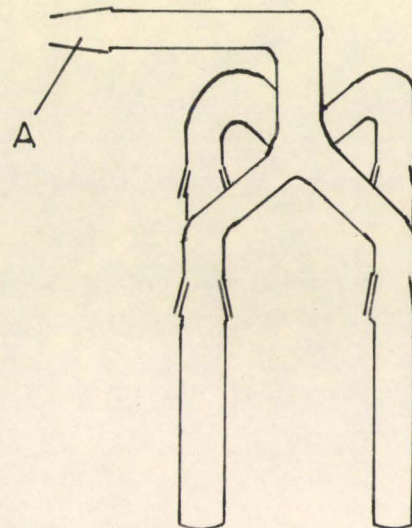
(d) NUCLEAR MAGNETIC RESONANCE SPECTROSCOPY

The n.m.r. measurements were made on a Varian Associates, high resolution, n.m.r. spectrometer operating at 56.4 Mc/sec. The spectra obtained were calibrated by the side-band technique using a Muirhead-Wigan, D-890-A, decade oscillator. Some spectra were integrated on a Varian Associates n.m.r. integrator, model V-3521.

Low temperatures were obtained by passing the cold air from a liquid air boiler through a Varian Associates variable temperature n.m.r. probe accessory, model V-4340. Temperatures were measured by a copper-constantan thermocouple connected to a Leeds and Northrup temperature potentiometer.

Samples were sealed in tubes made of selected 5 mm. glass tubing.

In all of the spectra presented in this thesis, the field strength increases from left to right, and the separation between peaks is given in frequency units (cycles per second).

CHAPTER IV

THE DETERMINATION OF FREEZING POINTS

AND THE CRYOSCOPIC CONSTANT

(a) DETERMINATION OF THE CRYOSCOPIC CONSTANT

The expression relating the freezing-point depression produced by a solute to its concentration is, for dilute solutions,[61,62]

$$\Delta T = (\frac{RT^2M}{\Delta H1000})m$$

$$= k_f \ m$$

where ΔT is the freezing-point depression;

R   is the gas constant;

T   is the freezing point of the pure solvent ($^{\circ}A$);

M   is the molecular weight of the solvent;

ΔH is the latent heat of fusion of pure solvent at the

temperature of its freezing point;

k_f is the cryoscopic constant ;

m   is the concentration of solute in molal units.

This expression was derived for a solute which does not dissociate in solution.

The more general expression

$$\Delta T = k_f \nu m \qquad\qquad\qquad 4.1$$

describes a system in which m moles of solute per 1000 g. of solvent dissolve to give ν moles of particles for each mole of solute.

The cryoscopic constant, k_f, for fluorosulphuric acid was determined experimentally in the following manner. A freezing-point depression-

45

molality curve was determined for each of a series of solutes for which
ν is known. If 4.1 is rearranged,

$$k_f = \frac{\Delta T}{m} \frac{1}{\nu}$$

it may be seen that the limiting slope of the freezing-point depression-
molality curve for a solute is $\frac{\Delta T}{m}$. Knowing ν it is then possible to deter-
mine k_f.

For a non-electrolyte, then, $\nu = 1$ and the limiting slope of its
freezing-point depression-molality curve yields k_f. Because of the very
high acid strength of fluorosulphuric acid, it is not easy to find solutes
which do not ionize in this solvent. In sulphuric acid it has been found
that several aromatic polynitro-compounds behave as non-electrolytes[63].
Barr, however, measured the conductivities of a series of aromatic nitro-
compounds in fluorosulphuric acid and found that they all behave as bases.
He did not study 1, 3, 5-trinitrobenzene and it was hoped that this solute
would behave as a non-electrolyte. Conductivities of trinitrobenzene
solutions are given in Table I and are compared with those of the strong
base nitrobenzene[42] in Fig. 18. It may be seen that trinitrobenzene is
a very weak electrolyte in fluorosulphuric acid.

Nevertheless, a value of k_f was obtained from the freezing-point
data on trinitrobenzene by first determining its degree of ionization from
conductivity data. Barr[42] determined the degrees of ionization of aro-
matic nitro-compounds by comparing the concentration of each required to
produce a given value of conductivity, with the concentration of nitrobenzene
required to produce the same conductivity. In this way the degree of
ionization of trinitrobenzene at a concentration of 0·01 molal was found
to be 0·02.

It will be shown later in this chapter that the degree of ioniza-
tion of a 0·01 molal solution of 2:4 dinitrotoluene at -90°C is approxi-
mately 10% greater than its degree of ionization at 25°C. If one assumes
analogous behaviour for trinitrobenzene, then the degree of ionization of
a 0·01 molal solution of this solute at its freezing point is approximately
0·022.

The freezing-point depressions produced by solutions of trinitro-
benzene are given in Table II and Fig. 19. The limiting slope of the
freezing-point depression-molality curve, shown by the dotted line, is 3·4
±0·05. The slope of this curve at the concentration 0·01 molal is essen-
tially the same, i.e. 3·4 ±0·05. At this concentration the degree of
ionization has been estimated above to be 0·022, which gives a ν value of
1·022. Hence k_f is found to be 3·33 ± 0·05.

Because of our failure to find other non-electrolytes in this
solvent, it was necessary to confirm the cryoscopic constant obtained above,
from freezing-point data on electrolytes.

Barr[42] has shown that the alkali metal fluorosulphates and benzoic
acid behave as strong bases in fluorosulphuric acid according to the
following equations.

$$MSO_3F \rightleftharpoons M^+ + SO_3F^-$$

$$C_6H_5COOH + HSO_3F \rightleftharpoons C_6H_5COOH_2^+ + SO_3F^-$$
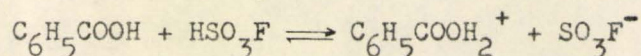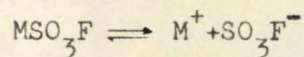
Thus ν = 2 for these solutes. Table III contains freezing-point
depression data for potassium, rubidium and cesium fluorosulphates and
benzoic acid, and the results for dilute solutions are shown graphically
in Fig. 19. These solutes all give essentially the same freezing-point
curve at low concentrations and the limiting slope of this curve (dotted

line) is $6 \cdot 7 \pm 0 \cdot 1$. Since $\nu = 2$, $k_f = 3 \cdot 35 \pm 0 \cdot 05$.

It will be shown in a later chapter that barium fluorosulphate is a strong electrolyte in fluorosulphuric acid, ionizing as follows:

$$Ba(SO_3F)_2 \rightleftharpoons Ba^{2+} + 2SO_3F^-$$
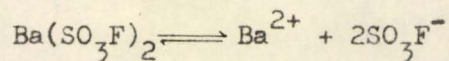
and hence $\nu = 3$. The freezing-point depressions for solutions of $Ba(SO_3F)_2$ are given in Table III and Fig. 19. The limiting slope is $10 \cdot 05 \pm 0 \cdot 05$ and since $\nu = 3$, $k_f = 3 \cdot 37 \pm 0 \cdot 03$.

From the above results the cryoscopic constant for fluorosulphuric acid was taken as $3 \cdot 35 \pm 0 \cdot 05$.

Table I

SOLUTIONS OF TRINITROBENZENE : CONDUCTIVITY AT $25^{\circ}C$

W_{HSO_3F} = $142 \cdot 00$ g.

$\mathcal{K}_o$ = $1 \cdot 110 \times 10^{-4}$ ohm^{-1} cm^{-1}

W	m^s	$10^4 \mathcal{K}$
0·0258	0·000834	1·184
0·0759	0·00245	1·351
0·1828	0·005910	1·649
0·4485	0·01450	2.210
0·6380	0·02063	2·554
1·2752	0·04123	3·390
1·5004	0·08083	4·519
3·5247	0·11395	5·248
4·2763	0·13824	5·561

Table II

SOLUTIONS OF TRINITROBENZENE : FREEZING—POINT DEPRESSIONS

W_{HSO_3F} = $148 \cdot 79$ g.

T_O = $-88 \cdot 998^{\circ}C.$

W	m^s	ΔT
0·5588	0·01762	0·060
1·1258	0·03550	0·129
1·7250	0·05440	0·210
2.4146	0.07615	0·306
3·3218	0.10476	0·421
4.2716	0·13471	0·567
5·6115	0.17697	0·789

Table III

SOLUTIONS OF SOME ELECTROLYTES : FREEZING-POINT DEPRESSIONS

Solute	Expt.	T_o	W_{HSO_3F}	W_{solute}	m^s	ΔT
KSO_3F	62	-88.999	144.02	1.0444	0.05249	0.382
				2.6592	0.13364	1.081
				4.2762	0.21490	1.825
KSO_3F	63	-89.026	152.45	1.0754	0.05106	0.379
				3.9959	0.18971	1.656
				5.5383	0.26293	2.450
KSO_3F	141	-89.005	138.17	0.1392	0.005424	0.030
				0.3233	0.01260	0.081
				0.4671	0.01820	0.122
				0.6316	0.02461	0.168
				0.8098	0.03156	0.223
				0.9444	0.03680	0.266
$CsSO_3F$	67	-88.999	124.67	0.9847	0.03405	0.243
				1.8611	0.06435	0.483
				3.0022	0.10381	0.822
				3.7402	0.12933	1.042
$RbSO_3F$	70	-88.999	135.43	1.5064	0.06037	0.443
				2.8644	0.11461	0.903
				3.8184	0.15278	1.272
				4.7238	0.18900	1.621
				5.5825	0.22336	1.956
$RbSO_3F$	74	-89.007	132.78	0.4997	0.02039	0.135
				0.7327	0.02990	0.211
				1.0440	0.04261	0.307
				1.9983	0.08137	0.619
				2.3988	0.09789	0.780
C_6H_5COOH	68	-89.134	121.72	0.4568	0.03073	0.232
				1.0872	0.07314	0.546
				1.8792	0.12642	0.967
				2.6761	0.18003	1.390
				3.3445	0.22500	1.844
$Ba(SO_3F)_2$	131	-89.027	173.06	0.2539	0.004373	0.039
				0.7384	0.01272	0.127
				1.4414	0.02483	0.249
				2.2177	0.03820	0.391
				3.7489	0.06457	0.656
				5.5941	0.09635	0.986
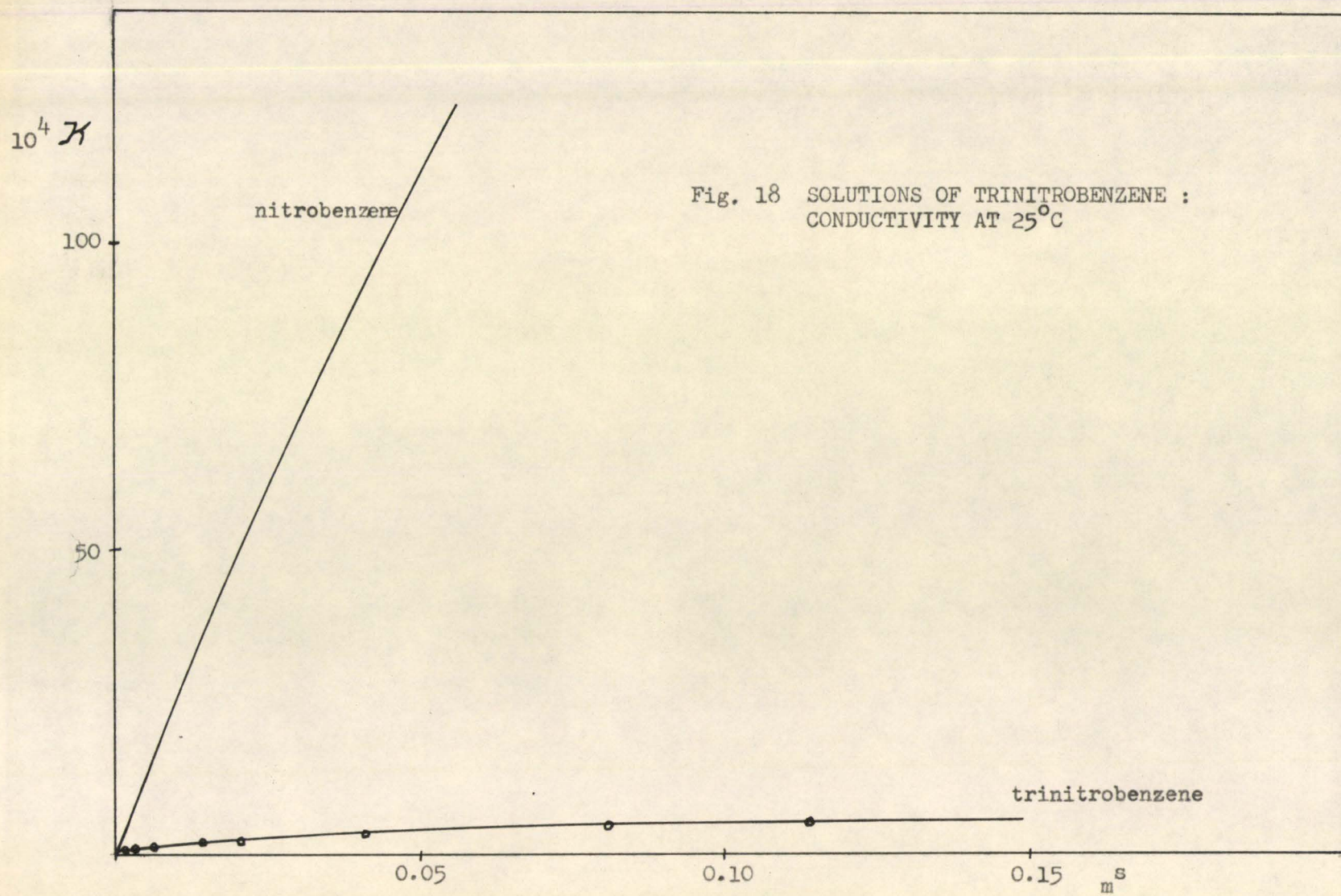
Fig. 18   SOLUTIONS OF TRINITROBENZENE :
CONDUCTIVITY AT 25°C

Fig. 19 SOLUTIONS OF SOME ELECTROLYTES : FREEZING-
POINT DEPRESSIONS

ΔT

0·8

0·6

0·4

0·2

o Trinitrobenzene
● KSO₃F
◓ RbSO₃F
◒ CsSO₃F
□ Benzoic Acid
■ Ba(SO₃F)₂

0.02   0.04   0.06

m^s
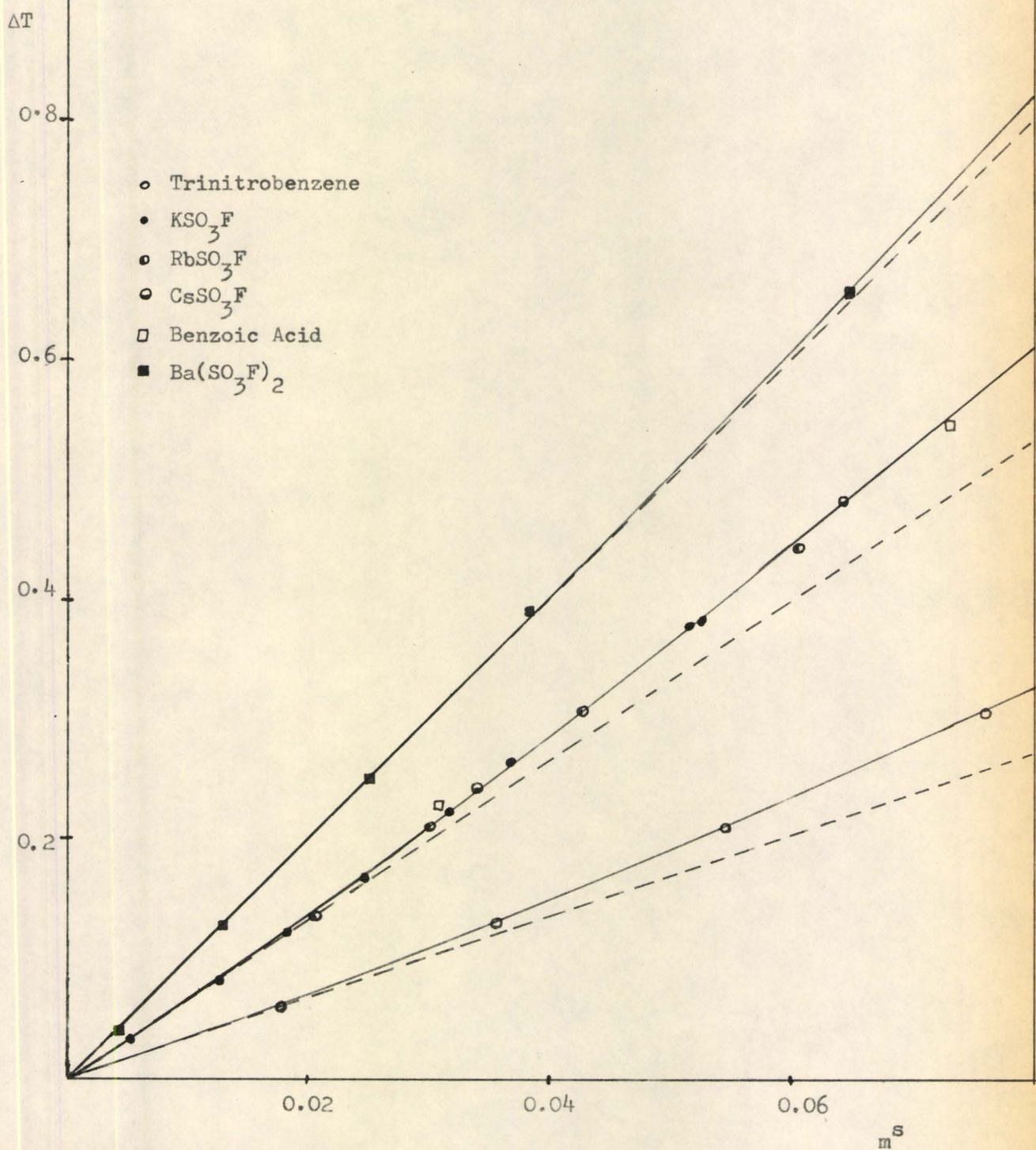
(b) DISCUSSION OF NON-IDEALITY

Deviations from ideality of solutions of alkali metal fluoro-
sulphates in fluorosulphuric acid are observable at freezing-point depres-
sions as low as $0 \cdot 1^{\circ}C$ (Fig. 19). Bass, Gillespie and Oubridge[64] have
expressed the degree of non-ideality of solutions in sulphuric acid, in
terms of the osmotic coefficient ϕ defined by the equation

$$\phi = \Delta T(1 + 0 \cdot 002\Delta T)/k_f \sum m_{ij}$$

where ΔT is the freezing-point depression;

k_f is the cryoscopic constant;

$\sum m_{ij}$ is the total concentration of solute species;

$0 \cdot 002\Delta T$ is a term which allows for the variation of the heat

of fusion with temperature.

Using a simplified version of this equation, setting $(1 + 0 \cdot 002\Delta T) = 1$,
values of ϕ for solutions of KSO_3F were calculated at various concentrations
and are given in Table IV. A graph showing the variation of ϕ with con-
centration of KSO_3F in HSO_3F is given in Fig. 20 along with a similar plot
for solutions of $KHSO_4$ in H_2SO_4[63] for comparison.

For solutions in sulphuric acid Bass, Gillespie and Oubridge have
accounted for the variation of the osmotic coefficient with concentration,
by means of an equation of the form

$$\phi = 1 + \phi^{el} + b \sum m_i$$

where ϕ^{el} is the contribution of interionic forces to the osmotic

coefficient;

b is an arbitrary parameter;

53

$\sum m_i$ is the total concentration of ionic species in solution. The term $b\sum m_i$ contains contributions arising from ionic solvation and the entropy of mixing of the solvated ions and the solvent molecules. For a number of solutes in sulphuric acid, these authors calculated ϕ^{el} and b. From the values of b, they were able to estimate solvation numbers for several cations.

Such detailed interpretations were not attempted at this time for solutions in fluorosulphuric acid for several reasons. The cryoscopic constant is not known very accurately and until the latent heat of fusion of fluorosulphuric acid is determined directly, interpretation of cryoscopic data must remain essentially semi-quantitative. Moreover, calculation of ϕ^{el} is not possible since the dielectric constant of the acid is not known, and it would be especially difficult to determine its value at $-90^{o}C$. The value $\mathcal{E} = 80$ at $25^{o}C$ is assumed in the discussion of conductimetric data in Chapter IX. This is only a rough guess, arrived at by assuming that $\mathcal{E}$ for HSO_3F would be approximately the same as $\mathcal{E}$ for water at $25^{o}C$. In any case there seems to be no reasonable way of converting this value to $-90^{o}C$. This value, 80, cannot be regarded as sufficiently reliable for the calculation of ϕ^{el}.

Bass, Gillespie and Oubridge[63] showed it was necessary to allow for the entropy of mixing of the solvent molecules and the solvated ions, in order to obtain reliable solvation numbers. To do this it was necessary to know the partial molar volumes of the solvated ions. Although partial molar volumes of some cations in fluorosulphuric acid have been determined by Barr[42] from density measurements at $25^{o}C$, it is uncertain that these quantities will be the same at $-90^{o}C$.

Since interionic attractions cause the osmotic coefficient to be less than unity while ion-solvation effects cause it to be greater than unity, the values given in Table IV show that ion-solvation effects must be considerably more important in these solutions than the effect of interionic attractions.

Solutions of barium fluorosulphate in fluorosulphuric acid appear to be ideal over a rather large range of concentrations (Fig. 19). It is possible that $Ba(SO_3F)_2$ is not completely ionized at moderate concentrations. This effect would tend to oppose non-ideality effects and this could result in apparent ideal behaviour. This incomplete ionization may be due to partial covalent character in $Ba(SO_3F)_2$. Some evidence for this is given by the fact that the salt hydrolyzes in aqueous solution. Potassium, rubidium and cesium fluorosulphates, which may be considered true ionic salts, do not undergo any appreciable hydrolysis in water; in fact, they may be recrystallized from water. Any hydrolysis which does occur is extremely slow at room temperature. Fluorosulphuric acid, on the other hand, which may be considered a covalent fluorosulphate, hydrolyzes fairly rapidly when added to water. In general it appears that covalent fluorosulphates hydrolyze more rapidly than ionic fluorosulphates. Thus the hydrolysis of $Ba(SO_3F)_2$ in aqueous solution may be attributed to some covalent character in the $Ba-OSO_2F$ bonds.

Table IV

SOLUTIONS OF KSO_3F : OSMOTIC COEFFICIENTS

m	ΔT	ϕ
0·01	0·067	1·000
0·02	0·137	1·022
0·03	0·211	1·050
0·04	0·287	1·071
0·05	0·365	1·090
0·06	0·447	1·112
0·07	0·528	1·126
0·08	0·610	1·139
0·09	0·695	1·153
0·10	0·785	1·172
0·11	0·870	1·181
0·12	0·963	1·198

Fig. 20   SOLUTIONS OF KSO_3F : OSMOTIC COEFFICIENTS

KSO_3F in HSO_3F

$KHSO_4$ in H_2SO_4

ϕ

1·12

1·08

1·04

1·00

0·96

0.02

0.04

0.06

m^s
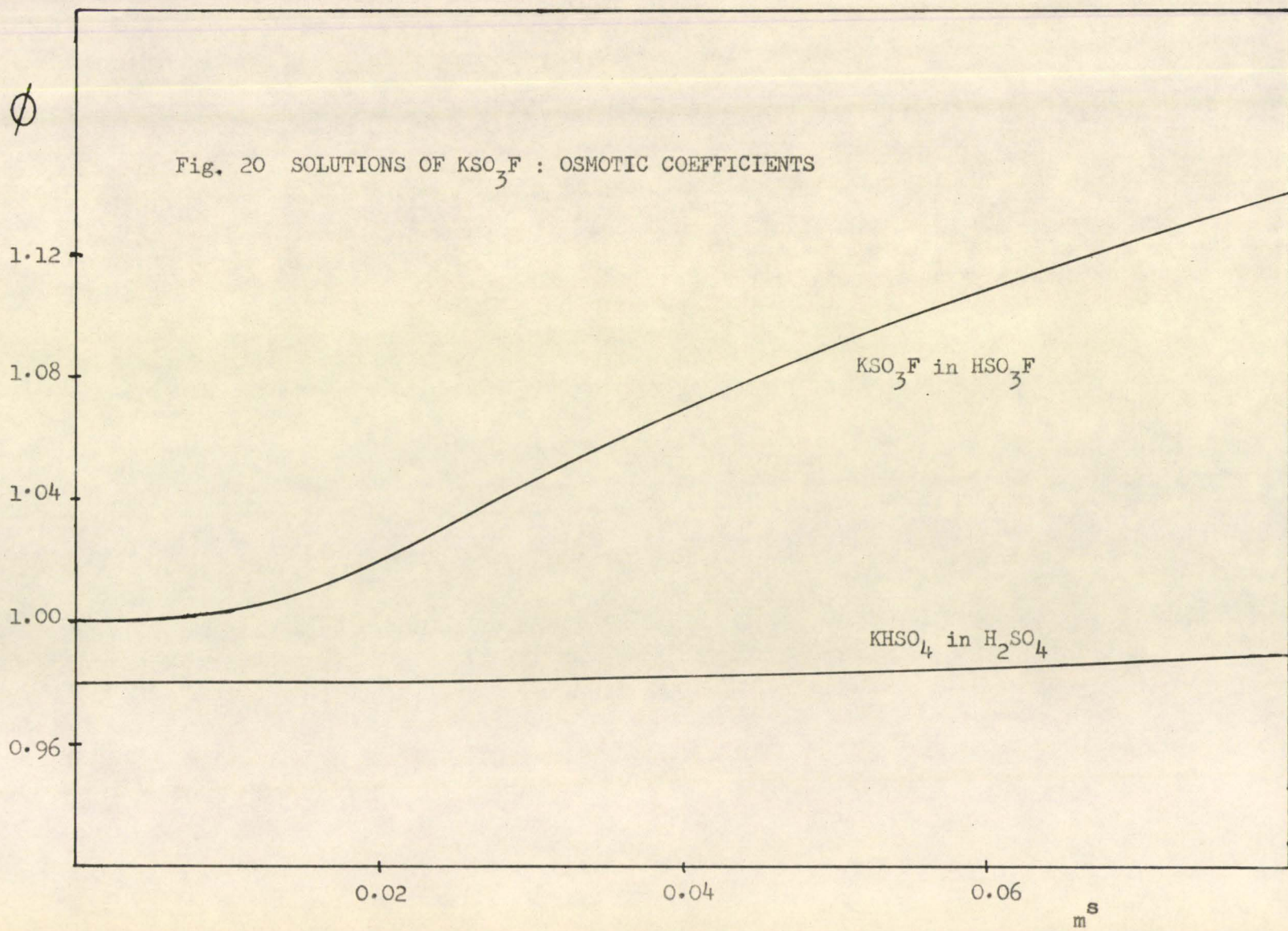
(c) ESTIMATION, FROM CRYOSCOPIC DATA, OF THE DEGREE OF IONIZATION
OF A WEAK BASE AT -90°C

Although the mode of ionization of a solute in fluorosulphuric
acid is, no doubt, generally the same at -90°C as at 25°C, the degree of
ionization is probably different at the two temperatures. In order to
gain some idea of the effect of temperature change on the degree of ioni-
zation of a weak base, α' was determined by cryoscopy, for the base 2:4
dinitrotoluene, and this value was compared to α, the degree of ionization
determined from conductivity. The 2:4 dinitrotoluene used in this experi-
ment was obtained from the sample purified by Barr[42].

Fig. 21 is the freezing-point curve obtained for 2:4 dinitro-
toluene and Table V lists the experimental data. Table VI lists values
for α, at different concentrations of base, as determined by Barr[42] from
conductivity results, and values of α' as determined in this work from
freezing-point results. The values of α' were calculated from the relation-
ship

$$\alpha' = \nu - 1$$

where $$\nu = \frac{\Delta T}{m^s \times 3.35}$$

Non-ideality effects limit the accuracy with which degrees of
ionization can be obtained from freezing-point measurements. Since, in
most solutions, deviations from ideality become noticeable at freezing-
point depressions as small as 0·15°C (Fig 19), the values of α' calculated
for solutions of 2:4 dinitrotoluene above 0·025 molal concentration cannot
be considered accurate. However, even at lower concentrations than this

58

(Table V) the value of α' is greater than that of α. It would appear then that 2:4 dinitrotoluene is more ionized in fluorosulphuric acid at -90°C than at $+ 25^{\circ}$C.

Table V

SOLUTIONS OF 2:4 DINITROTOLUENE : FREEZING-
POINT DEPRESSIONS

W_{HSO_3F} = 162.20 g.

T_o = -89.007°C.

W	m^s	ΔT
0.3151	0.01067	0.063
0.6631	0.02245	0.129
0.9944	0.03366	0.189
1.4428	0.04882	0.279
2.5322	0.08572	0.448

Table VI

SOLUTIONS OF 2:4 DINITROTOLUENE : DEGREES OF IONIZATION
CALCULATED FROM CONDUCTIVITY AND FREEZING-POINT RESULTS

m^s	α	α'
0.0026	0.855	0.89
0.0057	0.752	0.78
0.0092	0.678	0.74
0.0135	0.619	0.72
0.0185	0.558	0.72
0.0239	0.508	0.70
0.0369	0.443	0.70

Fig. 21 SOLUTIONS OF 2:4 DINITROTOLUENE : FREEZING-POINT DEPRESSIONS
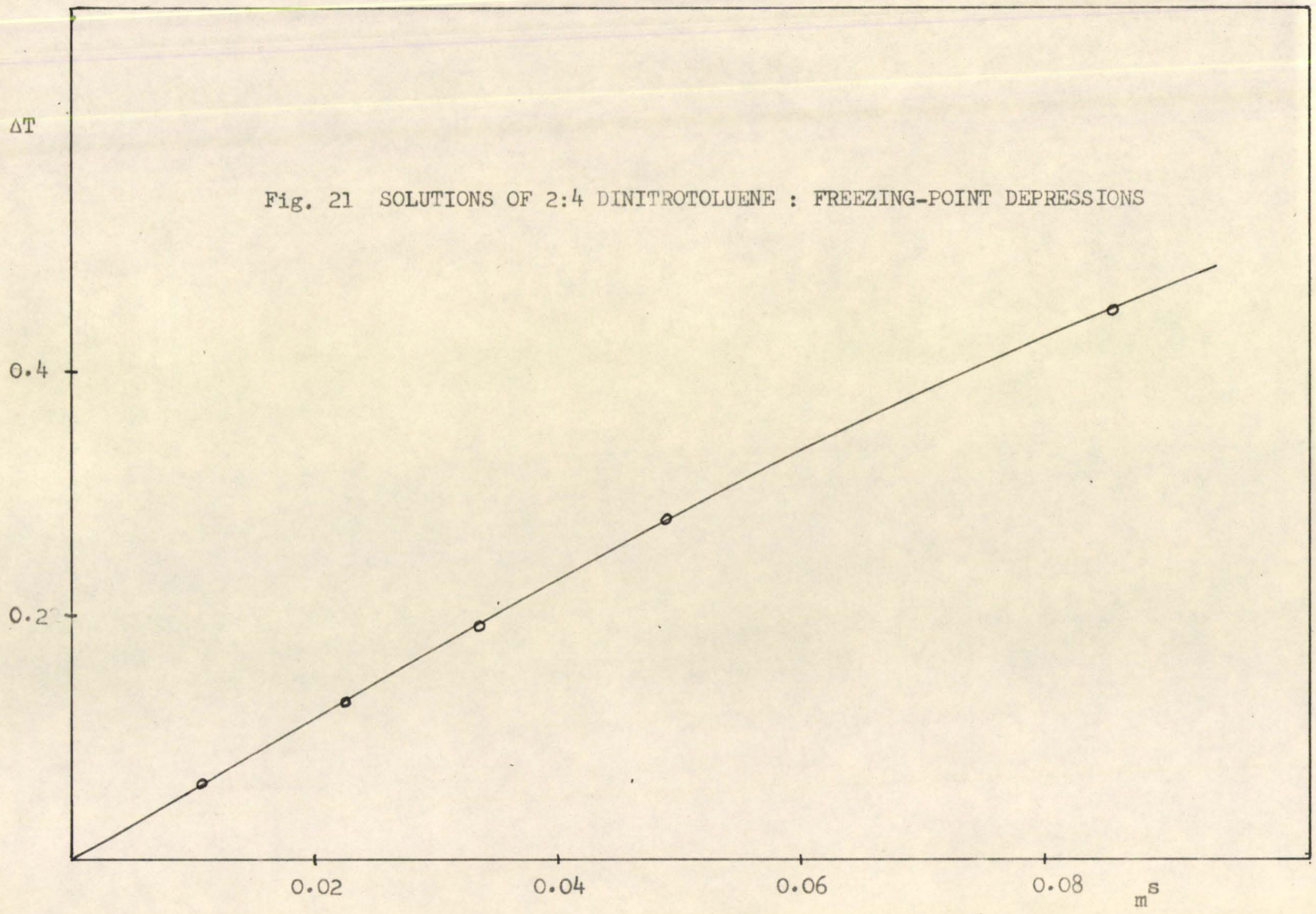
CHAPTER V

SOLUTIONS OF ANTIMONY PENTAFLUORIDE

(a) INTRODUCTION

Woolf[36] and Barr[42] both investigated solutions of antimony pentafluoride in fluorosulphuric acid. Their work was discussed briefly in Chapter I. Woolf suggested two possible modes of ionization for this solute, namely

$$SbF_5 + 2HSO_3F \rightleftharpoons SbF_5SO_3F^- + H_2SO_3F^+ \qquad 1.4$$

$$SbF_5 + 2HSO_3F \rightleftharpoons SbF_6^- + SO_3 + H_2SO_3F^+ \qquad 1.5$$
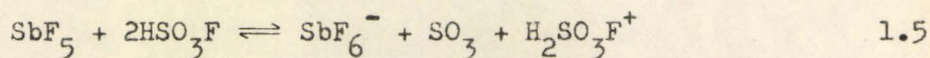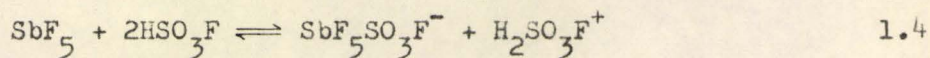
Woolf suggested that 1.5 is more probable than 1.4 because the structure $SbF_5SO_3F^-$ would require abnormal five-fold coordination of sulphur while the alternate structure $SbF_6SO_3^-$ would require seven-fold coordination of antimony. Barr, however, pointed out that if the fluorosulphate group is bonded to antimony via oxygen, no abnormal coordination is required.

Evidence presented in this chapter and in chapter VI supports 1.4 and no supporting evidence for 1.5 has been found in this work.

(b) CONDUCTIVITY MEASUREMENTS

In order to measure the conductivity of solutions of SbF_5, the solute was added as a concentrated solution in HSO_3F. This solution was made by distilling SbF_5 into a dropper tube (Fig. 9(b))which contained freshly distilled HSO_3F. The data for several experiments are given in Table VII and Fig. 22.

The solid line in Fig. 22 is the experimental conductivity curve for SbF_5. Assuming that 1.4 describes the behaviour of SbF_5 in fluorosulphuric acid, theoretical curves were determined for different values of K_1, where

$$K_1 = \frac{\left[SbF_5SO_3F^-\right]\left[H_2SO_3F^+\right]}{\left[SbF_5\right]}$$

The square brackets refer to concentrations in molal units. $\left[SbF_5\right]$ refers to m_{SbF_5}, the concentration of unionized SbF_5 in solution, not to be confused with $m_{SbF_5}^s$, the stoichiometric concentration of SbF_5. The theoretical curves appear as the dotted lines in Fig. 22.

In order to obtain the theoretical curves it was necessary to estimate the conductivities of the ions K^+, $SbF_5SO_3F^-$, and $H_2SO_3F^+$ at various concentrations. These conductivity-molality curves are shown in Fig. 23. The details of how these curves were obtained will be given later in this section. Thus for the value of $K_1 = 2.0 \times 10^{-3}$ the concentrations of the species resulting from 1.4 were calculated for different concentrations of SbF_5 ($m_{SbF_5}^s$). From the graphs in Fig. 23 the expected conductivity at each value of $m_{SbF_5}^s$ was calculated (curve 1,Fig. 22). The procedure was repeated for $K_1 = 0.003$, 0.0035, 0.0037, 0.0039 and 0.0045,

and the resulting curves are 2, 3, 4, 5 and 6 respectively in Fig. 22.

For $K_1 = (3.7 \pm 0.2) \times 10^{-3}$, good agreement between experimental and theoretical is obtained for low concentrations of SbF_5 ; however, at high concentrations the agreement is poor. When K_1 is given a larger value, 4.5×10^{-3}, agreement is obtained at high concentrations but now there is no agreement at low concentrations. Although one would not expect an equilibrium constant based on concentrations instead of activities to accurately describe the behaviour of a partially dissociated acid over a large concentration range, Barr[42] found that when concentration equilibrium constants were calculated for weak bases in fluorosulphuric acid, the values change at most by only a few percent over a large concentration range. For example, the dissociation constant of 2:4 dinitrochlorobenzene, $K = 1.64 \times 10^{-3}$, remains unchanged over the concentration range $0.0489 - 0.1055$ m, and for the somewhat stronger base, nitromethane, the constant varies from 29.0×10^{-3} to 32.0×10^{-3} over the range $0.055 - 0.125$ m. It appears, as is reasonable, that the variation in K is greater for stronger bases, i.e. for solutions of greater ionic strength. Since, at low concentrations, SbF_5 has an equilibrium constant of about 3.7×10^{-3}, one might expect a change in K_1 of a few percent over the range $0.05 - 0.20$ m. However, in order to obtain agreement between the experimental and theoretical curves, Fig. 22, K_1 would have to increase by 40% over this range.

It would appear, then, that SbF_5 becomes more ionized as its concentration is increased, contrary to normal behaviour for weak electrolytes. Aqueous solutions of HF exhibit a very similar behaviour and this system is described in a paper by Bell, Bascombe and McCoubrey[64]. In dilute solutions HF is a weak acid with a dissociation constant of approximately

7×10^{-4}. Kinetic and indicator experiments show that the acidity of HF solutions increases very rapidly in the range 10 to 50 weight % HF. They attribute this behaviour to the formation, at higher concentrations, of strong polymeric acids of HF which ionize to give the dimeric and trimeric anions, HF_2^- and $H_2F_3^-$, and even higher polymers.

The behaviour of SbF_5 in fluorosulphuric acid can be explained in an analogous manner. It is assumed that dimerization occurs and that there are two equilibria involved, the one being represented by equation 1.4 with an equilibrium constant $K_1 = 3 \cdot 7 \times 10^{-3}$, and the other being represented by 5.1

$$2SbF_5SO_3F^- + H_2SO_3F^+ \rightleftharpoons (SbF_5)_2SO_3F^- + 2HSO_3F \qquad 5.1$$
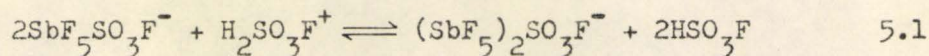
with an equilibrium constant K_2 defined by the expression

$$K_2 = \frac{\left[(SbF_5)_2SO_3F^-\right]}{\left[SbF_5SO_3F^-\right]^2 \left[H_2SO_3F^+\right]}$$

Using the values $K_1 = 3 \cdot 7 \times 10^{-3}$ and $K_2 = 450$ the concentrations of all the species in 1·4 and 5·1 were calculated at different values of $m_{SbF_5}^s$. The total conductivity at each $m_{SbF_5}^s$ was then determined from the curves in Fig. 23, and the theoretical conductivity curve 1 (Fig. 24) was thus determined. In these calculations the approximation was made that $(SbF_5)_2SO_3F^-$ has the same ionic mobility as $SbF_5SO_3F^-$. This procedure was repeated for $K_2 = 700$ and 950 (curves 2 and 3 in Fig. 24). Good agreement is obtained between experimental and theoretical for $K_1 = 3 \cdot 7 \times 10^{-3}$ and $K_2 = 700$.

A 0·188 m solution of SbF_5 in fluorosulphuric acid was titrated conductimetrically with KSO_3F and a minimum was observed at $r(KSO_3F/SbF_5) = 0 \cdot 4$ (not at $r = 1 \cdot 0$ as previously claimed by Woolf[36]). The experimental

data are given in Table VIII and Fig. 25. The dotted line is a theoretical curve calculated as follows. For $r(KSO_3F/SbF_5) = 0.2, 0.4, 0.6$ and 0.8 the concentrations of all species in solution were calculated assuming ionization of SbF_5 according to 1.4 and 5.1, with $K_1 = 3.7 \times 10^{-3}$ and $K_2 = 700$. From the curves in Fig. 23 the theoretical conductivity at each r was calculated and the curve drawn through these calculated values appears as the dotted line in Fig. 25.

The deviation of the experimental points from the theoretical curve is not too surprising since the latter is calculated on the assumption that the activities of ions can be represented by their concentrations. As was discussed previously, this is a reasonable approximation for solutions of low ionic strength, e.g. solutions of SbF_5 alone. However, when SbF_5 is titrated with KSO_3F, the ionic strength increases rapidly due to the formation of the highly ionized salt $KSbF_5SO_3F$ and appreciable deviations from ideal behaviour are to be expected.

The details of how the conductivity-molality curve for $H_2SO_3F^+$ (Fig. 23) was obtained will be given in Chapter VI. Barr found that in KSO_3F solutions the transport number of K^+ is 0.11. Thus the curve for K^+ was obtained by assuming that 11% of the conductivity of a KSO_3F solution[42] is due to K^+. The curve obtained is very nearly linear (the maximum deviation from linearity is not more than 0.5×10^{-4} ohm^{-1} cm.$^{-1}$) indicating that over the concentration range studied, the variation of the mobility of K^+ with concentration is essentially linear.

The curve for $SbF_5SO_3F^-$ was found as follows. In Fig. 25 the conductivity at $r(KSO_3F/SbF_5) = 1.0$ is due to the salt $KSbF_5SO_3F$ and its solvolysis products. A first approximation to the curve was made by

ignoring solvolysis. Thus at $r = 1.0$, $\mathcal{K} = 88 \times 10^{-4}$ ohm^{-1} cm.$^{-1}$ (Fig. 25). $\mathcal{K}$ for 0.188 m K$^+$ is 46×10^{-4} ohm^{-1} cm.$^{-1}$ and thus $\mathcal{K}$ for a 0.188 m solution of SbF$_5$SO$_3$F$^-$ is 42×10^{-4} ohm^{-1} cm.$^{-1}$. Assuming linear mobility-concentration dependance for this ion from m = 0 to 0.188, the dotted line in Fig. 23 was obtained. Using the procedure outlined previously, a series of curves were drawn as in Fig. 22 for different values of K_1. For concentrations up to 0.05 m the curves obtained were identical to those shown in Fig. 22. This is due to the fact that at such low concentrations the conductivity due to SbF$_5$SO$_3$F$^-$ is so small that the theoretically deter-mined curves are not affected by large changes in the assumed mobility of this ion. Thus $K_1 = 3.7 \times 10^{-3}$ was taken as the value for the equilibrium constant for 1.4. It was now possible to calculate a corrected conduc-tivity-molality curve for SbF$_5$ SO$_3$F$^-$ by allowing for solvolysis.

We have

$$K_s = K_{ap}/K_1$$

where K_s is the equilibrium constant for the solvolysis

$$SbF_5SO_3F^- \underset{K_s}{\rightleftharpoons} SbF_5 + SO_3F^-$$
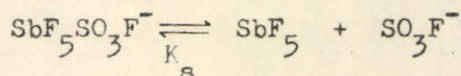
K_{ap} = autoprotolysis constant = 3.6×10^{-8} (Chapter X)

K_1 = 3.7×10^{-3}

$\therefore K_s$ = 1×10^{-5}

Thus for a 0.188 molal solution of KSbF$_5$SO$_3$F we find

$$\left[SbF_5SO_3F^-\right] = 0.1866 \text{ m}$$

$$\left[SbF_5\right] = 0.0014 \text{ m}$$

$$\left[SO_3F^-\right] = 0.0014 \text{ m}$$

$$\left[K^+\right] = 0.188 \text{ m}$$

The conductivity due to 0.0014 molal SO$_3$F$^-$ (89% of the conductivity of

0.0014 molal KSO$_3$F) is 6 x 10^{-4} ohm^{-1} cm.$^{-1}$, the conductivity due to 0.188 molal K$^+$ is 46 x 10^{-4} ohm^{-1} cm.$^{-1}$, and therefore, the conductivity due to 0.1866 m SbF$_5$SO$_3$F$^-$ is 36 x 10^{-4} ohm^{-1} cm.$^{-1}$. Assuming the change in the mobility of SbF$_5$SO$_3$F$^-$ is linear over the concentration range 0 to 0.1866 m, the curve shown in Fig. 23 was obtained. Since the curve for K$^+$ is linear over the concentration range considered, the assumption of linearity in the case of SbF$_5$SO$_3$F$^-$, made above, is probably justified. In any case, in considering the conductivity of solutions of SbF$_5$ alone, the conductivity due to SbF$_5$SO$_3$F$^-$ is only a very small percentage of the total conductivity; thus any slight curvature of the conductivity-molality curve for this ion would not produce any appreciable effect in the theoretical curves. It is possible, however, that such an effect would be noticeable in the theoretical curve for the titration (Fig. 25). This could account in part for the disagreement between the experimental results and the theoretical curve in this case.

The approximation was made that the dimer (SbF$_5$)$_2$SO$_3$F$^-$ has the same mobility as the monomer SbF$_5$SO$_3$F$^-$. Again, for the interpretation of the conductivity of solutions of SbF$_5$ this approximation is probably quite good since these ions conduct only a small portion of the current.

Table VII

SOLUTIONS OF SbF_5 : CONDUCTIVITY AT 25°C

Expt.	$10^4 \chi_o$	W_{SbF_5}	W_{HSO_3F}	m^s	$10^4 \chi$
89	1·107	1·0575	113·11	0·043132	37·747
91	1·153	0·6400	113·81	0·02594	25·880
96	1·314	5·2439	135·62	0·17838	90·693
97	1·096	3·1157	122·99	0·11687	70·039
129	1·148	1·1703	137·32	0·039317	35·025
138	1·498	1·4933	99·58	0·069182	48·448
138	1·498	2·3734	100·32	0·10914	65·286
138	1·498	2·7058	100·60	0·12408	70·928
138	1·498	3·3528	101·15	0·15292	81·490
138	1·498	4·1477	101·83	0·18791	93·656
139	1·287	0·2447	135·21	0·008349	14·44
139	1·287	0·4877	135·41	0·01662	21·12
139	1·287	0·8172	135·69	0·02778	28·36
139	1·287	1·1880	135·01	0·040296	35·16
139	1·287	2·9383	137·49	0·098593	61·14
139	1·287	4·6515	138·94	0·15445	82·06

Table VIII

SOLUTIONS OF SbF_5 - KSO_3F : CONDUCTIVITY AT 25^oC

W_{HSO_3F} = 101·83 g.

$m^s_{SbF_5}$ = 0·1879

K_o = 1·498 x 10^{-4} ohm^{-1} $cm.^{-1}$

W_{KSO_3F}	$r(KSO_3F/SbF_5)$	$10^4 K$
0·0	0·0	93.656
0·0923	0·03491	86.087
0·2141	0·08098	78.025
0·3377	0·1277	71.834
0·5057	0·1913	65.978
0·6910	0·2614	62.147
0·8988	0·3400	60.155
1·0993	0·41580	59.868
1·4935	0·56491	61.989
1·7949	0·67891	65.032
2·0287	0·76734	67.829
2·2123	0·83678	70.292
2·3850	0·90212	73.380
2·5512	0·96499	82.477
2·6742	1·0115	92.762
2·9618	1·1218	121.390
3·2399	1·2255	151.326

Fig. 22 SOLUTIONS OF SbF_5 : CONDUCTIVITY AT $25^{\circ}C$

THEORETICAL CONDUCTIVITY CURVES
FOR IONIZATION OF SbF_5 ACCORDING
TO 1.4

Fig. 23 ESTIMATED CONDUCTIVITY-MOLALITY CURVES
FOR VARIOUS IONS (25°C)
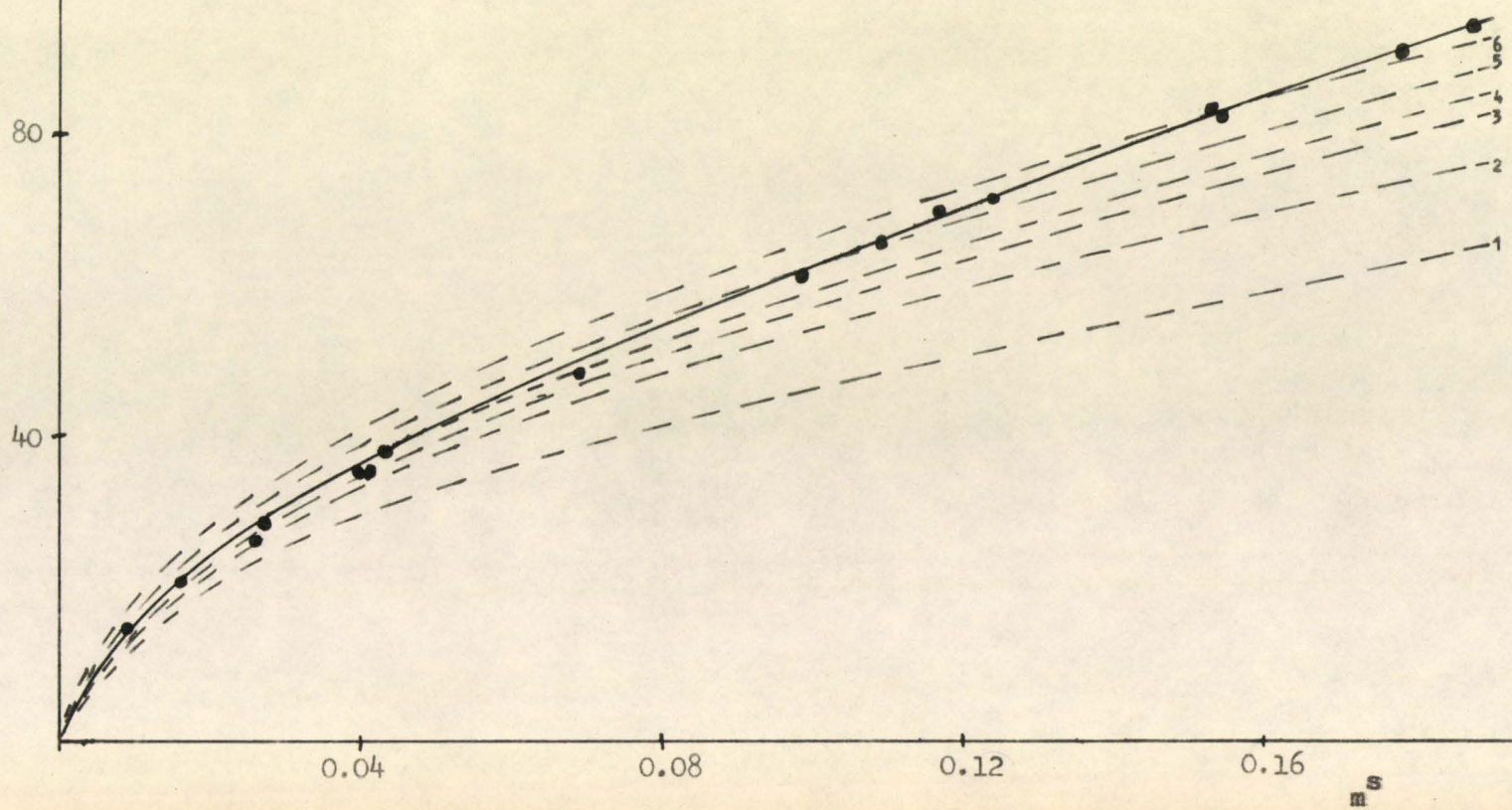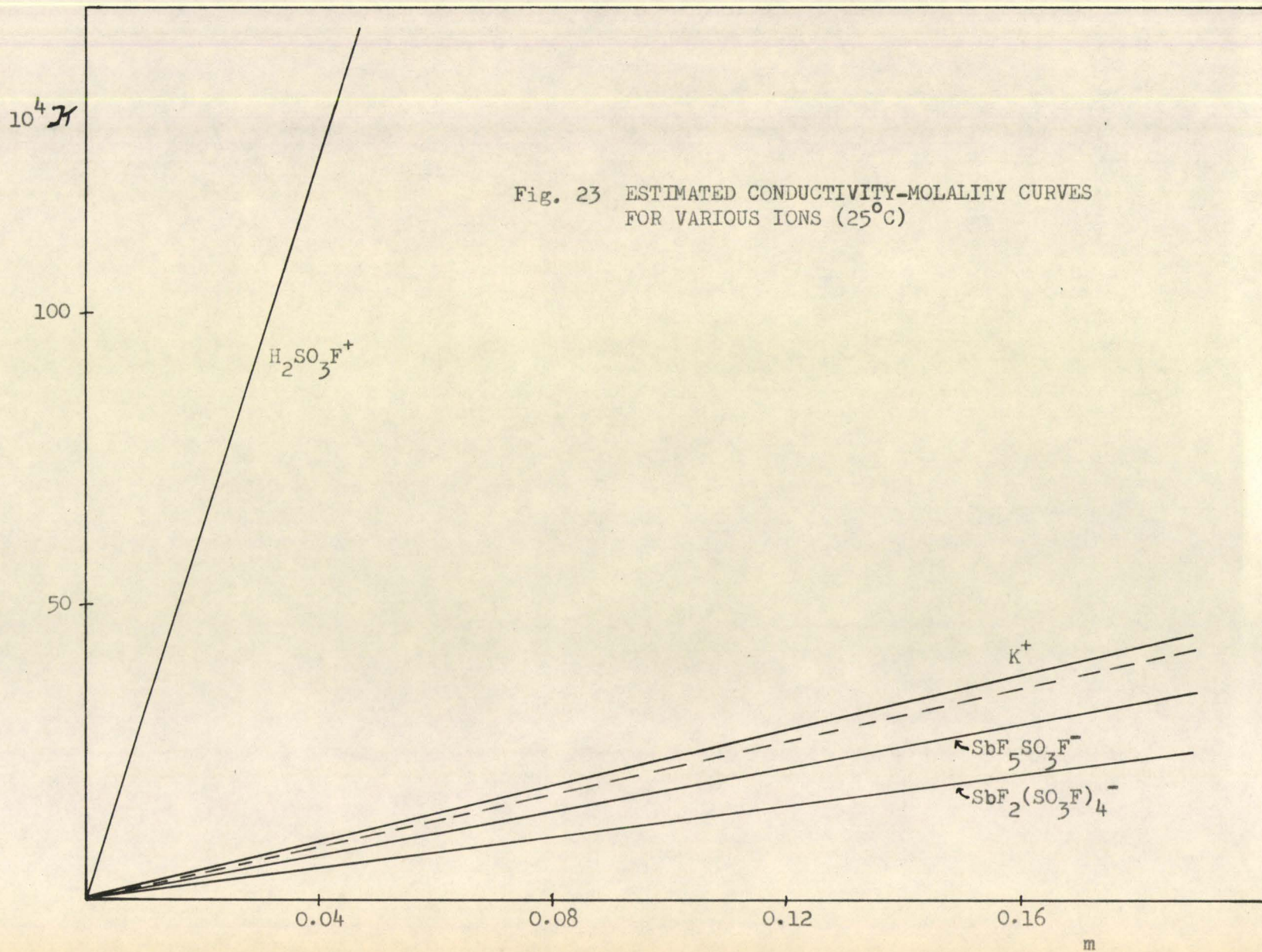
Fig. 24   SOLUTIONS OF SbF$_5$: THEORETICAL CONDUCTIVITY CURVES FOR
IONIZATION OF SbF$_5$ ACCORDING TO 1.4 and 5.1 (25°C)

Fig. 25 SOLUTIONS OF SbF$_5$ - KSO$_3$F : CONDUCTIVITY AT 25°C

$10^4 \mathcal{K}$

r(KSO$_3$F/SbF$_5$)
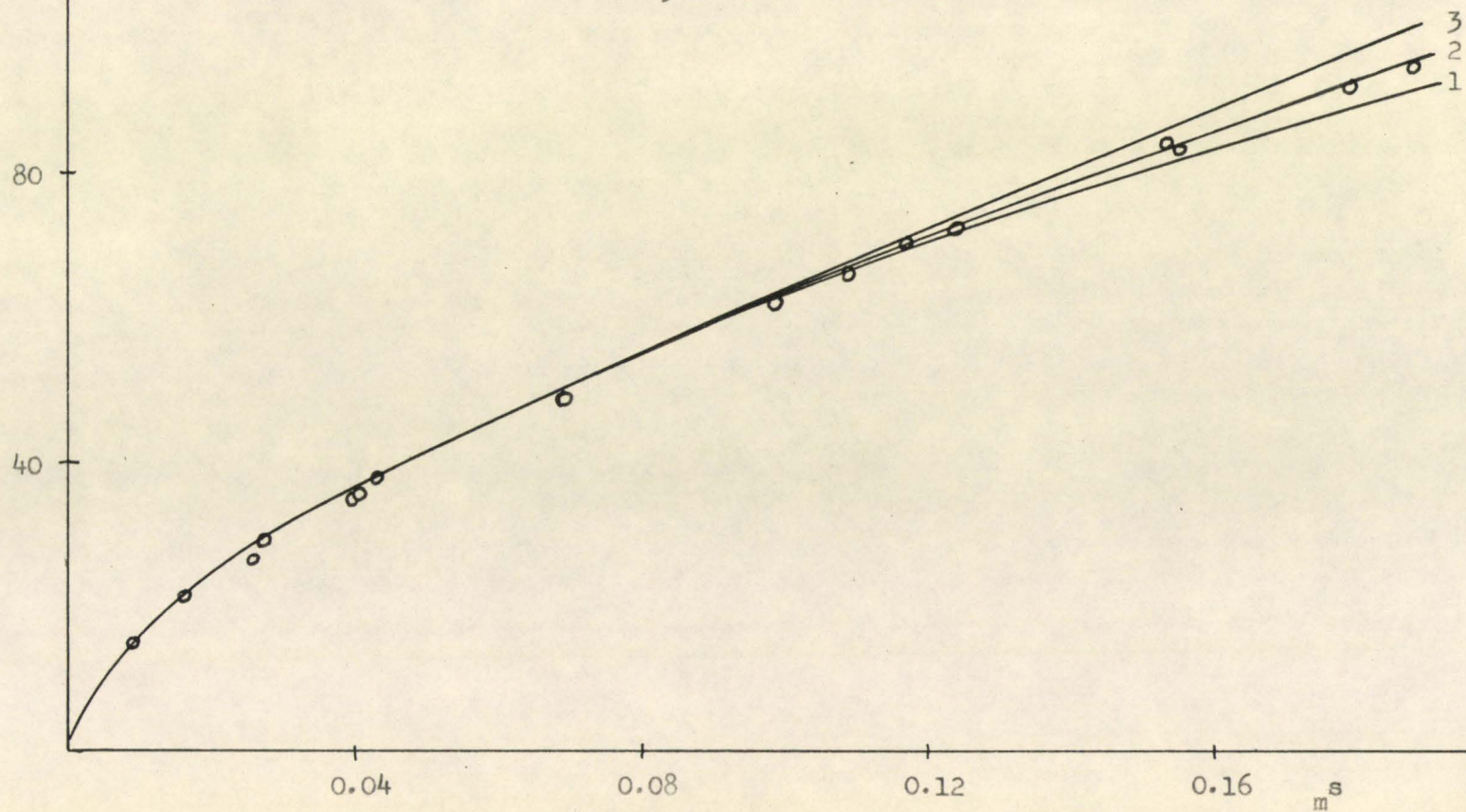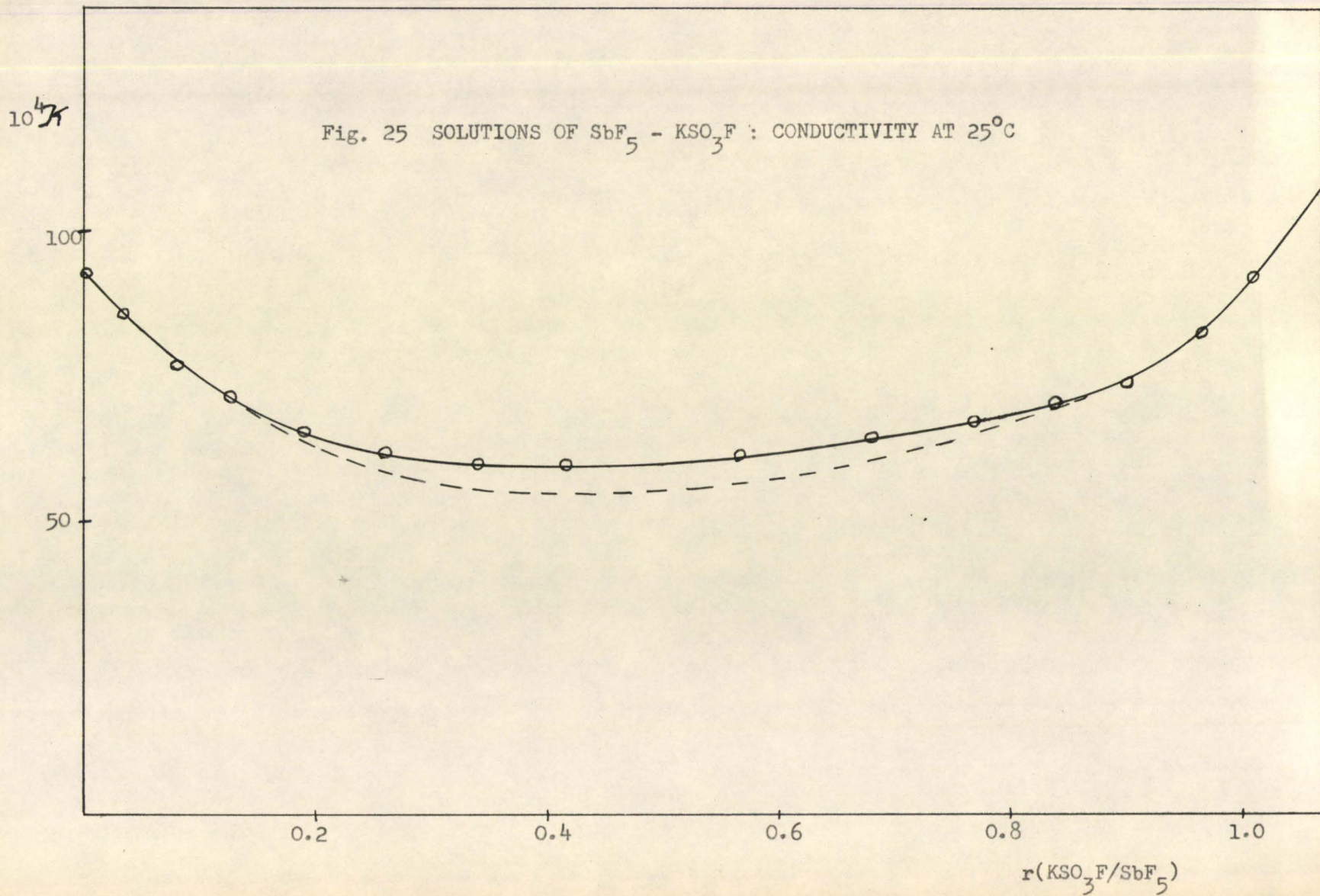
(c) FREEZING-POINT MEASUREMENTS

Table IX gives experimental data for two experiments involving freezing-point measurements on solutions of SbF_5 and for a titration of SbF_5 with KSO_3F. In experiment 80, KSO_3F was added to a 0.2687 molal solution of SbF_5. In Table IX the column headed m^s_{solute}, for this portion of the experiment, refers to the molal concentration of KSO_3F present in a solution of $m^s_{SbF_5} = 0.2687$.

The experimental results are shown graphically in Fig. 26. The region of the graph from 0.0 to 0.2687 m^s represents the freezing-point depression curve for SbF_5. The region from 0.2687 to 0.5394 m^s represents the freezing-point depressions produced by KSO_3F when added to a solution of 0.2687 $m^s_{SbF_5}$. The concentration values in this region of the graph refer to $m^s_{SbF_5}$ plus $m^s_{KSO_3F}$. This is, then, the titration portion of the curve and at the concentration 0.5394 m^s, $r(KSO_3F/SbF_5)$ is 1.0 and the end point of the titration is reached. At higher concentrations than 0.5394 m^s the curve represents the freezing-point depressions produced by the excess KSO_3F.

In Fig. 26 the solid line represents the experimentally determined freezing-point curve. Curve 1 is a theoretical curve obtained by assuming ionization of SbF_5 according to 1.4. This curve was obtained in the following manner. It was assumed that for a stoichiometric concentration of SbF_5 of 0.05 m, the solution is ideal. For different arbitrary values of K_1 the concentrations of all the species produced in 1.4 were calculated and the theoretical freezing point determined using $k_f = 3.35$. It was found that for K_1 equal to $(2.5 \pm 0.5) \times 10^{-3}$ the resulting ΔT was 0.2 $\pm$

75

$0.003^{\circ}C$, in agreement with the experimental value of 0.200 for a 0.05 m solution of SbF_5. Using $K_1 = 2.5 \times 10^{-3}$ the total concentration of all the solute species was calculated for different values of $m^s_{SbF_5}$ and the expected freezing-point depressions were then calculated and plotted (curve 1). The titration portion of this curve was determined similarly. From a knowledge of K_1, the concentrations of all the solute species can be calculated at different values of $r(KSO_3F/SbF_5)$ and hence the expected freezing-point depressions can be obtained. If solvolysis occurs to the same extent as found in the conductivity experiment (Chapter V (b)), then it may be shown that it would have a negligible effect on the freezing-point depression and it has therefore been ignored.

Curve 2 is a theoretical curve obtained by assuming ionization of SbF_5 according to 1.4 and 5.1, with equilibrium constants K_1 and K_2. This curve was obtained in the following manner. K_1 was assumed to have the value found from the conductivity experiments at $25^{\circ}C$, namely 3.7×10^{-3}. Then different values were assumed for K_2 until, for a 0.05 m^s solution of SbF_5, the calculated freezing-point depression agreed with experiment. Hence a value of K_2 equal to $(2.5 \pm 0.5) \times 10^3$ was obtained. Using values of K_1 and K_2 equal to 3.7×10^{-3} and 2.5×10^3 respectively, the theoretical freezing-point curve 2 was obtained. K_2 is larger in this case than was observed from the conductivity results. This is not too surprising since one would expect a higher degree of polymerization at $-90^{\circ}C$ than at $25^{\circ}C$. Using the limiting values for the equilibrium constants given above produces virtually no change in the theoretical curves.

From 0.0 to 0.2687 m there is not much difference between the two theoretical curves, the experimental curve deviating from both due to

non-ideality effects. However, in the titration portion of the graph the
two theoretical curves have different general shapes. Evidently the shape
of the experimental curve is much closer to that of 2 than 1 (Fig. 26).
This is considered supporting evidence for the conclusion that the simple
picture for the ionization of SbF_5, according to 1·4, is not adequate and
the further mode of ionization as represented by 5·1 must also be considered.

As $r(KSO_3F/SbF_5)$ approaches 1·0 the experimental curve approaches
curve 2. In other words, the solution appears, somewhat surprisingly, to
become ideal. This could be explained in two possible ways. If non-
ideality is due almost entirely to the solvation of the autoprotolysis
ions through hydrogen-bonding (I), then as the titration continues the con-
centration of $H_2SO_3F^+$ decreases, and at $r(KSO_3F/SbF_5) = 1·0$ there are
essentially no autoprotolysis ions present, and the solution becomes ideal.
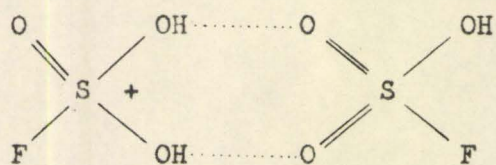
(I)

(II)
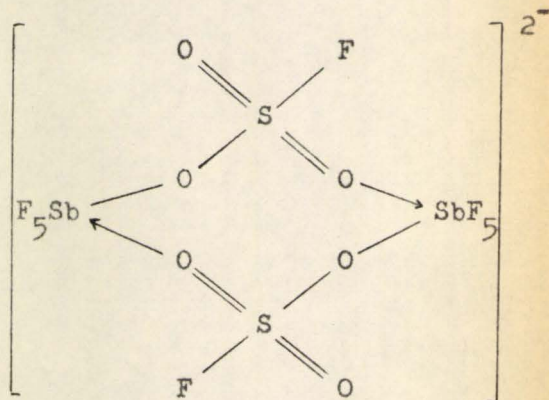
Another possiblility is that the dimeric doubly-charged ion (II)
is formed, to some extent, with increasing concentration of $SbF_5SO_3F^-$. Thus
it may be assumed that non-ideality effects give lower freezing points than
expected while the formation of (II) causes higher freezing points than
expected, and that the two effects cancel each other giving, what appears
to be, ideal behaviour.

Table IX

SOLUTIONS OF SbF_5 AND OF SbF_5-KSO_3F : FREEZING-POINT DEPRESSIONS

T_o (expt. 78) = $-88.999^{\circ}C$

T_o (expt. 80) = $-89.006^{\circ}C$

Expt.	Solute	W_{solute}	W_{HSO_3F}	m^s_{solute}	ΔT
78	SbF_5	0.9430	130.48	0.03334	0.131
78	SbF_5	1.9600	132.00	0.068502	0.270
78	SbF_5	3.0293	133.61	0.10460	0.424
80	SbF_5	2.9032	139.50	0.09601	0.394
80	SbF_5	5.7358	142.72	0.18541	0.746
80	SbF_5	8.4960	145.85	0.26873	1.096
80	KSO_3F	0.6713	145.85	0.03331	1.104
80	KSO_3F	1.8661	145.85	0.092603	1.151
80	KSO_3F	3.7731	145.85	0.18724	1.392
80	KSO_3F	5.6192	145.85	0.27885	1.902
80	KSO_3F	7.3778	145.85	0.36612	2.709
80	KSO_3F	8.5009	145.85	0.42185	3.209

Fig. 26 SOLUTIONS OF SbF_5 AND OF SbF_5 - KSO_3F: FREEZING-POINT DEPRESSIONS
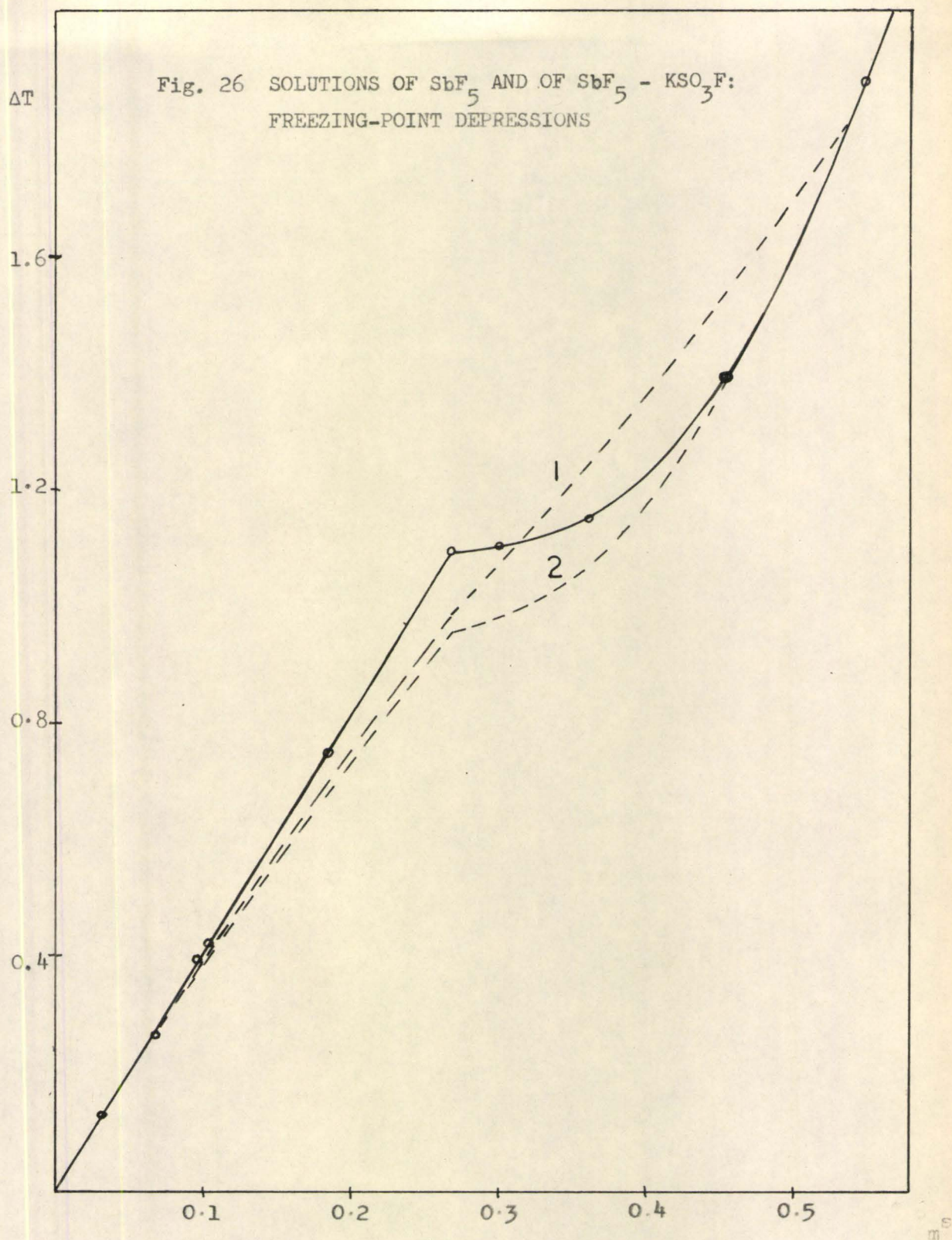
(d) NUCLEAR MAGNETIC RESONANCE SPECTROSCOPY

Several books dealing with nuclear magnetic resonance (n.m.r.) spectroscopy, its theory and application, have been published[66, 67]. Recently Gillespie and White[68] published an article giving a number of examples of the application of n.m.r. spectroscopy to structural and stereochemical problems. No attempt will be made to give a review of the field here; however, since much use is made in this work of the effect of electron-coupled spin-spin interaction, this effect will be described briefly. Also, since the work is concerned with F^{19} n.m.r. spectroscopy only, the discussion will be limited to this nucleus.

F^{19} has a nuclear spin quantum number, I, of 1/2. This nucleus has a magnetic dipole which, when placed in a magnetic field, can take up one of two possible orientations, each orientation being associated with a particular energy of the nuclear magnet. When the nuclear magnet, in a magnetic field, is irradiated with electromagnetic radiation of the correct frequency, ν_o, it is possible to cause transitions between the allowed energy levels. The value of ν_o that will excite the nuclear magnet depends on H_o, the magnetic field at the particular nucleus, and the value of H_o, in turn, depends on the magnitude of the applied field, H_{app}, and the chemical environment of the nucleus. This gives rise to the effect known as chemical shift. Thus nuclei which are not in the same chemical (or electronic) environment will give separate peaks in the n.m.r. spectrum. For example, n.m.r. peaks arising from fluorine nuclei bonded to antimony occur at a much higher field strength than peaks arising from fluorine nuclei bonded to sulphur. The separation between S-F and Sb-F peaks is

generally of the order of 10,000 cycles per second (c/s). Thus the spectra described in this chapter and in chapter VI are conveniently divided into two regions, the region due to fluorine bonded to sulphur, and the region due to fluorine bonded to antimony.

The effect known as electron-coupled spin-spin interaction arises from the fact that nuclear magnets at one position in a molecule may affect the nuclear magnets in another part of the molecule, the effect being transmitted by the bonding electrons. For example, consider a molecule containing two non-equivalent fluorine nuclei, F_1 and F_2. F_1 exists in each of two possible spin states, and each of these states produces a slightly different magnetic field at F_2. Thus F_2 "sees" two slightly different magnetic fields and, therefore, its n.m.r. signal is split into a symmetrical doublet. The doublet is symmetrical since each spin state of F_1 is equally probable. Similarly the signal due to F_1 is split into a doublet by F_2. The separation between components (in this case between the 2 peaks of the doublet) is termed the spin coupling constant J_{12} (the subscript referring to the fact that the coupling is between the fluorines labelled 1 and 2).

Consider, now, the case in which a molecule contains two fluorine atoms, F_2, which are equivalent to each other, and a third fluorine atom, F_1, which is not equivalent to the other two. The signal due to the F_2 fluorine atoms will be split into a doublet by coupling with F_1 for the reasons given above. Each of the fluorines, F_2, can exist in two possible spin states, $+ 1/2$ and $- 1/2$. The four possible ways of combining these spins are shown in Fig. 27.

Figure 27

Spin arrangements of two equivalent fluorine atoms

	Total Spin
↑↑	+ 1
↑↓	0
↓↑	0
↓↓	− 1

Since each combination is equally probable the possible total spins due to the two equivalent nuclei are +1, 0, −1 and the corresponding probabilities are 1, 2, 1. Each possible spin combination produces a slightly different magnetic field at F_1, and consequently the spectrum due to this atom is split into a triplet whose individual peaks have the relative intensities 1:2:1.

Similar arguments show that an equivalent set of three fluorine nuclei gives rise to a quartet for the resonance signal of a neighbouring fluorine nucleus, and the relative intensities of the component signals are 1:3:3:1. Also, an equivalent set of four fluorine nuclei splits the signal of a neighbouring fluorine nucleus into a quintet with components of relative intensities 1:4:6:4:1.

This simple method for deriving the number and relative intensities of the components of a spin-spin multiplet applies only if the coupling constant J is small compared with the chemical shift between the inter-acting nuclei $(v_1 - v_2)$. When the chemical shift is approximately of the same order of magnitude as J_{12}, the relative intensities of the lines are changed, and there may be more lines than would be expected from the simple considerations given above. Spectra of this type show a general enhancement

in intensity toward the centre of the spectrum, and the greater number of signals results from the fact that some of the spin states, which are degenerate when $\nu_1 - \nu_2$ is large, now become split because of mixing of states, induced by the magnetic field. A more complete discussion of spectra of this kind, together with methods of analysis, is given in reference 66.

In describing individual spectra in this work it is convenient to use the following systematic notation. An $A_n X_m$ spectrum refers to the n.m.r. spectrum arising from a molecule containing n atoms of A (where A represents fluorine atoms which are equivalent to each other but not equivalent to the fluorine atoms, X) which are spin-spin coupled with m atoms of X. The chemical shift between A and X ($\nu_A - \nu_X$) is large compared to J_{AX} and the resulting spectrum is predicted by the simple rules given above. An AX_4 spectrum, for example, consists of a doublet and a quintet. Since the signal intensity is proportional to the number of nuclei responsible for the signal, the relative areas of the doublet and quintet are 4:1. The notation $A_n B_m$ is used when the chemical shift ($\nu_A - \nu_B$) is of the same order of magnitude as J_{AB}. The spectra in this case cannot be predicted by the simple rules given above.

An SbF_5 solution in fluorosulphuric acid was prepared in an n.m.r. tube. The tube was weighed, freshly distilled HSO_3F was introduced by means of a capillary dropper, and the tube was weighed again to determine the amount of acid used. Freshly distilled SbF_5 was then added in the same manner. The capillary dropper consisted of a piece of 7 mm. glass tubing drawn at one end to a long, narrow capillary. The tip of this dropper was lowered into the n.m.r. tube until it was about one inch from the bottom,

before the liquid in the dropper was allowed to enter the tube. Thus, exposure of the contents of the dropper to the atmosphere was minimized. The solution studied contained 0.6242 g. of HSO_3F and 0.2298 g. of SbF_5. The concentration was thus 1.698 m^s SbF_5.

The spectra obtained at room temperature showed a broad peak in the region due to fluorine bonded to sulphur, and another very broad peak in the region due to fluorine bonded to antimony. The resonances were presumably broadened by fluorine exchange and therefore spectra were run at low temperatures in order to slow down this exchange.

Fig. 28 is the F^{19} n.m.r. spectrum obtained at $-66.5^{\circ}C$. Chemical shifts are measured in cycles per second from the peak due to the solvent. The spectrum shows the presence of two peaks in the region due to fluorine bonded to sulphur, the large peak being the solvent peak. At higher field, in the region of the spectrum due to fluorine bonded to antimony, two complex resonances appear. One, between $8,000$ and $9,000$ c/s to high field of the solvent peak, appears to be an unsymmetrical triplet and the other, at approximately $10,000$ c/s to high field of the solvent peak, appears to be a sextet. However, when each of these regions was examined in more detail, using a slower sweep-rate, the spectra shown in Figs. 29, 30 and 31 were obtained.

Fig. 29 shows the region of the spectrum due to fluorine bonded to sulphur, at $-66.5^{\circ}C$. In addition to the large solvent peak there are two other peaks of relative intensity approximately 8 to 1. Fig. 30 shows the region of the spectrum between $8,000$ and $8,600$ c/s to high field of the solvent peak $(-82^{\circ}C)$. It is evident that this region of the spectrum consists of two doublets (P and Q) of relative intensity approximately 4

to 1, and not an unsymmetrical triplet. Fig. 31 shows the region of the spectrum around 10,000 c/s to high field of the solvent peak $(-81^{\circ}C)$; it consists of two, overlapping quintets (P and Q), of approximate relative intensity 4 to 1, and not a sextet.

These spectra are consistent with the following description of the behaviour of SbF_5 in fluorosulphuric acid. On solution in HSO_3F, SbF_5 forms the mono-solvated species I, Fig. 32,(having an approximately octahedral arrangement of groups about antimony) which is partially ionized (5.2) to give the anion $SbF_5SO_3F^-$ (II in Fig. 32). For simplicity the negative charge has been omitted in the diagram.

$$HSbF_5SO_3F + HSO_3\textbf{F} \rightleftharpoons SbF_5SO_3F^- + H_2SO_3F^+ \qquad 5.2$$
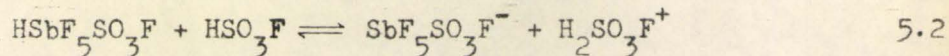
Rapid proton exchange between I and II is very probable and thus only one combined n.m.r. signal would be expected from these species. The fluorines designated F_3 in I and II thus give rise to peak A in Fig. 29, 72 c/s to low field of the solvent peak. Consider now the fluorines bonded to antimony in I and II. Four of these fluorines, designated F_1, are in a plane cis to the fluorosulphate group and thus are equivalent to each other and not equivalent to the fluorine, F_2, which is trans to the fluorosulphate group. These five fluorines, spin-spin coupled with each other,give rise to the large doublet P and the large quintet P shown in Figs. 30 and 31 respectively. This is an AX_4 spectrum. The chemical shift $(\nu_1 - \nu_2)$, measured between the middle of the doublet and the middle of the quintet, is 1662 ± 1 c/s,and the coupling constant J_{12} is 100 ± 1 c/s.

There remains in the spectrum one small peak B in the region due to fluorine bonded to sulphur, and a small doublet Q and quintet Q in the

region due to fluorine bonded to antimony. These can be explained by assuming the formation of the dimeric anion III (Fig. 32) according to equation 5.1. Again the negative charge has been omitted from the diagram for simplicity. Although the diagram shows a coordinate-covalent bond to the SbF_5 group on the left of III, it is assumed that the fluorosulphate group is symmetrically placed between the two SbF_5 groups, and thus the structure with the coordinate-covalent bond to the SbF_5 group on the right of III is equally probable. In other words the two halves of the dimer, on either side of the bridging fluorosulphate group, are identical. The fluorine designated F_6 gives rise to peak B in Fig. 29, 34 c/s to low field of the solvent peak. The remainder of the fluorines (designated F_4 and F_5) are bonded to antimony and give rise to the peaks Q in Figs. 30 and 31 respectively. This is an AX_4 spectrum. In this case $\nu_4 - \nu_5$ is 1415 ± 1 c/s and J_{45} is 100 c/s.

If 20% of the SbF_5 is present as dimer and 80% as monomer, then the relative intensities of the peaks in the spectrum are explained. Table X gives the values of $\nu_A - \nu_X$ and J_{AX} obtained from the spectrum in the region due to fluorine bonded to antimony.

TABLE X

SOLUTIONS OF SbF_5 : ANALYSIS OF N.M.R. SPECTRUM

Peaks considered	Spectrum type	$\nu_A - \nu_X$	J_{AX}	$\dfrac{\nu_A - \nu_X}{J_{AX}}$
P	AX_4	1662	100	16.6
Q	AX_4	1415	100	14.2

Summarizing: Conductivity results show that the behaviour of SbF_5 in fluorosulphuric acid cannot be described satisfactorily in terms of the simple ionization 1.4. However if one assumes, in addition, the existence of an equilibrium involving the formation of dimeric anions, 5.1, the conductivity results can be explained quantitatively. It is not possible to distinguish between ionization of SbF_5 according to 1.4 only, or according to the combination of 1.4 and 5.1, from the freezing-point depression curve of SbF_5. However, the freezing-point depression curve for a titration of SbF_5 with KSO_3F yields a very small slope at low values of $r(KSO_3F/SbF_5)$. Such behaviour cannot be accounted for on the basis of 1.4 alone, but, again, can be accounted for if one assumes the existence of the two equilibria 1.4 and 5.1. The n.m.r. results cannot be interpreted in terms of the existence of monomeric SbF_5 alone, but can be interpreted in terms of the existence of dimeric anions in addition to monomeric species. The n.m.r. results present a slight modification to the picture, however. Since the spectra do not show the existence of unsolvated SbF_5, the behaviour of SbF_5 is best described in terms of 5.2 and 5.1 instead of 1.4 and 5.1. This conclusion could not have been reached from the conductivity evidence or cryoscopic results since these techniques cannot distinguish between 1.4 and 5.2.

Therefore all three experimental techniques described in this chapter agree in showing that in solutions of SbF_5 in fluorosulphuric acid there exist two equilibria,

$$HSbF_5SO_3F + HSO_3F \rightleftharpoons SbF_5SO_3F^- + H_2SO_3F^+ \qquad 5.2$$

$$2SbF_5SO_3F^- + H_2SO_3F^+ \rightleftharpoons (SbF_5)_2SO_3F^- + 2HSO_3F \qquad 5.1$$
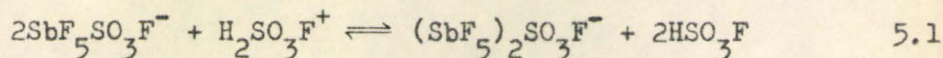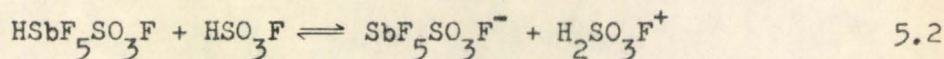
At $25^{\circ}C$ the equilibrium constant for 5.2 is 3.7×10^{-3} and the equilibrium constant for 5.1 is 7.0×10^{2}.

Fig. 28 SOLUTION OF SbF$_5$: F^{19}
N.M.R. SPECTRUM

- 66.5°C
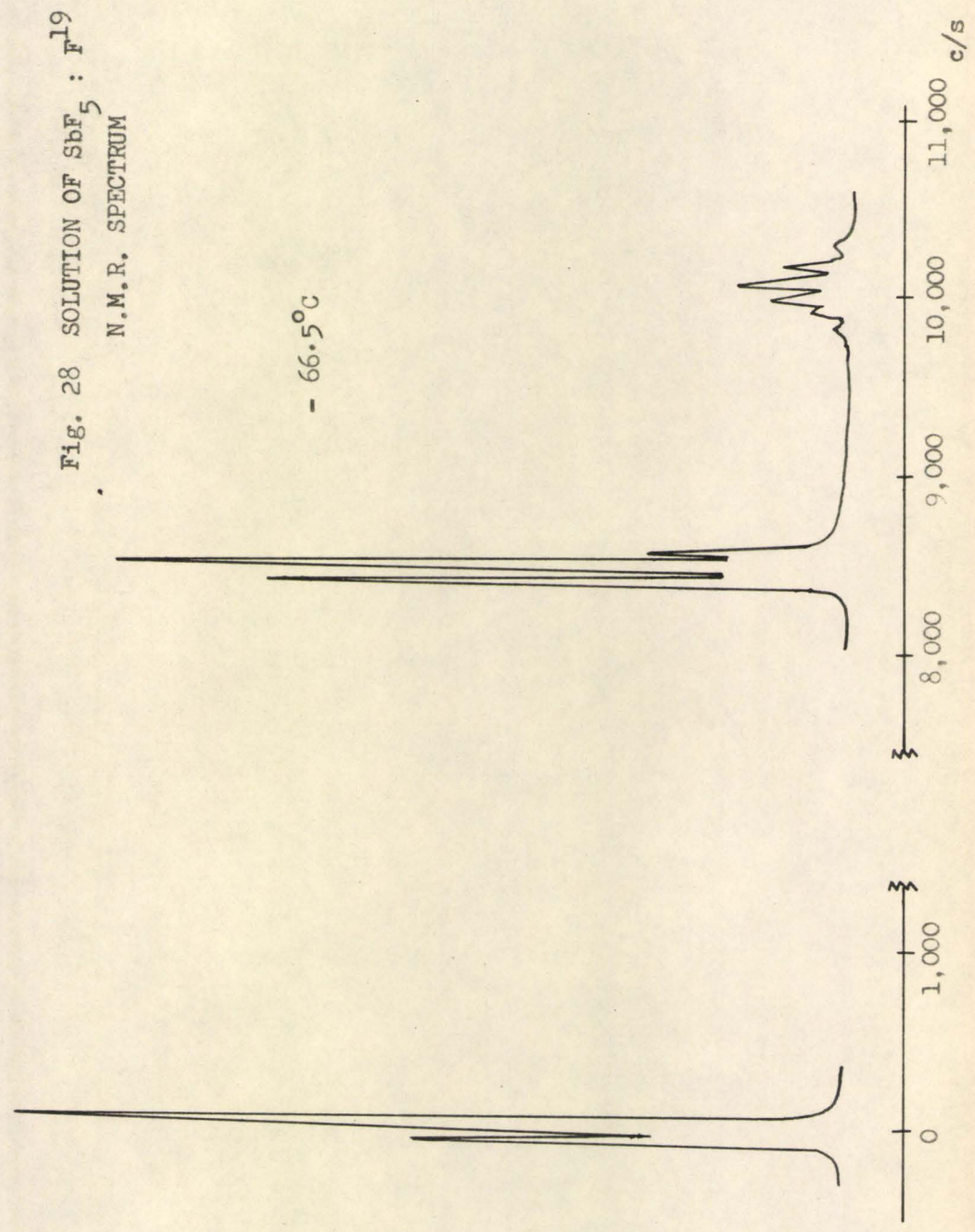
Fig. 29 SOLUTION OF SbF$_5$: F^{19} N.M.R.
SPECTRUM, FLUORINE BONDED TO
SULPHUR REGION

A

B

−66.5°C

−100   −50   0
c/s
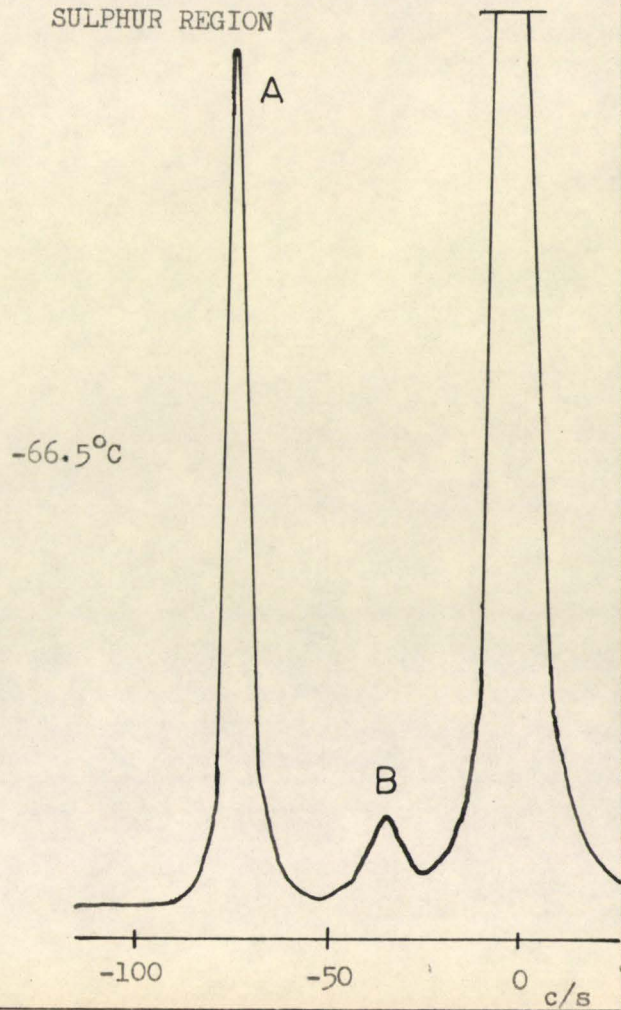
Fig. 30 SOLUTION OF SbF$_5$: F^{19} N.M.R.
SPECTRUM, FLUORINE BONDED TO
ANTIMONY REGION
(8,300 to 8,700 c/s)

P

P

Q

Q

−82°C

8,400   8,600
c/s
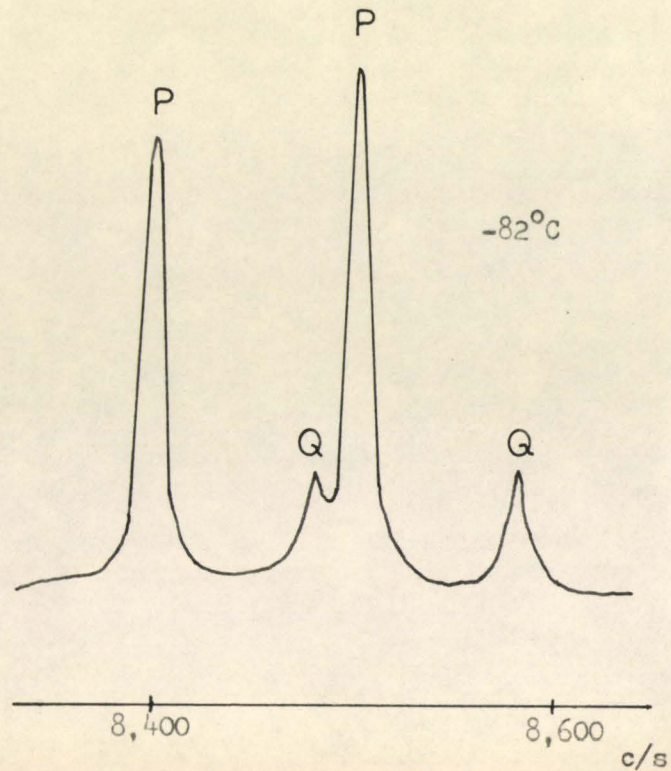
Fig. 31 SOLUTION OF SbF$_5$: F^{19} N.M.R. SPECTRUM, FLUORINE BONDED TO ANTIMONY REGION (9,700 to 10,300 c/s)
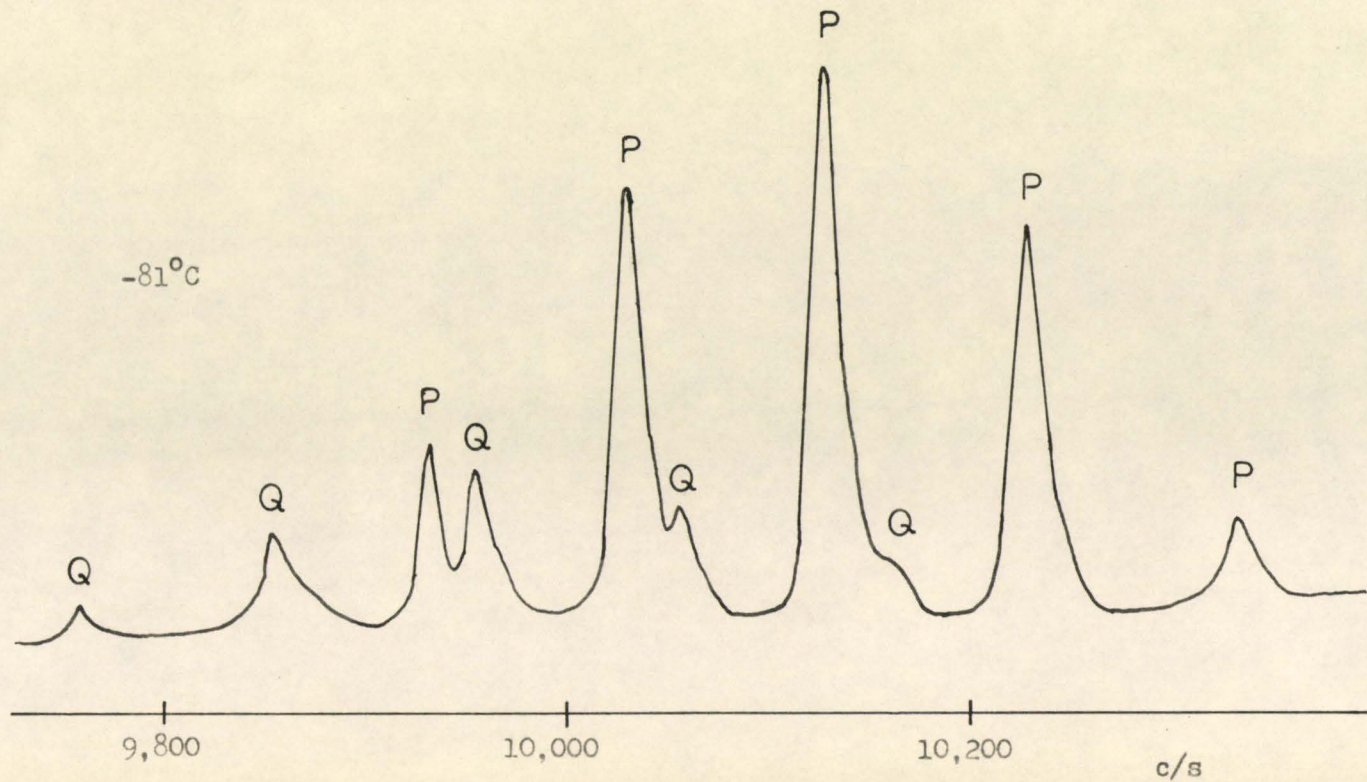
Fig. 32 STRUCTURES OF SPECIES PRESENT IN SOLUTIONS
         OF SbF₅
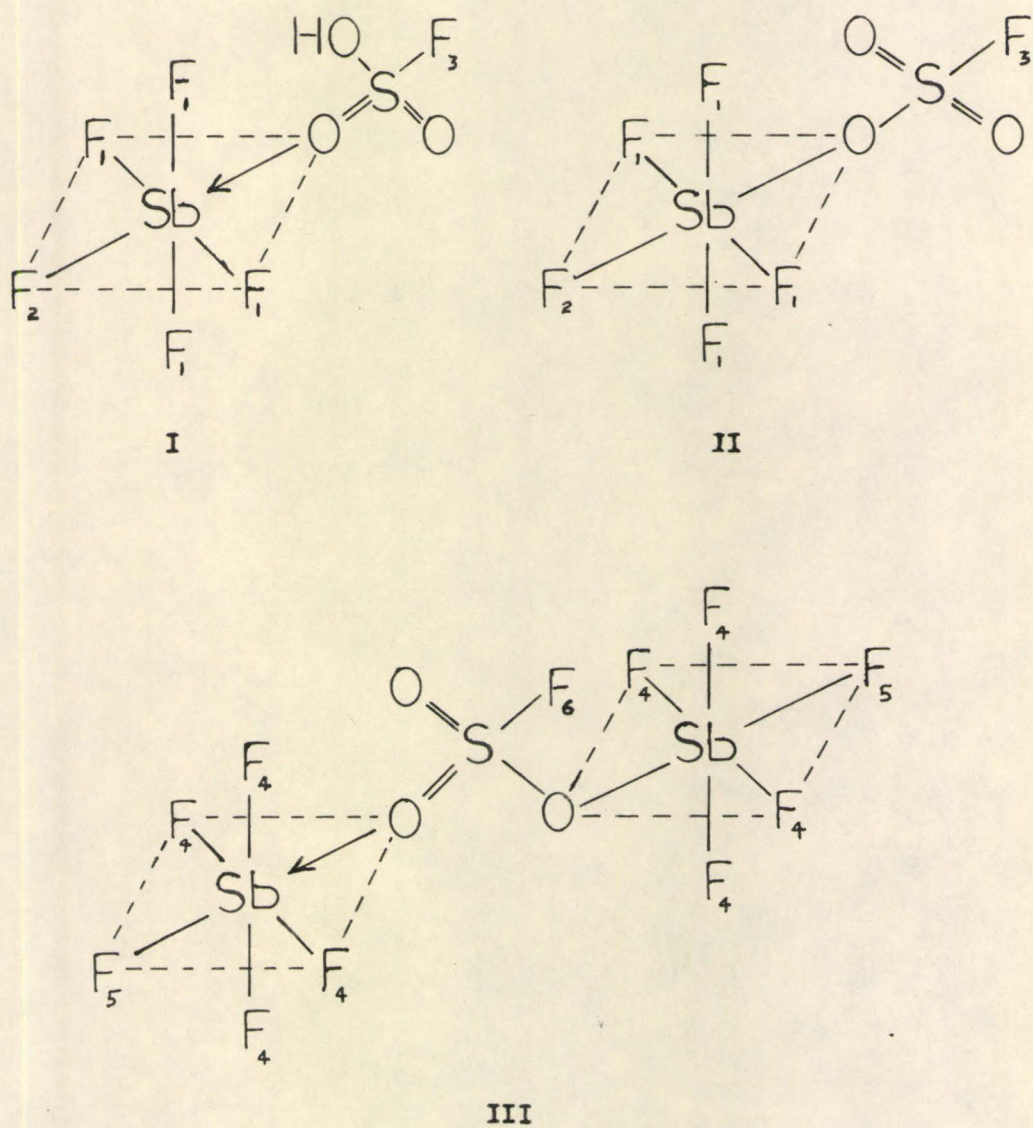
CHAPTER VI

THE REACTION OF ANTIMONY PENTAFLUORIDE WITH
SULPHUR TRIOXIDE IN FLUOROSULPHURIC ACID

(a) CONDUCTIVITY MEASUREMENTS

When sulphur trioxide is added to a solution of antimony penta-
fluoride in fluorosulphuric acid the conductivity of the solution increases.
Since Barr[42] has shown that SO_3 is a non-electrolyte in fluorosulphuric
acid, then it must be concluded that SO_3 reacts with SbF_5 in solution to
form a product which is a stronger acid than SbF_5.

One experiment for studying this reaction was carried out as follows
(experiment 91). A solution of SbF_5 in fluorosulphuric acid was prepared
in a conductivity cell and the conductivity was determined. A few drops
of a concentrated solution of SO_3 in HSO_3F were then added and the con-
ductivity of the resulting solution was determined. Further additions of
SO_3 were made until no change in the conductivity was observed (Curve A,
Fig. 33). SbF_5 was then added in the form of a concentrated solution so
that $r(SO_3/SbF_5)$ was less than 2.0, and the conductivity was again deter-
mined. Further additions of SO_3 were made, until no further change in
conductivity was observed (Curve B, Fig. 33). More SbF_5 was added so that
$r(SO_3/SbF_5)$ was less than 3.0, and the conductivity was recorded. SO_3 was
added again until no change in the conductivity occurred (Curve C, Fig. 33).
The experimental data are given in Table XI.

The reaction between SbF_5 and SO_3 is not instantaneous. After each
addition of SO_3 the resistance decreased with time. Resistance readings

93

were taken at intervals of time for two to three hours. A plot of resistance versus time was extrapolated to the apparent limiting resistance. These extrapolated values are recorded in Table XI. Fig. 34 gives one of these resistance-time plots. The final resistance in this case was taken as 4,975 ohms.

In later experiments, in which only the maximum conductivity value was required for different initial SbF_5 concentrations, sufficient SO_3 was added to give $r(SO_3/SbF_5)$ greater than 3.0 and the solutions were left for at least 8 hours. After this time the resistance readings were constant and it was assumed that true equilibrium had been attained.

The above experimental results can be explained in the following manner. SO_3 reacts with SbF_5 in solution in HSO_3F to form, first, a 1:1 complex, $SbF_5 \cdot SO_3$. This complex is a stronger acid than SbF_5; thus the conductivity of the solution increases. At higher values of $r(SO_3/SbF_5)$ a 2:1 complex, $SbF_5 \cdot 2SO_3$, is formed. This complex is a stronger acid than the 1:1 complex. For $r(SO_3/SbF_5)$ greater than 2.0 a still stronger acid, the 3:1 complex, is formed. At values of $r(SO_3/SbF_5)$ greater than 3.0 no change in the conductivity was observed. It is possible that no species with $r(SO_3/SbF_5)$ greater than 3.0 are formed; it is equally possible that these species are formed, but that their acid strength is not sufficiently greater than the strength of $SbF_5 \cdot 3SO_3$ to cause a noticeable change in the conductivity of the solution.

Throughout the work which will now be described, solutions in which $r(SO_3/SbF_5)$ is greater than 3.0 were studied. It will be assumed that the acid species present in these solutions has the composition $SbF_5 \cdot 3SO_3$. It is recognized that in these solutions, acids of the general

formula $SbF_5 \cdot nSO_3$, where n is greater than 3, may be present. However, since these acids appear to be of the same acid strength as $SbF_5 \cdot 3SO_3$, our conclusions will not be affected by ignoring their presence. N.m.r. investigations (Chapter VI (b)) show that the acid $SbF_5 \cdot 3SO_3$ probably has the structure $SbF_2(SO_3F)_3$ and, therefore, it will be written with this structure throughout the remainder of the thesis.

In order to obtain the conductivity-molality curve for the acid $SbF_2(SO_3F)_3$, the following experiment was carried out. To a solution of SbF_5 in HSO_3F enough SO_3 was added to make $r(SO_3/SbF_5)$ greater than 3·0. The solution was then allowed to stand for several hours until the conductivity no longer changed with time. The experimental results are given in Table XII. A plot of $\mathcal{K}$ versus $m^s_{SbF_5}$ yields the conductivity-molality curve for the acid $SbF_2(SO_3F)_3$. This curve is shown in Fig. 35, together with the conductivity curve for SbF_5, for comparison. If the values for the conductivity of the acid $SbF_2(SO_3F)_3$ obtained from experiment 91 were included in the graph in Fig. 35, they would appear slightly below the curve given there. Experiment 91 involved a number of small additions of SO_3 before a maximum was reached. Presumably, during each addition very small amounts of water were introduced to the cell. The water, which is a base in fluorosulphuric acid, partially neutralized the acid formed, and this resulted in a low value for the conductivity of the acid. In experiments 96 and 129, which gave the results shown in Fig. 35, each point is the result of only one addition of SO_3, and therefore, there was less opportunity for traces of water to enter the cell.

A solution of 0.0854 $m^s_{SbF_2}(SO_3F)_3$ was titrated conductimetrically with KSO_3F and the results are given in Table XIII and Fig. 36. In order

to obtain the theoretical conductivity curves described later in this chapter, it was necessary to obtain the conductivity-molality curve for the ion $SbF_2(SO_3F)_4^-$. This curve is shown in Fig. 23, and was obtained in much the same manner as the curve for $SbF_5SO_3F^-$ in Chapter V(b). In the titration curve (Fig. 36) it was assumed that at $r(KSO_3F/SbF_5)$ equal to 1.0 there exists, in the solution, 0.0854 m $KSbF_2(SO_3F)_4$. Solvolysis of this salt was ignored since the corresponding acid is very strong (Fig. 35). From the graph in Fig. 23 the conductivity due to 0.0854 m K^+ is 20.5×10^{-4} ohm^{-1} cm.$^{-1}$; from the minimum in the conductivity curve (Fig. 36) the conductivity due to 0.0854 m $KSbF_2(SO_3F)_4$ is 32.0×10^{-4} ohm^{-1} cm.$^{-1}$; therefore, the conductivity due to 0.0854 m $SbF_2(SO_3F)_4^-$ is 11.5×10^{-4} ohm^{-1} cm.$^{-1}$. This gives one point on the conductivity curve. Assuming that the conductivity is proportional to the concentration of the ion (cf. Chapter V(b)), the curve in Fig. 23 was obtained.

Simple ionization for the acid $SbF_2(SO_3F)_3$ was considered.

$$SbF_2(SO_3F)_3 + 2HSO_3F \underset{K_3}{\rightleftharpoons} SbF_2(SO_3F)_4^- + H_2SO_3F^+ \qquad 6.1$$
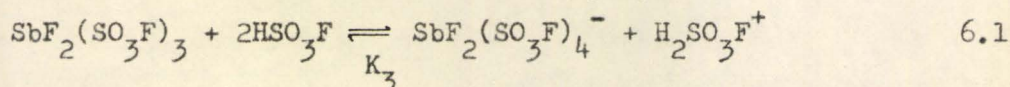
Theoretical titration curves based on ionization according to 6.1 were obtained in the following manner. An arbitrarily chosen value of 0.061 was assigned to K_3, where

$$K_3 = \frac{\left[SbF_2(SO_3F)_4^-\right]\left[H_2SO_3F^+\right]}{\left[SbF_2(SO_3F)_3\right]}$$

For the value $m^s_{SbF_2(SO_3F)_3} = 0.0854$, the concentrations of all the species in 6.1 were determined. This yielded the value 0.048 m for the concentrations of $H_2SO_3F^+$ and $SbF_2(SO_3F)_4^-$ in this solution. The total conductivity of this solution (Fig. 37) is 107×10^{-4} ohm^{-1} cm.$^{-1}$. The conductivity due

to 0.048 m $SbF_2(SO_3F)_4^-$ is 6.0×10^{-4} ohm^{-1} cm.$^{-1}$ (from Fig. 23), and

thus the conductivity due to 0.048 m $H_2SO_3F^+$ is 101×10^{-4} ohm^{-1} cm.$^{-1}$.

This gave one point on the conductivity-molality curve for $H_2SO_3F^+$. It

was assumed that this curve is linear over the concentration range 0 to

0.048 m. Thus the curve designated 1 in Fig. 37 was obtained. The con-

ductivity curve for KSO_3F [42] is linear over this range and, therefore,

the above assumption is probably justified. A theoretical titration curve

for the titration of a 0.0854 m solution of $SbF_2(SO_3F)_3$ with KSO_3F, was

obtained as follows. Assuming ionization according to 6·1 and an equili-

brium constant of 0.061, the concentrations of all the species present in

solution were calculated for different values of $r(KSO_3F/SbF_2(SO_3F)_3)$.

Then, from the conductivity curves for the different species, the con-

ductivity due to each species was obtained, and thus the total conductivity

at each value of r was determined. A plot of this theoretically determined

conductivity versus $r(KSO_3F/SbF_2(SO_3F)_3)$ gave the theoretical titration

curve which appears as the dotted line 3 in Fig. 38. The solid line in

this graph is the experimental curve. There is obviously very poor agree-

ment between the experimental and theoretical curves. The dotted line 1

is the theoretical curve obtained assuming K_3 is ∞, in other words,

assuming the acid is a simple strong acid. The agreement here is even

worse.

The above procedure was repeated: more values were given to

K_3, the conductivity curve for $H_2SO_3F^+$ for each value was determined,

and then a theoretical titration curve was determined. When K_3 was given

the values 0.16, 0.044, and 0.02, the conductivity curves for $H_2SO_3F^+$

labelled 6, 2, and 3 in Fig. 37, were obtained. The corresponding

theoretical titration curves appear as the dotted lines 2, 4, and 5 in Fig. 38. None of the theoretical titration curves appearing in Fig. 38 agrees with the experimental curve.

However, it could possibly be argued that curve 4 (Fig. 38) agrees with experimental values within the error of the approximations involved. This curve was obtained using K_3 for a 0.0854 molal solution of $SbF_2(SO_3F)_3$ equal to 0.044, and using the conductivity curve for $H_2SO_3F^+$, 2, in Fig. 37. Using this conductivity curve it is possible to calculate the value of K_3 at concentrations from 0.02 to 0.12 $m^s_{SbF_2(SO_3F)_3}$. When this calculation was done it was found that the equilibrium constant varied from 0.02 to 0.05. Such a large change in the equilibrium constant would not be expected. Thus it is not possible to reasonably describe the behaviour of $SbF_2(SO_3F)_3$ according to 6.1 alone.

Since SbF_5, in solution in fluorosulphuric acid, exists partially as a fluorosulphate bridged dimer (Chapter V), it is reasonable to assume that $SbF_2(SO_3F)_3$ also exists partially in a dimeric form in solution. The behaviour of this acid will now be discussed in terms of complete ionization according to 6.1 (i.e. $K_3 = \infty$), together with partial dimerization according to 6.2,

$$\left[SbF_2(SO_3F)_3\right]_2 \; SO_3F^- + 2HSO_3F \underset{K_4}{\rightleftharpoons} 2SbF_2(SO_3F)_4^- + H_2SO_3F^+ \qquad 6.2$$
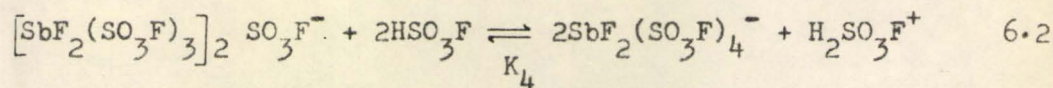
where $K_4 = \dfrac{\left[SbF_2(SO_3F)_4^-\right]^2 \left[H_2SO_3F^+\right]}{\left[SbF_2(SO_3F)_3\right]_2 \; SO_3F^-}$.

This mode of ionization was tested theoretically in exactly the same manner as 6.1 alone was tested. In the calculations the approximation was made

that the mobility of the dimer is equal to that of the monomer. This approximation is adequate, since in all the cases considered, the dimeric anion accounted for only a very small portion of the total conductivity; thus a large variation in the value assumed for its mobility, produced negligible affects on the total calculated conductivity.

When the values 1.0×10^{-3}, 3.0×10^{-3}, 4.0×10^{-3}, and 5.0×10^{-3} were assigned to K_4, the conductivity curves for $H_2SO_3F^+$ (4, 5, 6, and 7 respectively, in Fig. 37) were obtained in the manner outlined previously. As before, using these values for K_4 and the corresponding $H_2SO_3F^+$ conductivity curves, the theoretical titration curves 1, 2, 3, and 4 shown in Fig. 39 were obtained. The agreement between the experimental values and curve 3, Fig. 39, is very good. This curve was obtained with K_4 equal to 4×10^{-3}, and with curve 6 in Fig. 37 as the conductivity curve for $H_2SO_3F^+$. The entire titration curve is shown in Fig. 36. The solid line in this graph is the theoretical curve. The section of the theoretical curve for $r(KSO_3F/SbF_2(SO_3F)_3)$ greater than 1.0 was obtained from the conductivity curve for KSO_3F [42], since in this region the conductivity is due to excess KSO_3F. The conductivity values were obtained from the portion of the KSO_3F conductivity curve which corresponds to the same ionic strength as that in the solutions under consideration.

Thus curve 6, Fig. 37, is taken as the conductivity curve for $H_2SO_3F^+$. This curve, given in Fig. 23, was used in the interpretation of the SbF_5 results.

Assuming complete ionization according to 6.1 and partial dimerization according to 6.2, and using curve 6, Fig. 37, as the conductivity curve for $H_2SO_3F^+$, the value of K_4 was determined for various values of

$m^s_{SbF_2(SO_3F)_3}$ from $0\cdot02$ to $0\cdot12$. The value was found to be $0\cdot004 \pm 0\cdot0002$. We recall that in attempting to describe the behaviour in terms of $6\cdot1$ alone, the equilibrium constant varied considerably over this concentration range.

A more concentrated solution of $SbF_2(SO_3F)_3$ ($0\cdot168$ m^s) was titrated with KSO_3F. The results are given in Table XIV and Fig. 40. Assuming ionization according to $6\cdot1$ and $6\cdot2$ with $K_3 = \infty$ and $K_4 = 4\cdot0 \times 10^{-3}$, then for $m^s_{SbF_2(SO_3F)_3} = 0\cdot168$, the concentration of $H_2SO_3F^+$ was calculated to be $0\cdot1065$ m. The total concentration of the anions present is $0\cdot1065$ m, giving rise to a conductivity of $14\cdot5 \times 10^{-4}$ ohm^{-1} cm.$^{-1}$ due to these ions (Fig. 23). The total conductivity of this solution is $340\cdot6$ ohm^{-1} cm.$^{-1}$ (Table XIV); hence the conductivity due to $H_2SO_3F^+$ is $326\cdot1 \times 10^{-4}$ ohm^{-1} cm.$^{-1}$. This gave another point on the conductivity-molality curve for $H_2SO_3F^+$. This value for the conductivity of $0:1065$ m $H_2SO_3F^+$ is approximately 97% of the value which may be obtained by a linear extrapolation of the conductivity curve, given previously in this section, for low concentrations of this ion. In other words, the slope of the conductivity curve for $H_2SO_3F^+$ decreases slightly at high concentrations. This is reasonable behaviour since the conductivity curve for KSO_3F also shows a slight decrease in slope at high concentrations.

The theoretical titration curve obtained in the usual manner is the solid line in Fig. 40. Again, agreement between the experimental values and the theoretical curve is good.

In conclusion then, the behaviour of the acid $SbF_2(SO_3F)_3$ can best be explained in terms of complete ionization according to $6\cdot1$ together with $6\cdot2$.

$$\left[SbF_2(SO_3F)_3\right]_2 \; SO_3F^- + 2HSO_3F \underset{K_4}{\rightleftharpoons} 2SbF_2(SO_3F)_4^- + H_2SO_3F^+ \qquad 6.2$$
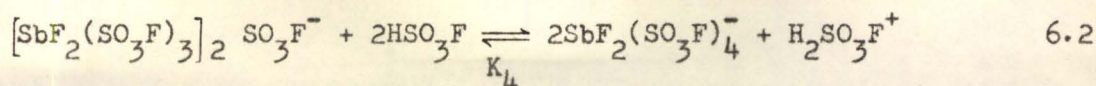
where $K_4 = 0.004 \pm 0.0005$ at $25^{\circ}C$.

Table XI

SOLUTIONS OF $SbF_5 - SO_3$: CONDUCTIVITY AT $25^{\circ}C$

W_{SbF_5}	W_{SO_3}	W_{HSO_3F}	$r(SO_3/SbF_5)$	$10^4 \mathcal{K}$
0.64003	0.0000	113.81	0.0000	25.880
0.64003	0.56026	114.64	2.3698	61.07
0.64003	0.62506	114.74	2.6439	62.85
0.64003	0.80936	115.01	3.4235	65.27
0.64003	0.87383	115.10	3.6962	65.62
0.64003	0.98680	115.27	4.1741	66.05
1.6418	0.98680	117.55	1.6272	104.9
1.6418	1.2166	117.89	2.0061	122.3
1.6418	1.8191	118.78	2.9996	147.0
1.6418	1.9811	119.02	3.2668	149.7
1.6418	2.5208	119.82	4.1567	152.4
1.6418	3.2624	120.92	5.3795	151.2
3.1498	3.2624	123.93	2.8040	237.7
3.1498	3.9375	124.93	3.3843	250.1
3.1498	4.8070	126.22	4.1316	253.2
3.1498	5.8381	127.75	5.0179	253.2

Table XII

SOLUTIONS OF $SbF_2(SO_3F)_3$: CONDUCTIVITY AT 25°C

$\mathcal{K}_o$ (expt. 129) = 1.15×10^{-4} ohm^{-1} cm.$^{-1}$

$\mathcal{K}_o$ (expt. 96) = 1.31×10^{-4} ohm^{-1} cm.$^{-1}$

Expt.	W_{HSO_3F}	W_{SbF_5}	W_{SO_3}	$r(SO_3/SbF_5)$	$m^s_{SbF_5}$	$10^4\mathcal{K}$
129	140.06	1.1703	2.6601	6.1537	0.03855	106.4
129	143.93	2.1380	4.9463	6.2633	0.06853	174.4
129	146.12	2.7041	6.2143	6.2846	0.08538	207.2
96	144.35	5.2439	6.2229	3.2158	0.16759	340.6

Table XIII

SOLUTIONS OF $SbF_2(SO_3F)_3$ - KSO_3F : CONDUCTIVITY AT 25°C

$\mathcal{K}_o$ = 1.15×10^{-4} ohm^{-1} cm.$^{-1}$

W_{SbF_5} = 2.7041 g.

W_{SO_3} = 6.2143 g.

W_{HSO_3F} = 146.12 g.

W_{KSO_3F}	$r(KSO_3F/SbF_2(SO_3F)_3)$	$10^4\mathcal{K}$
0.0000	0.0000	207.2
0.2703	0.1569	172.5
0.5555	0.3224	137.1
0.7485	0.4344	114.1
1.0444	0.6175	80.16
1.5528	0.9013	35.77
1.7756	1.0306	37.54
1.9792	1.1488	52.65
2.2812	1.3240	75.59

Table XIV

SOLUTIONS OF $SbF_2(SO_3F)_3$ – KSO_3F : CONDUCTIVITY AT $25^\circ C$

$\mathcal{K}_o = 1.31 \times 10^{-4}$ ohm^{-1} cm.$^{-1}$

$W_{SbF_5} = 5.2439$ g.

$W_{SO_3} = 6.2229$ g.

$W_{HSO_3F} = 144.35$ g.

W_{KSO_3F}	$r(KSO_3F/SbF_2(SO_3F)_3)$	$10^4 \mathcal{K}$
0.0000	0.00000	340.6
0.1592	0.04762	332.4
0.6668	0.1995	267.0
1.2113	0.3624	211.0
1.5773	0.4719	175.3
2.2536	0.6743	114.8
2.8584	0.8552	68.60
3.1904	0.9546	55.72
3.4257	1.0250	60.92
3.8858	1.1626	95.22
4.3286	1.2951	128.19

Fig.33   SOLUTIONS OF SbF_5-SO_3:
CONDUCTIVITY AT 25°C

Fig.34   SOLUTION OF SbF_5-SO_3:
RESISTANCE VERSUS TIME CURVE (25°C)

Fig.35 SOLUTIONS OF $SbF_2(SO_3F)_3$:
CONDUCTIVITY AT $25^{o}C$

10^4 $\mathcal{K}$

$SbF_2(SO_3F)_3$

SbF_5

0·04   0·08   0·12   0·16   0·20 m^s

Fig.36 SOLUTIONS OF $SbF_2(SO_3F)_3$-KSO_3F:
CONDUCTIVITY AT $25°C$

$10^4 \, \mathcal{K}$

200—

100—

0·2   0·4   0·6   0·8   1·0

$r(KSO_3F/SbF_2(SO_3F)_3)$

Fig.37 CALCULATED CONDUCTIVITY-MOLALITY CURVES FOR $H_2SO_3F^+$ (25°C)

Fig. 38 SOLUTIONS OF $SbF_2(SO_3F)_3$-KSO_3F: THEORETICAL CONDUCTIVITY CURVES FOR IONIZATION OF $SbF_2(SO_3F)_3$ ACCORDING TO 6.1 (25°C)

Fig. 39 SOLUTIONS OF $SbF_2(SO_3F)_3$-KSO_3F:
THEORETICAL CONDUCTIVITY CURVES FOR IONIZATION OF
$SbF_2(SO_3F)_3$ ACCORDING TO 6.1 AND 6.2 (25°C)

$10^4 K$

$r(KSO_3F/SbF_2(SO_3F)_3)$

Fig. 40   SOLUTIONS OF $SbF_2(SO_3F)_3$-KSO_3F: CONDUCTIVITY AT $25^{o}C$

$10^4 \varkappa$

300

200

100

50

0.2   0.4   0.6   0.8   1.0

$r(KSO_3F/SbF_2(SO_3F)_3)$

(b) NUCLEAR MAGNETIC RESONANCE SPECTROSCOPY

The reaction between sulphur trioxide and antimony pentafluoride in fluorosulphuric acid was studied by n.m.r. spectroscopy. Solutions were prepared as outlined in Chapter V (d). The weights of reactants are given in Table XV. The low temperature n.m.r. spectra of the region due to fluorine bonded to antimony are shown in Figs. 41, 42, and 43, and the low temperature n.m.r. spectra of the region due to fluorine bonded to sulphur are shown in Fig. 44. The scale at the bottom of each graph refers to the chemical shift (c/s) from the solvent peak.

Fig. 41 is the F^{19} n.m.r. spectrum, in the region due to fluorine bonded to antimony, for solution 1. This solution contains SO_3 and SbF_5 in the mole ratio 0·67 and therefore, may be considered to contain both SbF_5 and a 1:1 complex $SbF_5 \cdot SO_3$. In the regions marked C and E in Fig. 41, there occur two doublets and two quintets. This portion of the spectrum is essentially the same as that found in solutions of SbF_5 alone. The chemical shifts between doublets and quintets are almost the same and the spin-spin coupling constants are identical, (see Tables X and XVI). Therefore, this part of the spectrum has been assigned to the species arising from the ionization of SbF_5, as described in Chapter V (d).

The remaining peaks of the spectrum, then, must be due to the species produced in solution by the complex $SbF_5 \cdot SO_3$. The spectrum has been analyzed as follows. In region A there are two triplets, R and S. In region D it is assumed there are also two triplets, R and S, but they are not resolved. Peaks R (in regions A and D) form an A_2X_2 spectrum, and peaks S also form an A_2X_2 spectrum. The measured chemical shifts and

112

coupling constants are given in Table XVI. Two singlet peaks, T and U, are found in region B.

The possible structures proposed to explain this spectrum are given in Fig. 45. All structures given in this figure and Figs. 46 and 47, are structures of the anions produced in solution. These anions may exist in equilibrium with their corresponding neutral acids. However, since n.m.r. spectroscopy cannot distinguish between the anion and the acid, for the reason given in Chapter V (d), ignoring the presence of the acid will not affect the interpretation of the n.m.r. spectra. Also, in order to simplify the diagrams, the negative charge on each anion has been omitted, and coordinate-covalent bonds have not been indicated explicitly in the structures of dimers.

There are two possible structures for $SbF_4(SO_3F)_2^-$ and these are shown in Fig. 45, I and II . They are both based on an approximately octahedral arrangement of groups about antimony. In I the fluorosulphate groups are _trans_ to each other, and the fluorines bonded to antimony are all equivalent. These fluorines give rise to one of the peaks (T or U) in section B of Fig. 41. In II, the fluorosulphate groups are _cis_ to each other, and the two fluorines bonded to antimony, which are in the same plane as the fluorosulphate groups, are equivalent to each other but not equivalent to the two fluorines out of this plane. The latter two fluorines are equivalent to each other. Thus, the fluorines bonded to antimony in this species give rise to one of the A_2X_2 spectra in Fig. 41.

Fluorosulphate bridged dimers have been shown to exist in solutions of SbF_5 (Chapter V (d)). Analogous dimers are also present in solutions of $SbF_5 \cdot SO_3$ and two possible structures for these dimers are shown in Fig.

45, III and IV. In III, the fluorines bonded to antimony are all equi-
valent and give rise to the second single peak occurring in region B in
the spectrum in Fig. 41. As in the case of the cis monomer, the fluorines
bonded to antimony in IV produce the other A_2X_2 spectrum in Fig. 41.
Another possible structure for the dimer is V. If this species is present,
the half of the ion which contains the cis fluorosulphate group presumably
gives rise to a fluorine bonded to antimony spectrum which is indistinguish-
able from the spectrum produced by IV; the other half of the ion presumably
gives rise to a spectrum which is indistinguishable from the spectrum due
to III.

Since Fig. 41 is the spectrum produced by a mixture of SbF_5 and
$SbF_5 \cdot SO_3$, the existence of dimers in which the mole ratio of SbF_5/SO_3 is
2/1 is possible. Structures for these species are shown in Fig. 45, VI
and VII. Presumably the spectrum produced by one half of a dimer is
essentially independent of the structure and composition of the other half.
If this is so, then the left-hand sides of VI and VII, which contain no
non-bridging fluorosulphate groups, would be expected to have spectra which
are indistinguishable from the spectrum produced by the ion $(SbF_5)_2SO_3F^-$
(Fig. 32, III). In other words, the spectra arising from the fluorines
occurring in the left-hand side of VI and VII would appear in the high
field doublet and quintet (peaks Q) in Fig. 41. This could explain why,
in this spectrum, these peaks are larger, in comparison to the P peaks,
than was observed in the spectrum for pure SbF_5 in fluorosulphuric acid
(Figs. 30 and 31). Similarly, the right-hand sides of VI and VII, which
contain the non-bridging fluorosulphate groups, would give rise to spectra
indistinguishable from those produced by III and IV respectively (Fig. 45).

In summary, the complex $SbF_5 \cdot SO_3$ is present in solution as monomers and dimers, each giving rise to two triplets and one singlet. It is not possible to tell, however, which singlet or set of triplets is due to the monomeric species, and which is due to the dimeric species.

Fig. 42 is the F^{19} n.m.r. spectrum (fluorine bonded to antimony region) of solution 2 (Table XV). The peaks in the regions of the spectrum designated A, B and D are assigned to the species produced by the complex $SbF_5 \cdot SO_3$. The low field peaks in region A are superimposed on the two peaks, V, which occur in this spectrum. The peaks labelled V and W are new peaks which did not occur in the spectrum in Fig. 41, and are therefore assigned to the species produced in solution by the complex $SbF_5 \cdot 2SO_3$. The analysis of this portion of the spectrum follows. All the peaks, labelled V have been assigned to an AB_2 spectrum with $(\nu_1 - \nu_2)/J_{12} = 7 \cdot 5$. A theoretical AB_2 spectrum, for the value $(\nu_1 - \nu_2)/J_{12}$ equal to $7 \cdot 5$ was calculated from the information given on page 127 of reference 66. This spectrum appears schematically, below the observed spectrum for solution 2, in Fig. 42. The calculation involved determining only the position of the lines (i.e. the chemical shift between them); the intensities shown are only qualitative. The peak W is a singlet peak.

The possible structures proposed to explain this spectrum are shown in Fig. 46. In I the fluorosulphate groups are in one plane and, of the fluorines bonded to antimony, the two which are <u>trans</u> to each other are equivalent, but the third fluorine is not equivalent to these. This species, it is suggested, gives rise to the AB_2 spectrum observed in Fig. 42. In II the fluorosulphate groups are not in the same plane and all the fluorines bonded to antimony are equivalent. This anion produces the

singlet W in Fig. 42.

Thus all of the lines of Fig. 42 have been assigned. The dimeric anion III will, no doubt, also be present in these solutions and should give rise to an AB_2 spectrum. However, it is assumed that this spectrum is superimposed on the spectrum for I. Similarly, the spectrum for IV is superimposed on the spectrum for II. For solutions of SbF_5, the chemical shift between the peaks due to the monomeric and dimeric species is about 90 c/s. For the complex $SbF_5 \cdot SO_3$, the chemical shift between signals due to the monomeric and dimeric anions is so small that, although the low field triplets (region A) which have a separation of about 40 c/s can be resolved, the high field triplets (region D) cannot be resolved. Therefore it is not unexpected that for the complex $SbF_5 \cdot 2SO_3$ the spectra due to the monomeric and dimeric species are not resolvable.

Dimeric anions in which one half of the molecule has a structure analogous to III while the other has a structure analogous to IV, are possible. Also, dimers in which one half of the molecule has only one non-bonded fluorosulphate group while the other half has two non-bonded fluorosulphate groups, are possible. However, as was discussed previously, such species would not give rise to any new peaks in the n.m.r. spectrum of fluorine bonded to antimony.

Fig. 43 is the F^{19} n.m.r. spectrum of the region due to fluorine bonded to antimony for solution 3 (Table XV). In the regions B and D very small peaks, due to small quantities of $SbF_5 \cdot SO_3$, are present. The corresponding peaks expected for this complex in region A are superimposed on peaks arising from other complexes. V and W are recognizable as peaks resulting from the complex $SbF_5 \cdot 2SO_3$. Two new lines appear in this spectrum

and are labelled X and Y. These are singlet peaks and can be ascribed to the species produced in solution by the complex $SbF_5 \cdot 3SO_3$. Possible structures for these species are given in Fig. 47. In I and II the fluorines bonded to antimony are equivalent; consequently each anion gives rise to a single line (X and Y) in the spectrum. Again, the dimeric species III and IV probably produce spectra indistinguishable from those produced by I and II respectively. Mixed dimers may be present, as before, but they will give rise to no new lines.

Fig. 44 shows the low temperature F^{19} n.m.r. spectra of the region due to fluorine bonded to sulphur for all three solutions studied (Table XV). The large peak in all three cases is the solvent peak and from it, the chemical shifts of the other peaks are measured. Since there is a very large number of different fluorines bonded to sulphur (see Figs. 45, 46, and 47), it is difficult to rigorously assign the individual peaks observed in Fig. 44. However, the following tentative assignment is suggested.

Consider the spectrum obtained for solution 1. The peak A (-65 c/s) is assigned to the fluorines bonded to sulphur in I and II, Fig. 32. A small peak B (-32 c/s) is assigned to the fluorine bonded to sulphur in III, Fig. 32. C (-86 c/s) is assigned to the fluorines in the fluoro-sulphate groups of the monomeric anions of the complex $SbF_5 \cdot SO_3$ (I and II, Fig. 45). D (-98 c/s) is due to the fluorines in the non-bridging fluoro-sulphate groups which are cis to the bridging groups in IV, V, and VII, Fig. 45. E (-109 c/s) is assigned to the fluorines in the non-bridging fluorosulphate groups, trans to the bridge in III, V, and VI, Fig. 45. The peaks F, G, and H (at -155 c/s, -174 c/s, and -194 c/s respectively) are presumably due to fluorines in the bridging fluorosulphate groups in the

species III, IV, V, VI, and VII in Fig. 45.

Consider the spectrum obtained for solution 2. The peaks in the region C, D, E are due to fluorines in the non-bridging fluorosulphate groups in the anions shown in Fig. 45. K (-121 c/s) is due to fluorines in the fluorosulphate groups of I and II, Fig. 46. L (-138 c/s) arises from the fluorines in the non-bridging fluorosulphate groups in the species III and IV, Fig. 46. The broad peak M (-172 c/s) is assigned to fluorines in different bridging fluorosulphate groups, present in dimers produced by the complexes $SbF_5 \cdot SO_3$ and $SbF_5 \cdot 2SO_3$.

Consider the spectrum obtained for solution 3. The peak C, D, E (approximately -95 c/s) arises from fluorines in non-bridging fluorosulphate groups present in the species shown in Fig. 45. K (-121 c/s) and L (-138 c/s) are assigned to the same species as before. The peaks at lower field strength from L are presumably due to fluorines in bridging fluorosulphate groups as well as, possibly, fluorines in the non-bridging fluorosulphate groups of anions produced by $SbF_5 \cdot 3SO_3$ (Fig. 47).

The direct reaction between SbF_5 and SO_3 has been used by Hayek and Koller for the preparation of disulphuryl fluoride[69]. In some of the concentrated solutions of SbF_5 and SO_3 in fluorosulphuric acid, small peaks due to trace amounts of $S_2O_5F_2$ and $S_3O_8F_2$ were observed. These peaks were identified by adding small amounts of the pure compounds to the solution, according to the method of Gillespie, Oubridge and Robinson[70]. In solution 2, for example, two small peaks at -360 c/s and -441 c/s from the solvent peak, were identified as arising from $S_2O_5F_2$ and $S_3O_8F_2$ respectively.

In solution 3, $r(SO_3/SbF_5)$ is 3·2. However, the n.m.r. spectrum (Fig. 43) shows the presence, not only of the complex $SbF_5 \cdot 3SO_3$, but also

of a large amount of $SbF_5 \cdot 2SO_3$, and even of some $SbF_5 \cdot SO_3$. Therefore, in this solution, as well as in the other solutions studied in this portion of the work, free SO_3 must be present, presumably in equilibrium with the complexes described in this section.

Table XV

SOLUTIONS OF SbF_5 - SO_3 ; PREPARATIONS FOR N.M.R. STUDIES

Solution	W_{HSO_3F}	W_{SO_3}	W_{SbF_5}	$r(SO_3/SbF_5)$
1	0.5237	0.0935	0.3800	0.666
2	0.4192	0.1514	0.2232	1.837
3	0.5237	0.4514	0.3800	3.216

Table XVI

SOLUTIONS OF SbF_5 - SO_3 : ANALYSIS OF N.M.R. SPECTRA

Spectrum	$r(SO_3/SbF_5)$	Peaks Considered	$\nu_1 - \nu_2$	J_{12}	$\dfrac{\nu_1 - \nu_2}{J_{12}}$	Spectrum Type
Fig. 41	0.67	P	1556	100	15.6	AX_4
		Q	1438	100	14.4	AX_4
		R	1430	126	11.3	A_2X_2
		S	1388	126	11.0	A_2X_2
Fig. 42	1.8	V	948	126	7.5	AB_2

Fig. 41 SOLUTION OF SbF_5-SO_3 IN WHICH $r(SO_3/SbF_5) = 0.67$: F^{19} N.M.R. SPECTRUM, FLUORINE BONDED TO ANTIMONY REGION

$-63°C$
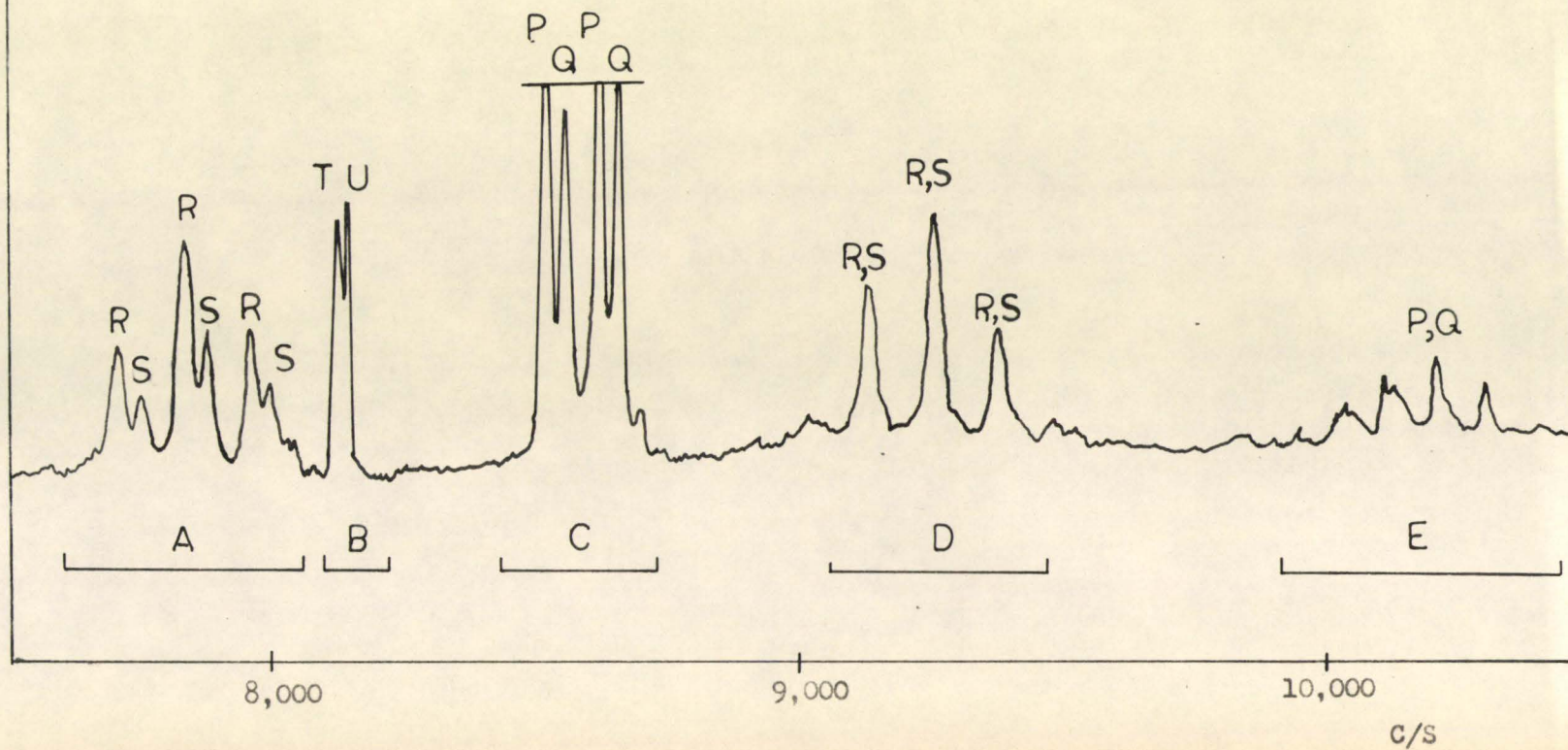
Fig. 42 SOLUTION OF SbF_5-SO_3 IN WHICH $r(SO_3/SbF_5) = 1.8$: F^{19} N.M.R. SPECTRUM, FLUORINE BONDED TO ANTIMONY REGION

$-67°C$

7,500

8,500

9,500

c/s
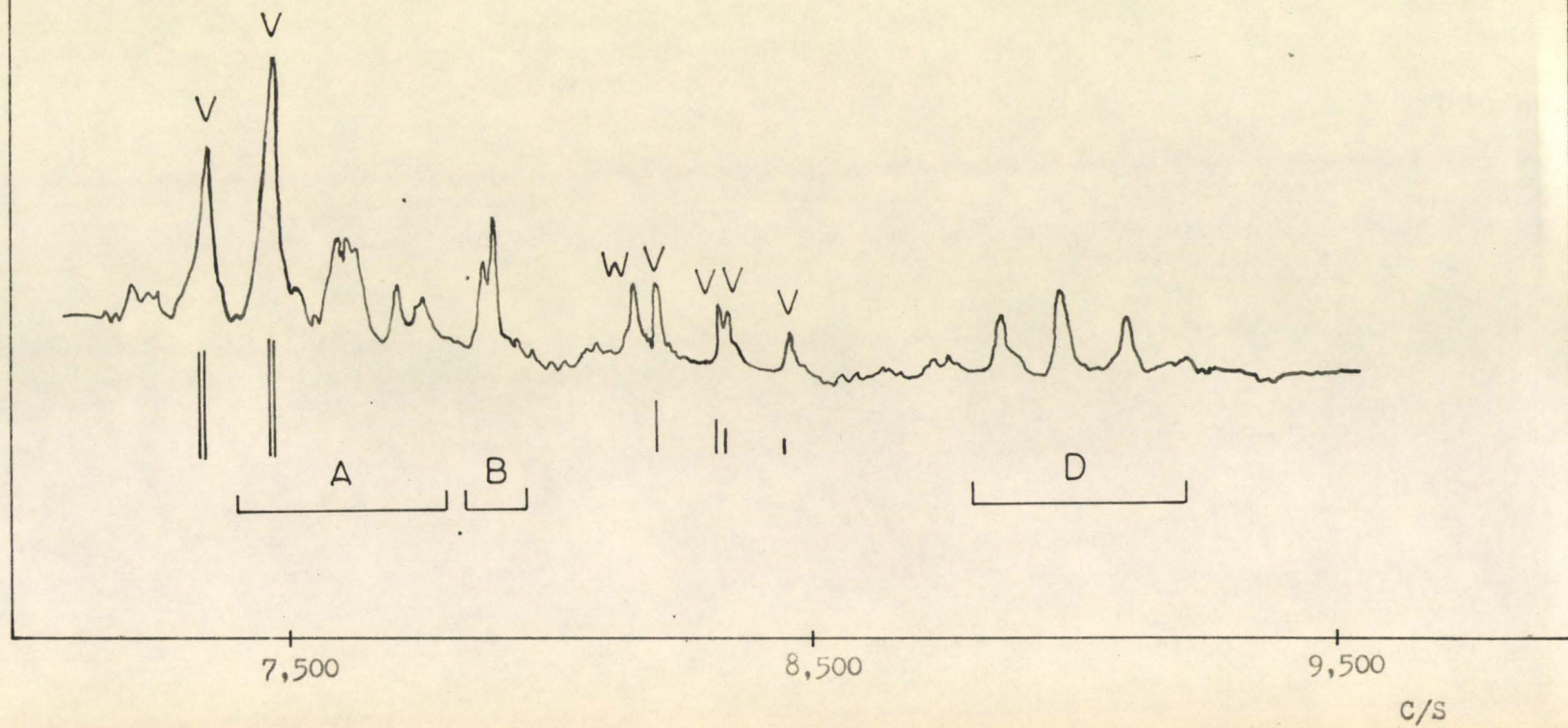
Fig. 43   SOLUTION OF SbF_5-SO_3 IN WHICH $r(SO_3/SbF_5)$ = 3·2: F^{19} N.M.R. SPECTRUM, FLUORINE BONDED TO ANTIMONY REGION

-71°C

7,500

8,500

9,500

c/s
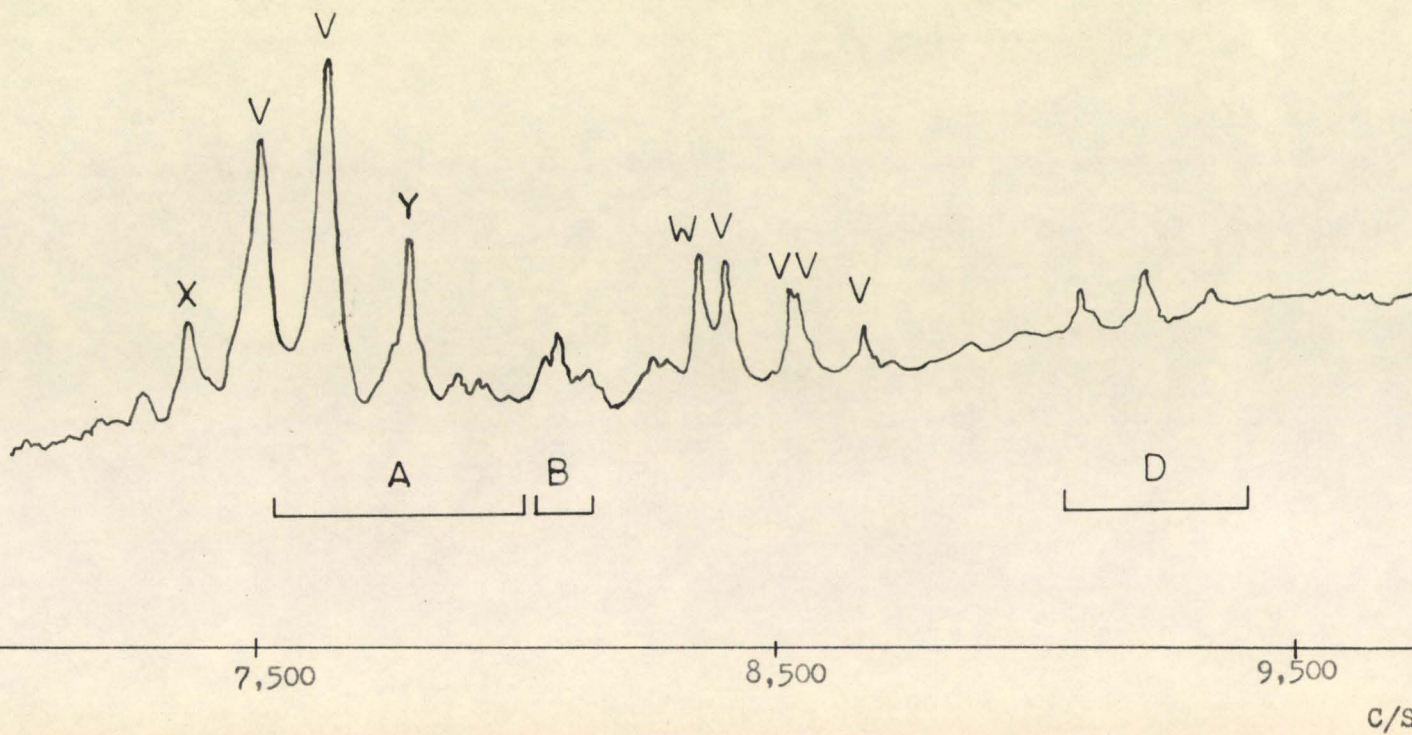
Fig. 44 SOLUTIONS OF SbF$_5$-SO$_3$: F^{19} N.M.R. SPECTRA, FLUORINE BONDED TO SULPHUR REGION
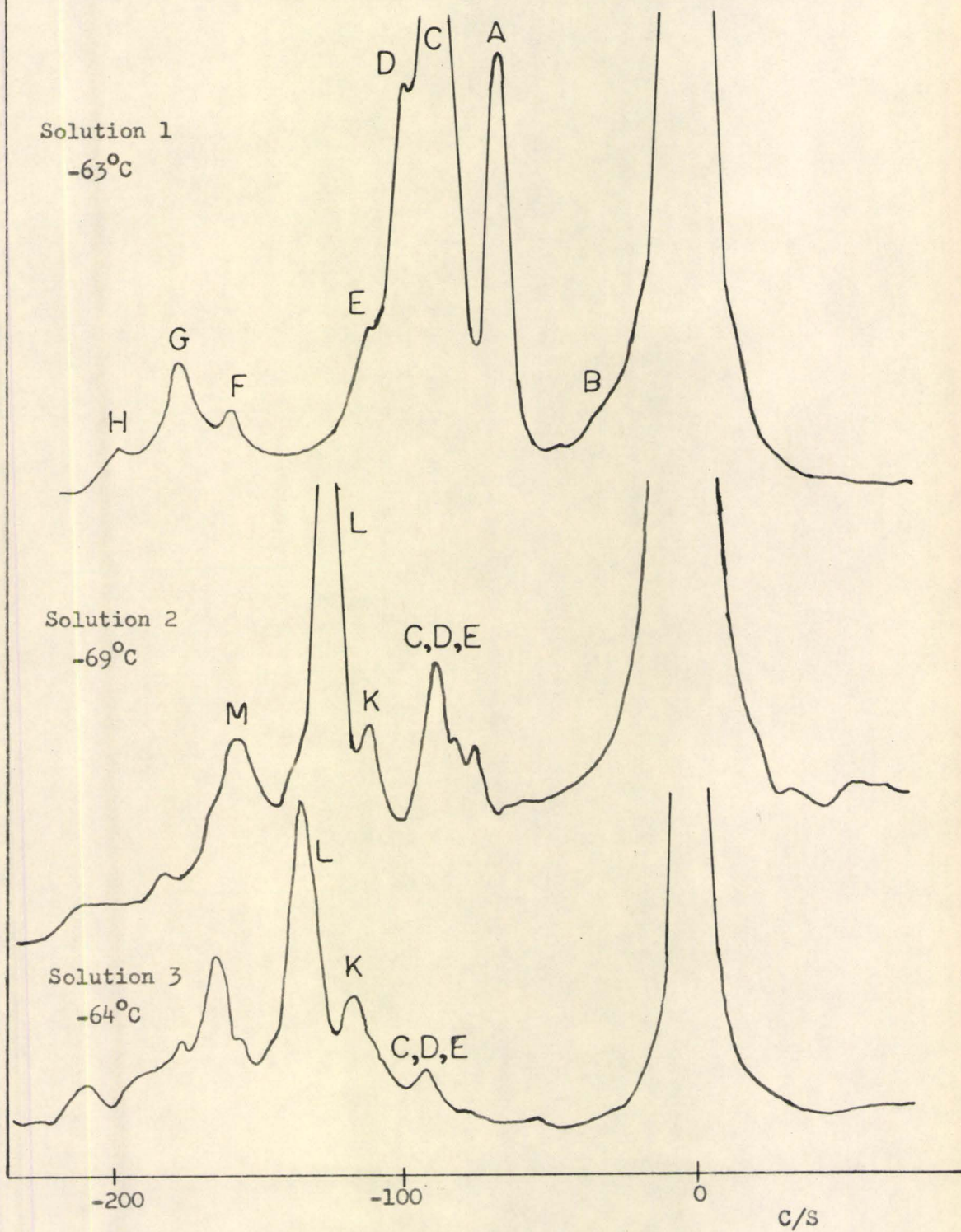
Fig. 45 STRUCTURES OF ANIONS PRESENT IN SOLUTIONS OF $SbF_5 \cdot SO_3$
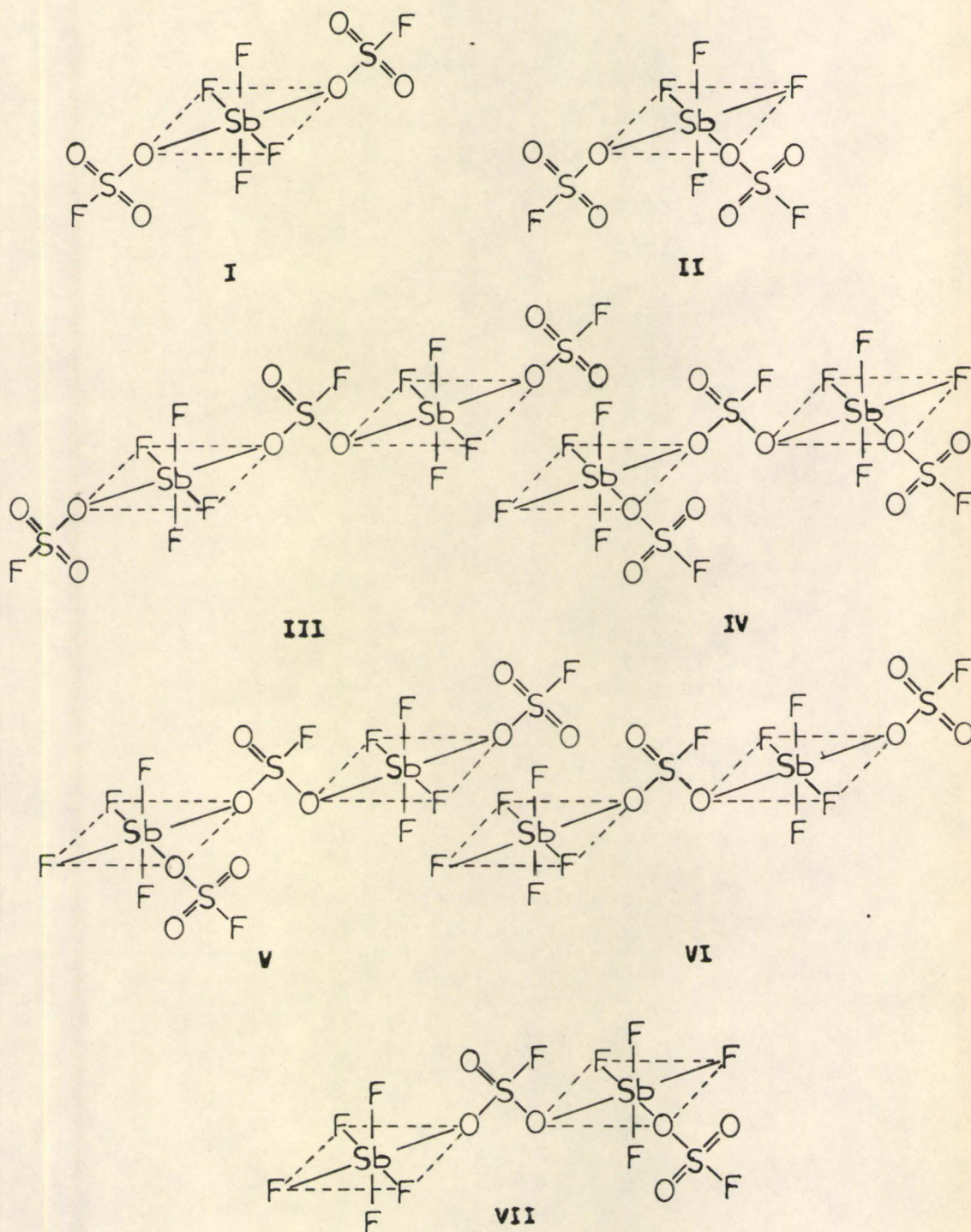
Fig. 46   STRUCTURES OF ANIONS PRESENT IN SOLUTIONS OF $SbF_5 \cdot 2SO_3$
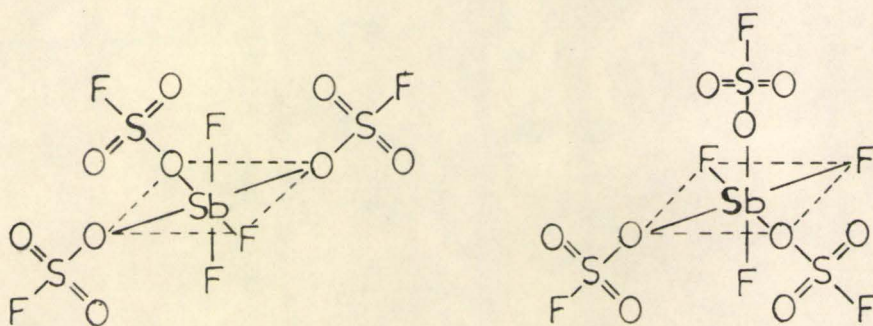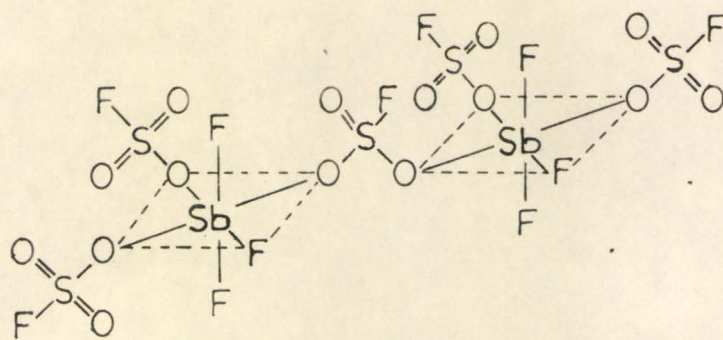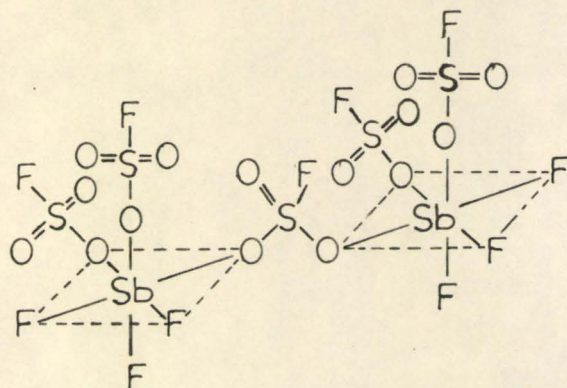
Fig. 47   STRUCTURES OF ANIONS PRESENT IN SOLUTIONS OF $SbF_5 \cdot 3SO_3$
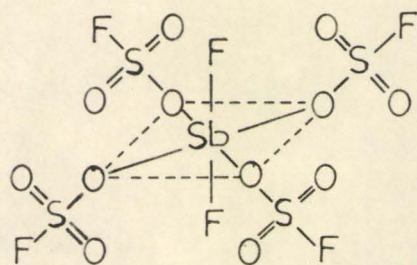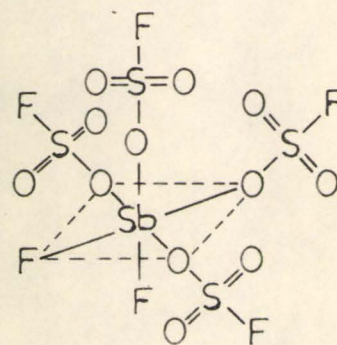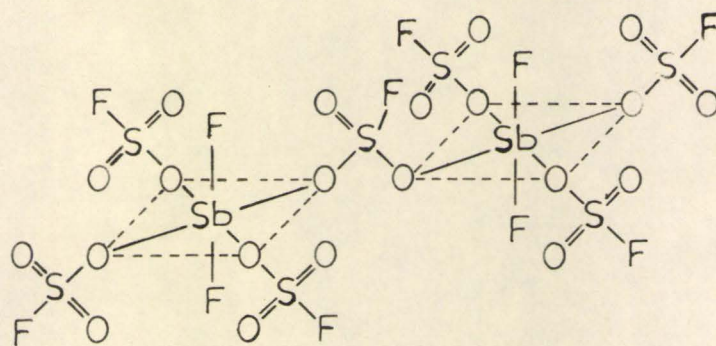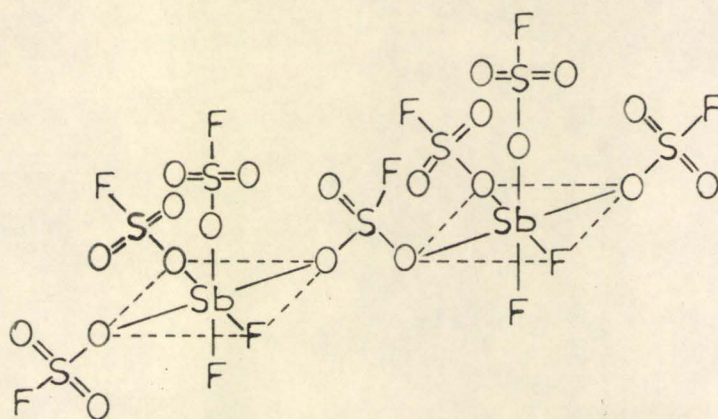
THE REACTION OF BORON TRIFLUORIDE WITH SULPHUR TRIOXIDE

(a) THE REACTION IN FLUOROSULPHURIC ACID

In fluorosulphuric acid, sulphur trioxide dissolves as a non-electrolyte[42]. Boron trifluoride is only slightly soluble in fluoro-sulphuric acid and, also, is essentially a non-electrolyte since a saturated solution raises the conductivity of fluorosulphuric acid from 1.17×10^{-4} to only 1.59×10^{-4} ohm^{-1} cm.$^{-1}$. However, when BF_3 was added to a solution of SO_3 in fluorosulphuric acid, the gas dissolved and the conductivity of the solution increased. Moreover, when a crystal of potassium fluorosulphate was added to the resulting solution, the conductivity decreased. Thus, BF_3 reacts with SO_3 in solution in HSO_3F, and the product is an acid in this system. The following is a description of a series of experiments carried out to investigate the nature of this reaction, and to determine the mode of ionization of the product.

A solution of SO_3 in fluorosulphuric acid was prepared in the conductivity cell designed for use with gases; this cell was described in Chapter III (a) (Fig. 8). Successive amounts of BF_3 were dissolved in the HSO_3F/SO_3 solution and the conductivity was measured after each addition. The results of two experiments are given in Table XVII and Fig. 48. After $r(BF_3/SO_3)$ reached the value of approximately 1/3, further amounts of boron trifluoride would not dissolve. The small increase in weight beyond this composition may be due to a slight excess of BF_3; however, it is largely attributed to the replacement, by BF_3, of the air above the solution in the cell. Thus it was assumed that the reaction involved the formation

128

of a compound of composition $BF_3 \cdot 3SO_3$, which ionizes as an acid in HSO_3F. To obtain the conductivity-molality curve for the acid, the conductivity cell, shown in Fig. 7, was fitted with the bubbler, shown in Fig. 49 (a). This bubbler was attached via the ground glass joint on one of the flasks of the cell. After each addition of SO_3 to the cell, (additions were made as concentrated solutions of SO_3 in HSO_3F) BF_3 was bubbled through the solution until it was saturated. The results are given in Table XVIII and Fig. 50. The values of $m^s_{BF_3 \cdot 3SO_3}$ were taken as $1/3\ m^s_{SO_3}$. By comparing the resulting curve with the conductivity curve for $H_2SO_3F^+$ (curve A, Fig. 50), it is clear that the acid formed is a weak acid.

If the values for the conductivity of the acid $BF_3 \cdot 3SO_3$, obtained in experiments 10 and 13, (i.e. the maximum conductivities shown in Fig. 48) were included in the graph in Fig. 50, they would appear below the curve. An analogous situation was described in Chapter VI (a). Experiments 10 and 13 involved several additions of BF_3 before the maximum was reached. Presumably, traces of water were introduced into the cell during each addition; this resulted in partial neutralization of the acid. Although this should not alter the significance of the conductivity levelling off at $r(BF_3/SO_3) = 1/3$, it would give a low value for the conductivity of the acid. In the experiment which gave the results shown in Fig. 50, only one addition of BF_3 was made after each addition of SO_3. In this case then, there was less opportunity for traces of water to enter the cell.

When excess SO_3 was added to a solution of $BF_3 \cdot 3SO_3$, the conductivity increased. The results of this experiment are given in Table XIX and Fig. 51. A solution of $0 \cdot 3204$ m SO_3 was saturated with BF_3 and the resulting conductivity is the first result in Table XIX and the first

point on the graph in Fig. 51. Thereafter, SO_3 additions were made with-out further additions of BF_3. In Table XIX the column under $m_{SO_3}^s$ refers to the total molality of SO_3; in Fig. 51 the abscissa also refers to the total molality of SO_3. Thus the addition of excess SO_3 appears to lead to the formation of stronger acids than $BF_3 \cdot 3SO_3$.

For freezing-point measurements on this system, the cryoscope head was redesigned (Fig. 49 (b)). A bubbler was incorporated into the apparatus. The sintered glass end of the bubbler was immersed in the acid throughout a run.

The fluorosulphuric acid in the cryoscope was saturated with BF_3 at a temperature below $15^{\circ}C$. The solution was allowed to warm to $15^{\circ}C$; the liquid air bath was then placed around the cryoscope and the freezing point of the solution was determined. Freezing-point depressions were measured from the freezing point of the saturated solution. Following each addition of SO_3 to the cryoscope, the solution was saturated with BF_3 by the procedure described above. By allowing the solutions, saturated at a low temperature, to warm to the same temperature before freezing, it was hoped that the concentration of excess BF_3 would be the same in each case. Two determinations on the same solution, saturated by this pro-cedure, did, in fact, yield the same freezing point.

The cooling curves obtained in this experiment were difficult to extrapolate since a long period of time (20 minutes after seeding) was required before equilibrium was reached. This is possibly explained by the fact that, in order to immerse the bubbler in the solution, a rather large amount of acid was used in this experiment, and therefore, stirring may not have been adequate. As a result there is a larger than normal

scatter in the experimental points ($\pm$ 0.04°C). The dotted line in Fig. 52 is the theoretical curve for ν = 3. Thus the acid $BF_3 \cdot 3SO_3$ dissociates at -90°C to give approximately three particles in solution. The experimental data are listed in Table XX, and plotted in Fig. 52.

In order to explain the above experimental results it is suggested that the following equilibria exist in these solutions.

$$
BF_3 + 3SO_3 \underset{7.1}{\rightleftharpoons}
\begin{matrix} OSO_2F \\ | \\ B - F \\ | \\ OSO_2F \end{matrix}
+ SO_3 \underset{7.2}{\rightleftharpoons}
\begin{matrix} O \\ \| \\ S = O \longrightarrow \\ \| \\ O \end{matrix}
\begin{matrix} OSO_2F \\ | \\ B - F \\ | \\ OSO_2F \end{matrix}
$$

$$
\qquad\qquad\qquad\qquad\quad A \qquad\qquad\qquad\qquad\qquad B
$$
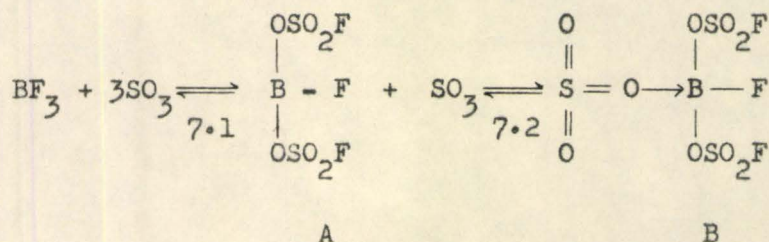
A is a strong acid, dissociating as follows:

$$
\begin{matrix} OSO_2F \\ | \\ B - F \\ | \\ OSO_2F \end{matrix}
+ 2HSO_3F \rightleftharpoons
\left[\begin{matrix} OSO_2F \\ | \\ FSO_2O - B - F \\ | \\ OSO_2F \end{matrix} \right]^{-}
+ H_2SO_3F^{+} \qquad 7.3
$$

$$
\qquad A \qquad\qquad\qquad\qquad\qquad\qquad C
$$
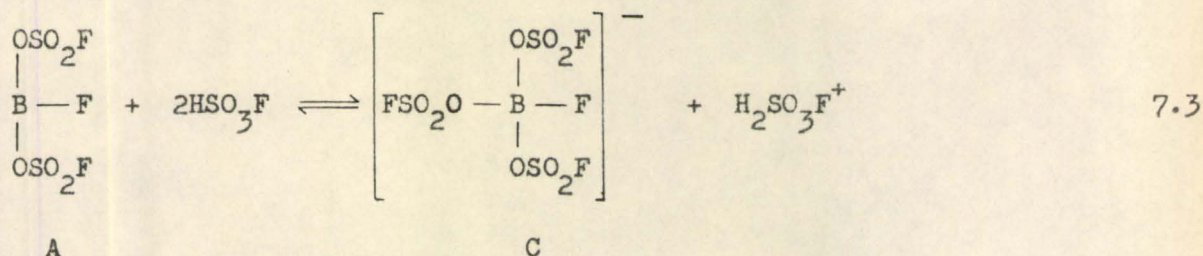
B is a weak acid, dissociating as follows:

$$
\begin{matrix} O \\ \| \\ S = O \longrightarrow \\ \| \\ O \end{matrix}
\begin{matrix} OSO_2F \\ | \\ B - F \\ | \\ OSO_2F \end{matrix}
+ 2HSO_3F \rightleftharpoons
\left[\begin{matrix} OSO_2F \\ | \\ FS_2O_5O - B - F \\ | \\ OSO_2F \end{matrix} \right]^{-}
+ H_2SO_3F^{+} \qquad 7.4
$$

$$
\quad B \qquad\qquad\qquad\qquad\qquad\qquad\qquad D
$$
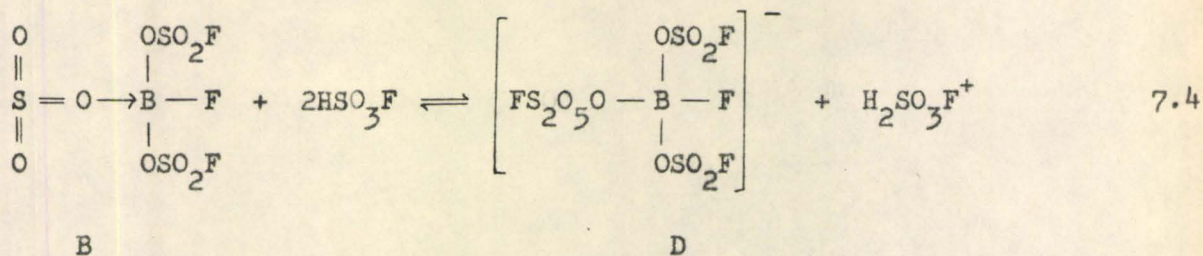
The observation that the conductivity reaches a maximum value when $r(BF_3/SO_3)$ = 1/3 is explained as follows. In a solution saturated with BF_3 at 25°C, there is very little free BF_3, SO_3, or A, and most of the boron is present as B and its corresponding anion D. The small solubility of BF_3 in HSO_3F plays an important role in determining the final equilibrium

position of reactions 7.1 to 7.4. If one could increase the concentration of BF_3 in these solutions, it would be expected that all of the complex $BF_3 \cdot 3SO_3$ would be converted into the complex $BF_3 \cdot 2SO_3$, A. However, it appears that when $r(BF_3/SO_3)$ reaches the value 1/3, the equilibrium amount of BF_3 is sufficient to saturate the solution, and no further increase in the concentration of dissolved BF_3 is possible.

Since the reactions involved in 7.2 result in merely the addition and loss of a weakly bonded SO_3 molecule, it may be assumed that both forward and reverse reactions are fast, and therefore, anything which changes the concentration of SO_3 in these solutions will have an immediate effect on the position of this equilibrium. Equilibrium 7.1, on the other hand, will not be affected to the same extent, for the following reason. When there is a large concentration of free SO_3 in solution, and BF_3 is added, the rate of the forward reaction (formation of fluorosulphate groups) is moderately fast. The rate of the reverse reaction, involving the breaking up of fluorosulphate groups, is, however, very slow. When $r(BF_3/SO_3)$ approaches 1/3, the concentration of free SO_3 is so small that the rate of the forward reaction now equals the rate of the reverse reaction, and equilibrium is established.

A further equilibrium will exist in these solutions[42, 71].

$$HSO_3F + SO_3 \rightleftharpoons HS_2O_6F \qquad\qquad 7.5$$
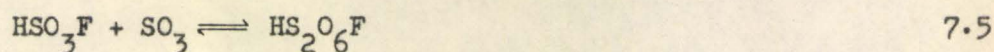
If it is assumed that at low temperatures the stability of HS_2O_6F increases, and, in general, the formation of fluorosulphate groups is favoured, then equilibria 7.1 and 7.2 will be affected by a decrease in temperature as follows. As the temperature is lowered, 7.5 will shift to the right,

decreasing the concentration of free SO_3 in the solution, and thus causing

7.2 to shift to the left. Although, by similar reasoning, one might

expect 7.1 to shift to the left (due to removal of free SO_3), this equili-

brium involves the formation of fluorosulphate groups (in going from

left to right) and thus it will presumably shift to the right. Therefore

at $-90^{\circ}C$ (the temperature of freezing-point measurements) the solution

will contain C (the ionized form of A), $H_2SO_3F^+$, and HS_2O_6F. Hence, three

particles are present, in agreement with the cryoscopic results.

Adding excess SO_3 increases the acid strength of these solutions

(Table XIX and Fig. 51). This is possibly the result of the formation of

E, a compound which is a stronger acid than B.

$$
\begin{array}{cccccc}
O & OSO_2F & & O & OS_2O_5F & \\
\| & | & & \| & | & \\
S = O \rightarrow B - F & + & SO_3 \rightleftharpoons & S = O \rightarrow B - F & & 7.6 \\
\| & | & & \| & | & \\
O & OSO_2F & & O & OSO_3F & \\
\\
\quad B & & & \quad E &
\end{array}
$$
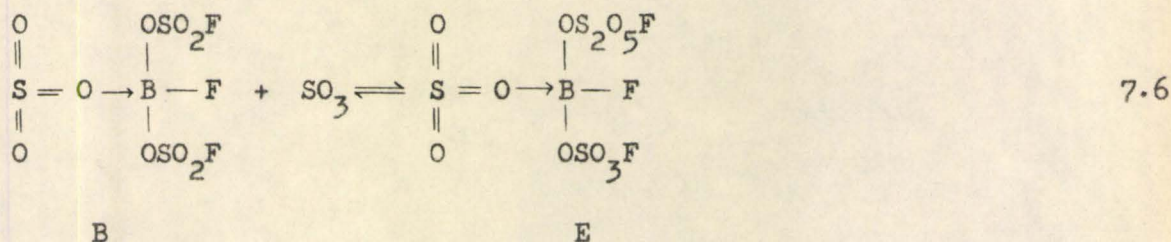
A further experiment involved a conductimetric study of the addition

of potassium fluoroborate to a solution of sulphur trioxide in fluoro-

sulphuric acid. It was first necessary to determine the behaviour of KBF_4

when added to HSO_3F alone. On solution in fluorosulphuric acid, KBF_4 decom-

poses to give BF_3, recognizable by the fumes produced. The conductivity

of the resulting solution is identical to that produced by potassium flu-

oride solutions (Table XXI and Fig. 53, curve 1). Thus KBF_4 dissociates

as follows:

$$KBF_4 \longrightarrow KF + BF_3 \qquad\qquad 7.7$$
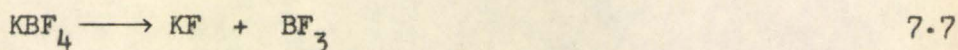
Since potassium fluoride solutions had not been previously studied,

it was necessary to obtain the conductivity curve for KF in this work.

The results are given in Table XXII and Fig. 53, curve 1. The dotted line below curve 1 is the conductivity curve for KSO_3F [42]. Potassium fluoride dissolves in fluorosulphuric acid to give KSO_3F and HF; therefore, the increased conductivity of these solutions over that of KSO_3F solutions alone must be the result of basic behaviour by HF.

According to 7.7, the addition of KBF_4 to an HSO_3F/SO_3 solution is equivalent to the addition of KF and BF_3 in equal amounts. The results of this experiment are given in Table XXIII and a plot of $\mathcal{K}$ versus $m_{KBF_4}^s$ is given in Fig. 53 (curve 2). Each mole of KF added will remove one mole of SO_3 by the reactions,

$$KF + HSO_3F \longrightarrow HF + KSO_3F \qquad\qquad 7.8$$

$$HF + SO_3 \longrightarrow HSO_3F \qquad\qquad 7.9$$
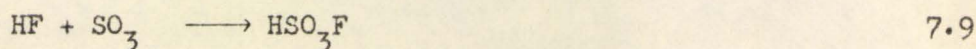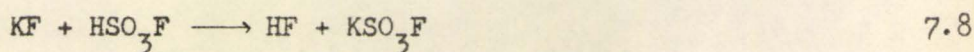
At X (curve 2, Fig. 53), $r(KBF_4/SO_3) = 1/4$, and presumably the salt F,

$$K^+ \begin{bmatrix} & OSO_2F & \\ & | & \\ FS_2O_5O - B - F \\ & | & \\ & OSO_2F & \end{bmatrix}^-$$

F
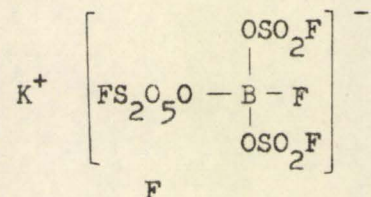
and its solvolysis product B, are present in solution in equilibrium with free SO_3 and A, according to 7.2. Further additions of KBF_4 will result in the removal of SO_3 by 7.8 and 7.9, causing a net conversion of B into A by the displacement of 7.2 to the left. One might expect further additions of KBF_4 to shift equilibrium 7.1 to the left; however, as mentioned previously, this reaction (the decomposition of fluorosulphate groups to fluoride and SO_3) is very slow, and does not occur to an appreciable extent during the measurements. Hence, once all of the boron has been converted to A, further additions of KBF_4 would be expected to give the

conductivity curve for KBF_4. Because A is a strong acid it will exist in these solutions as the stable salt G.

$$K^+ \quad \begin{bmatrix} & OSO_2F & \\ & | & \\ FSO_2O - & B & - F \\ & | & \\ & OSO_2F & \end{bmatrix}^-$$

G
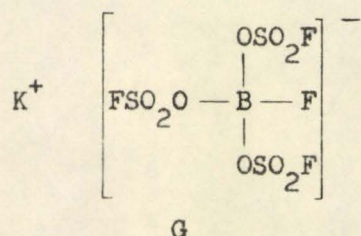
Since G contains KBF_4 and SO_3 in the mole ratio 1/3, one would expect a break to occur in the conductivity curve at $r(KBF_4/SO_3) = 1/3$. The experimental curve agrees with this very well since at Y on curve 2, Fig. 53, $r(KBF_4/SO_3) = 1/3$.

An n.m.r. investigation of the reaction between BF_3 and SO_3 in fluorosulphuric acid was attempted. However, in the concentrated solutions required for this study, a further complication was encountered. In some of the solutions studied, peaks due to small amounts of polysulphuryl fluorides, $S_2O_5F_2$ and $S_3O_8F_2$, were observed. These compounds were formed, presumably, by the decomposition of $BF_3 \cdot 3SO_3$. The peak due to $S_3O_8F_2$ was identified by the addition of a small amount of the pure compound to the sample tube. The line, produced by $S_2O_5F_2$, was identified by its chemical shift from the $S_3O_8F_2$ peak[70]. It is not surprising to find these products in the most concentrated solutions studied. The compound $S_3O_8F_2$ has been prepared by Lehmann and Kolditz[72], by passing BF_3 gas into liquid SO_3 and decomposing the white solid obtained, with 70% sulphuric acid. Gillespie, Oubridge and Robinson[70] have shown that this reaction also produces $S_2O_5F_2$.

Since these polysulphuryl fluoride peaks were observed in a solution in which $r(SO_3/HSO_3F) = 1/2.7$, but were not observed in a solution

in which $r(SO_3/HSO_3F) = 1/5.2$, it is reasonable to assume that poly-sulphuryl fluorides are not produced to any significant extent in solutions studied by cryoscopy and conductivity, where $r(SO_3/HSO_3F) = 1/100$.

A solution in which $r(SO_3/HSO_3F) = 1/1.12$ was saturated with BF_3 and its F^{19} n.m.r. spectrum was obtained at various temperatures, from room temperature to $-89^{o}C$. The spectra obtained at room temperature and $-37^{o}C$ are shown in Fig. 54. The scale in this figure refers to the chemical shift (c/s) from the solvent peak. The spectrum obtained at $-77^{o}C$ was essentially the same as that obtained at $-37^{o}C$. Identified as above, P and Q are due to $S_3O_8F_2$ and $S_2O_5F_2$ respectively. R is due to the fluorines in the solvent and, presumably, also to the fluorines in the fluorosulphate groups bonded to boron. At higher field another broad peak, S, occurs at room temperature. This peak splits into two peaks, T and U, at $-37^{o}C$.

A solution of 4.12 g. SO_3 in 21.32 g. HSO_3F was saturated with BF_3, and its low temperature ($-70^{o}C$), F^{19} n.m.r. spectrum (high field region) is shown in Fig. 55 (a). Chemical shifts are measured relative to the solvent peak. Peaks V and W correspond respectively to T and U, in Fig. 54. When 3.74 g. of SO_3 were added to this solution (with no further addition of BF_3), the spectrum, shown in Fig. 55 (b), was obtained. Since V disappears on addition of excess SO_3, this peak is tentatively assigned to BF_3. Thus T (Fig. 54) is also assigned to BF_3. Peak U, Fig. 54 (and also W, Fig. 55) is assigned to fluorines bonded to boron in the complexes $BF_3 \cdot 2SO_3$ and $BF_3 \cdot 3SO_3$.

It is extremely difficult to interpret these spectra quantitatively, in terms of the equilibria given earlier in this chapter. One cannot predict what effect the large difference in concentrations between the con-

ductivity and n.m.r. experiments will have on these equilibria. Also, in the solutions studied by n.m.r. the formation of polysulphuryl fluorides is a further complication.

Nevertheless, making the assumption that, in the production of polysulphuryl fluorides, the other products (probably containing -B-O-B- groups) do not contain fluorine, and therefore, do not affect the spectrum, an explanation of the relative areas of the peaks observed (Fig. 54) can be made in terms of the species produced by 7.1 and 7.2. The solution contains 1.12 moles of HSO_3F and 1 mole of SO_3. Consider the room temperature spectrum. In order to explain the relative areas of the peaks it is assumed that 0.21 moles of SO_3 were used in the formation of $S_3O_8F_2$ and 0.09 moles were used in the formation of $S_2O_5F_2$. The remainder of the SO_3 is assumed to be present in B (see equation 7.2). The area of peak S, assigned to fluorine bonded to boron, indicates that there are 0.06 moles of free BF_3 present. On this basis the following theoretical ratios were calculated: $P/R = 0.085$, $Q/R = 0.05$, and $S/R = 0.24$. The experimental ratios are 0.07, 0.04, and 0.24 respectively.

In cooling to $-37^{\circ}C$, presumably some of B is converted into A due to a shift of 7.2 to the left, as explained before. Assume 0.10 moles of B are converted into A. Then 0.1 moles of HS_2O_6F are produced. The HS_2O_6F reacts with 0.05 moles of BF_3 producing another 0.05 moles of A. Therefore, it is expected that in this solution there are 0.21 moles of $S_3O_8F_2$, 0.09 moles of $S_2O_5F_2$, 0.13 moles of B, 0.15 moles of A, and 0.01 moles of BF_3. Assuming that T is due to the fluorines in BF_3, and U is due to fluorines bonded to boron in A and B, the following theoretical ratios were calculated: $P/R = 0.08$, $Q/R = 0.05$, $T/R = 0.02$, and $U/R =$

0.16.   The experimental ratios are 0.07, 0.04, 0.02 and 0.15 respectively.

Table XVII

SOLUTIONS OF BF_3-SO_3 : CONDUCTIVITY AT $25^{\circ}C$

W_{HSO_3F} (expt. 10) = 44.1422 g.

W_{SO_3} (expt. 10) = 1.5184 g.

W_{HSO_3F} (expt. 13) = 42.9321 g.

W_{SO_3} (expt. 13) = 2.5266 g.

Expt.	W_{BF_3}	$r(BF_3/SO_3)$	$10^4 \varkappa$
10	0.0000	0.0000	2.2562
	0.0315	0.0245	6.0941
	0.0872	0.0678	20.210
	0.1296	0.1008	29.688
	0.4451	0.3461	64.536
	0.4986	0.3878	65.229
13	0.0000	0.0000	1.138
	0.1756	0.0820	41.123
	0.3327	0.1554	78.210
	0.4714	0.2202	101.74
	0.5784	0.2702	115.83
	0.6209	0.2901	118.11
	0.6941	0.3242	120.42
	0.7252	0.3388	119.88
	0.7929	0.3704	119.41
	0.8457	0.3952	119.18

Table XVIII

SOLUTIONS OF $BF_3 \cdot 3SO_3$: CONDUCTIVITY AT $25^{\circ}C$

$W_{HSO_3F} = 107.09$ g.

$\mathcal{K}_o = 1.459 \times 10^{-4}$ ohm^{-1} cm.$^{-1}$

W_{SO_3}	W_{HSO_3F}	$m^s_{BF_3 \cdot 3SO_3}$	$10^4 \mathcal{K}$
0.8282	108.33	0.03183	16.701
1.7798	109.76	0.06752	40.999
2.8062	111.30	0.10498	65.424
3.9096	112.96	0.14413	90.130
6.2337	116.45	0.22290	133.70
7.9192	118.91	0.27717	164.93

Table XIX

SOLUTIONS OF $BF_3 \cdot 3SO_3$ AND EXCESS SO_3 : CONDUCTIVITY AT $25^{\circ}C$

$\mathcal{K}_o = 1.358 \times 10^{-4}$ ohm^{-1} cm.$^{-1}$

W_{SO_3}	W_{HSO_3F}	$m^s_{SO_3}$	$10^4 \mathcal{K}$
2.8440	110.86	0.32041	63.460
2.9719	111.03	0.33431	65.357
3.1425	111.26	0.35276	68.055
4.0104	112.43	0.44551	82.799
4.8940	113.63	0.53793	96.091
5.6999	114.72	0.62055	106.46
6.4879	115.78	0.69988	114.81
7.3663	116.97	0.78655	123.07

Table XX

SOLUTIONS OF $BF_3 \cdot 3SO_3$: FREEZING-POINT DEPRESSIONS

Freezing Point of Saturated BF_3 Solution = $-89.460^\circ C$

W_{SO_3}	W_{HSO_3F}	$m^s_{BF_3 \cdot 3SO_3}$	ΔT
1.8187	201.09	0.03767	0.39
3.2162	203.04	0.06595	0.84
4.4245	204.72	0.08998	1.14
6.0626	206.00	0.1225	1.38

Table XXI

SOLUTIONS OF KBF$_4$: CONDUCTIVITY AT 25°C

W_{HSO_3F} = 95.47 g.

$\mathcal{K}_o$ = 1.67 x 10^{-4} ohm^{-1} cm.$^{-1}$

W	m^s	10$^4\mathcal{K}$
0.0807	0.006716	20.760
0.2088	0.01737	50.351
0.3570	0.02970	80.531
0.5252	0.043688	111.71
0.5988	0.04981	124.88
0.8892	0.07397	171.81
0.9919	0.08251	187.76
1.2746	0.10602	225.41

Table XXII

SOLUTIONS OF KF : CONDUCTIVITY AT 25°C

W_{HSO_3F} = 93.65 g.

$\mathcal{K}_o$ = 1.30 x 10^{-4} ohm^{-1} cm.$^{-1}$

W	m^s	10$^4\mathcal{K}$
0.0340	0.006249	16.328
0.1109	0.02038	52.082
0.2055	0.03777	94.455
0.2887	0.05306	128.770
0.3463	0.06364	151.883
0.4307	0.07916	184.76

Table XXIII

SOLUTIONS OF KBF_4-SO_3 : CONDUCTIVITY AT $25°C$

$\mathcal{K}_0$ = 2.20×10^{-4} ohm^{-1} cm.$^{-1}$

W_{HSO_3F} = 107.58 g.

W_{SO_3} = 2.3645 g.

m_{SO_3} = 0.27474

W_{KBF_4}	$m^s_{KBF_4}$	$10^4\mathcal{K}$
0.2590	0.01912	14.537
0.4381	0.032341	21.852
0.6512	0.04807	30.313
0.9737	0.071879	44.972
1.2476	0.092098	65.500
1.5320	0.11309	99.432
1.8472	0.13636	146.106
1.9660	0.1451	165.294

Fig. 48   SOLUTIONS OF BF_3-SO_3:   CONDUCTIVITY AT $25°C$

$10^4 \mathcal{K}$

$r(BF_3/SO_3)$

144
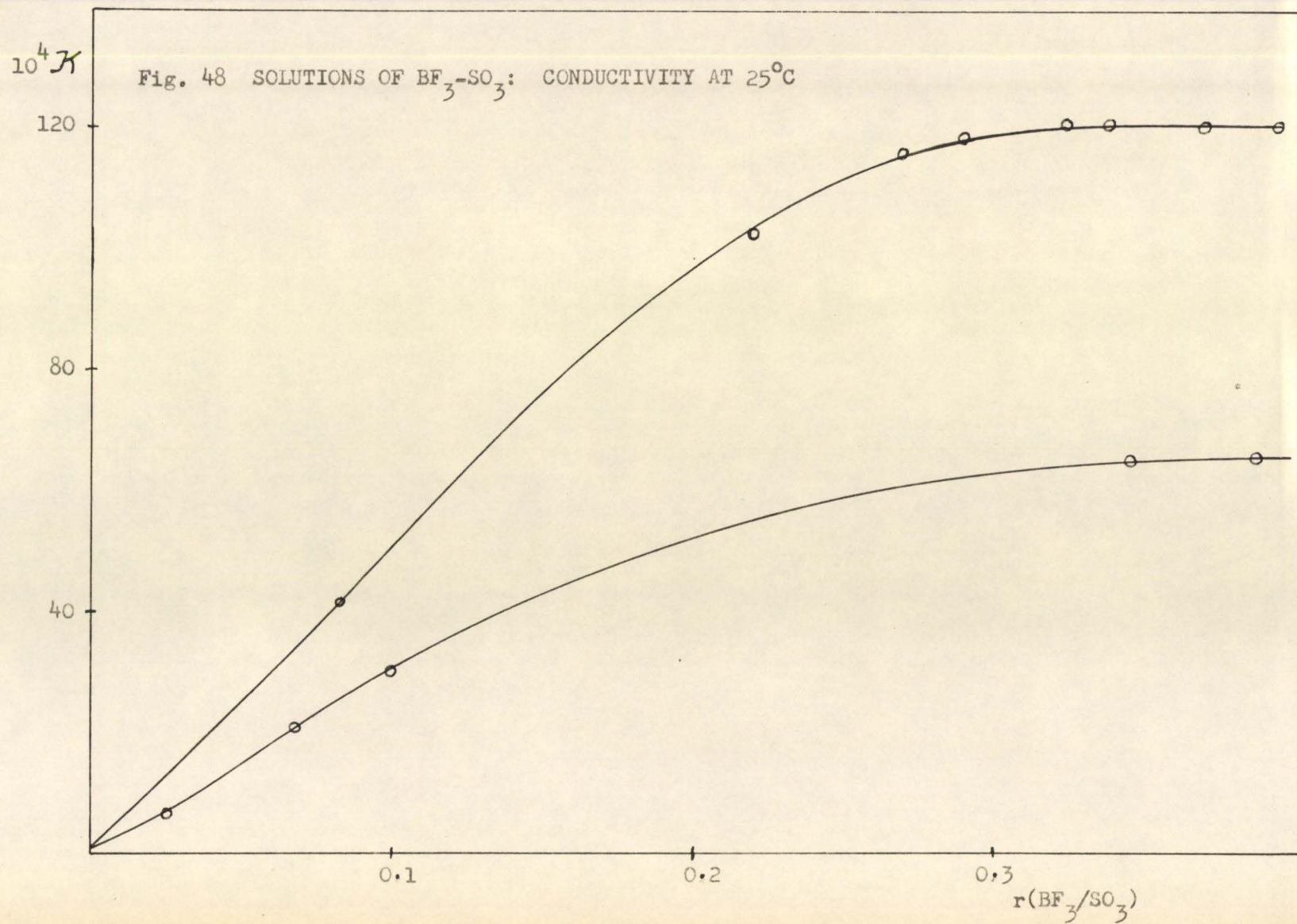
Fig. 49   APPARATUS USED FOR ADDITIONS OF BF_3 TO CONDUCTIVITY
CELL AND CRYOSCOPE

(a)   (b)

145

Fig. 50 SOLUTIONS OF $BF_3 \cdot 3SO_3$: CONDUCTIVITY AT $25^{\circ}C$

$10^4 \mathcal{K}$

Fig. 51 SOLUTIONS OF $BF_3 \cdot 3SO_3$ CONTAINING EXCESS SO_3: CONDUCTIVITY AT $25^{\circ}C$

120

80

40

0·2   0·4   0·6   0·8

$m^s_{SO_3}$

Fig. 52 SOLUTIONS OF $BF_3 \cdot 3SO_3$: FREEZING-POINT DEPRESSIONS

Fig. 53 SOLUTIONS OF KF, KBF₄,
AND KBF₄-SO₃:
CONDUCTIVITY AT 25°C
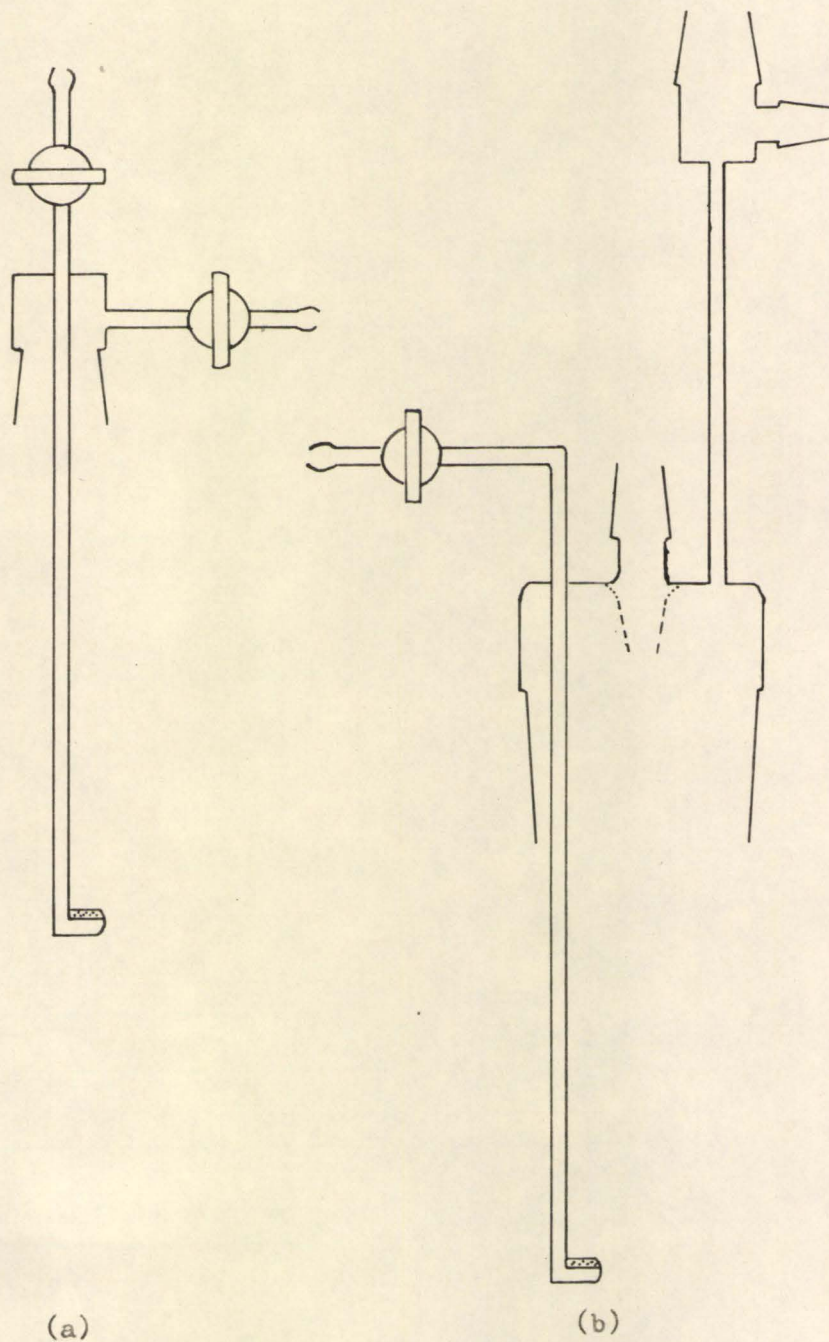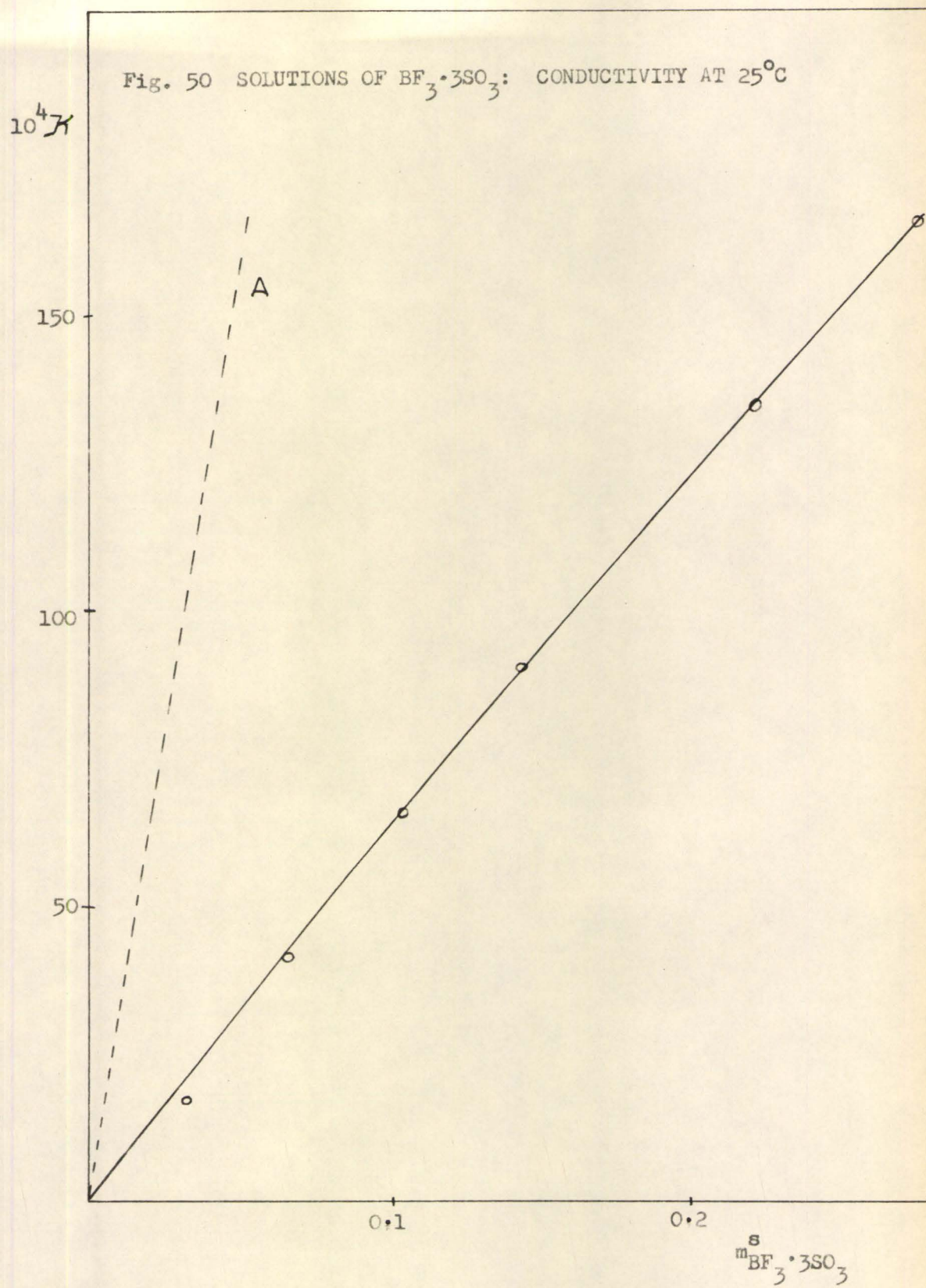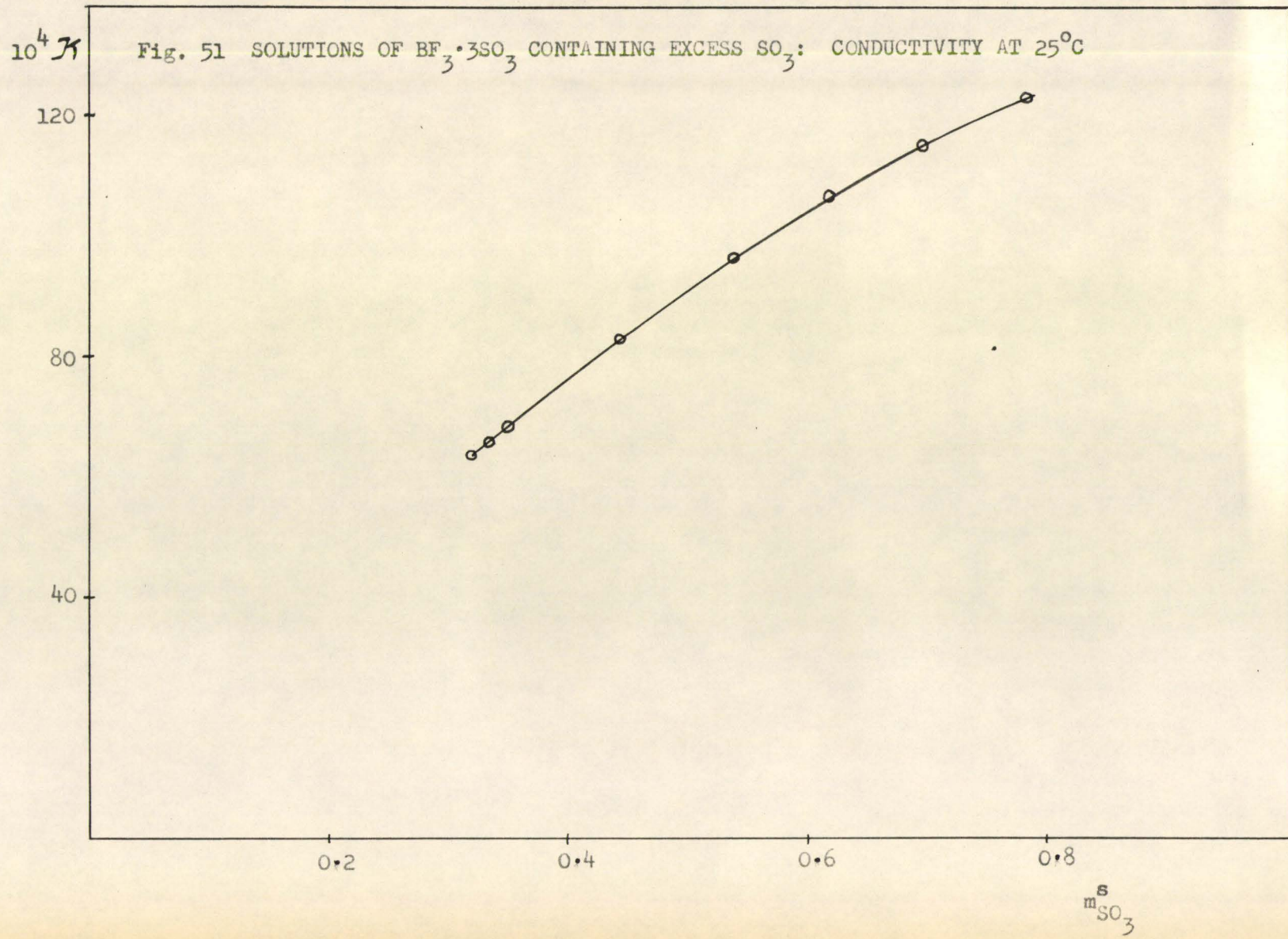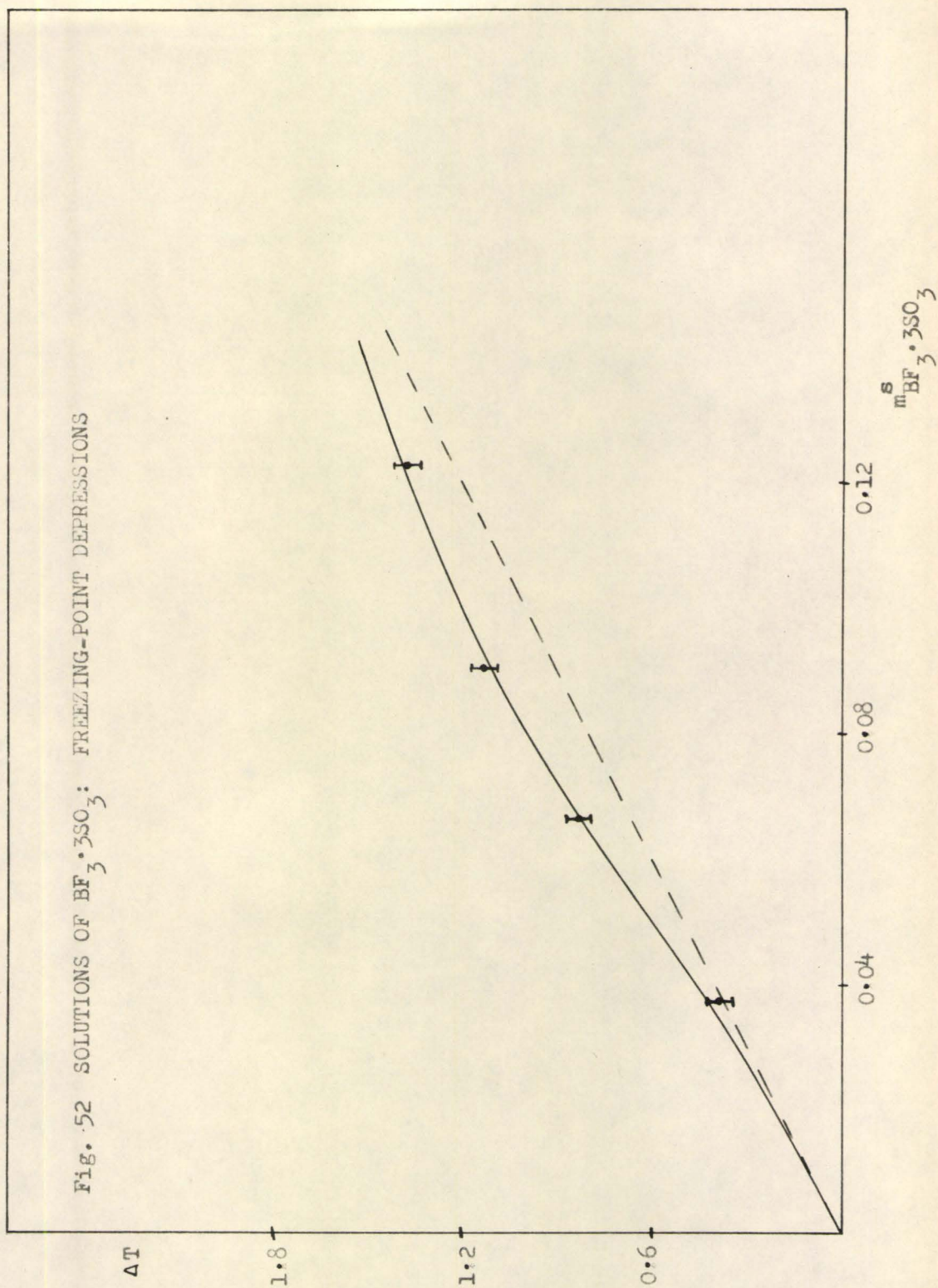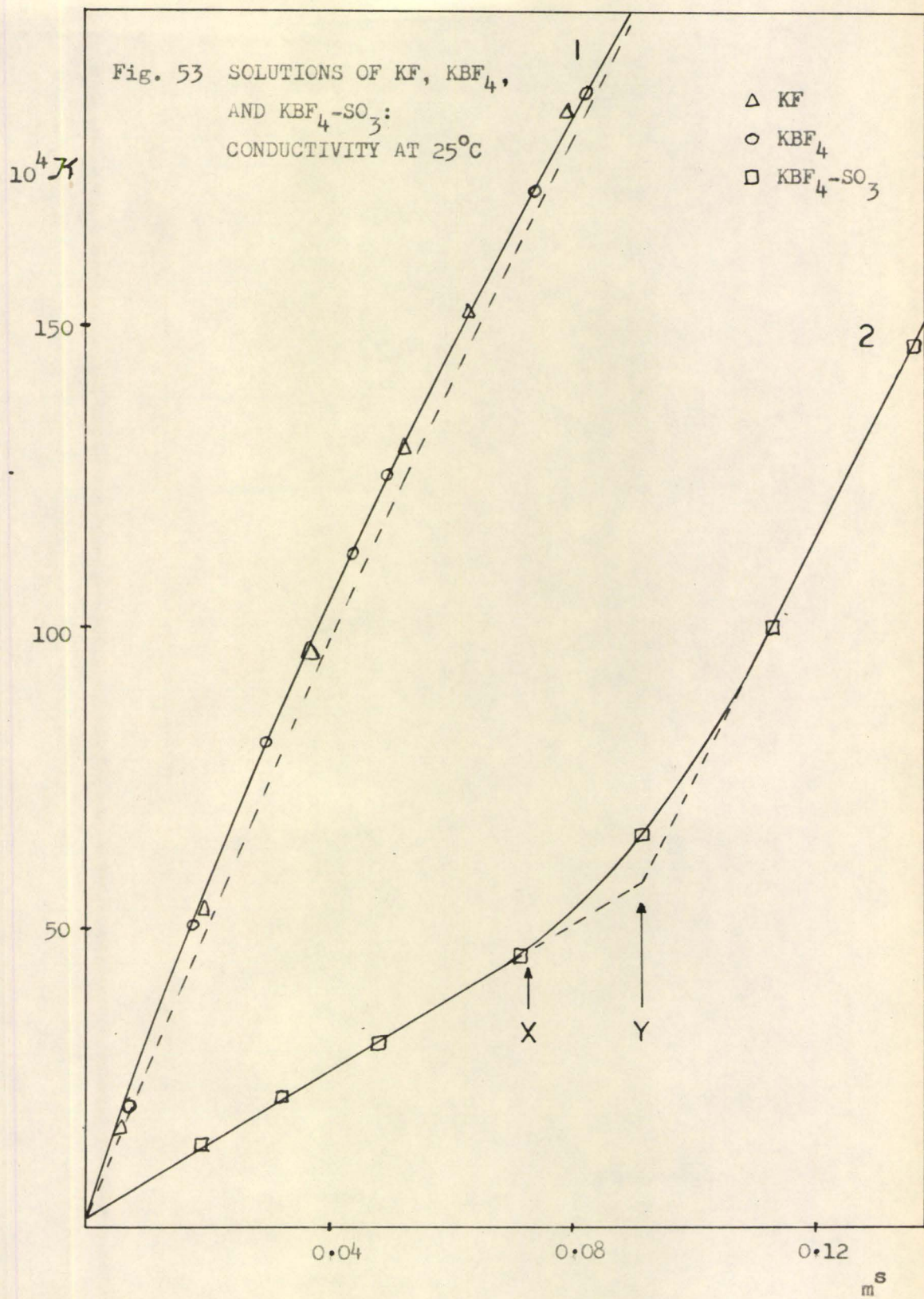
Fig. 54 SOLUTION OF BF_3-SO_3: F^{19} N.M.R. SPECTRA
ROOM TEMPERATURE
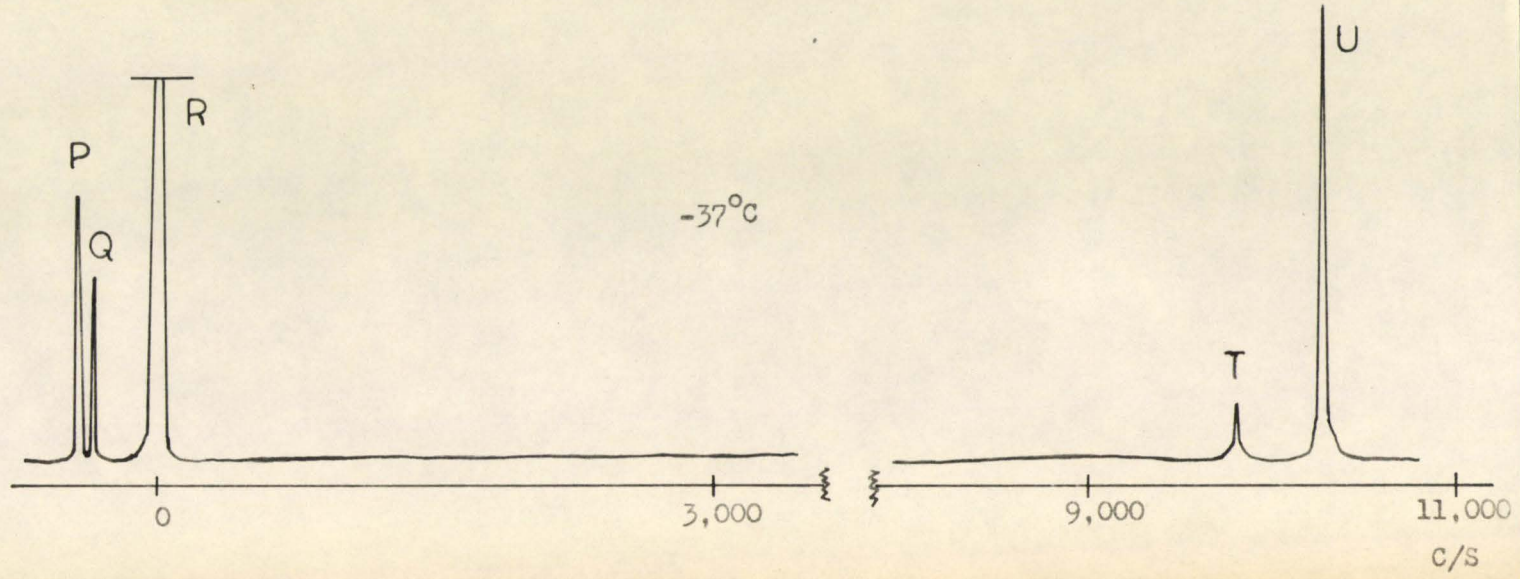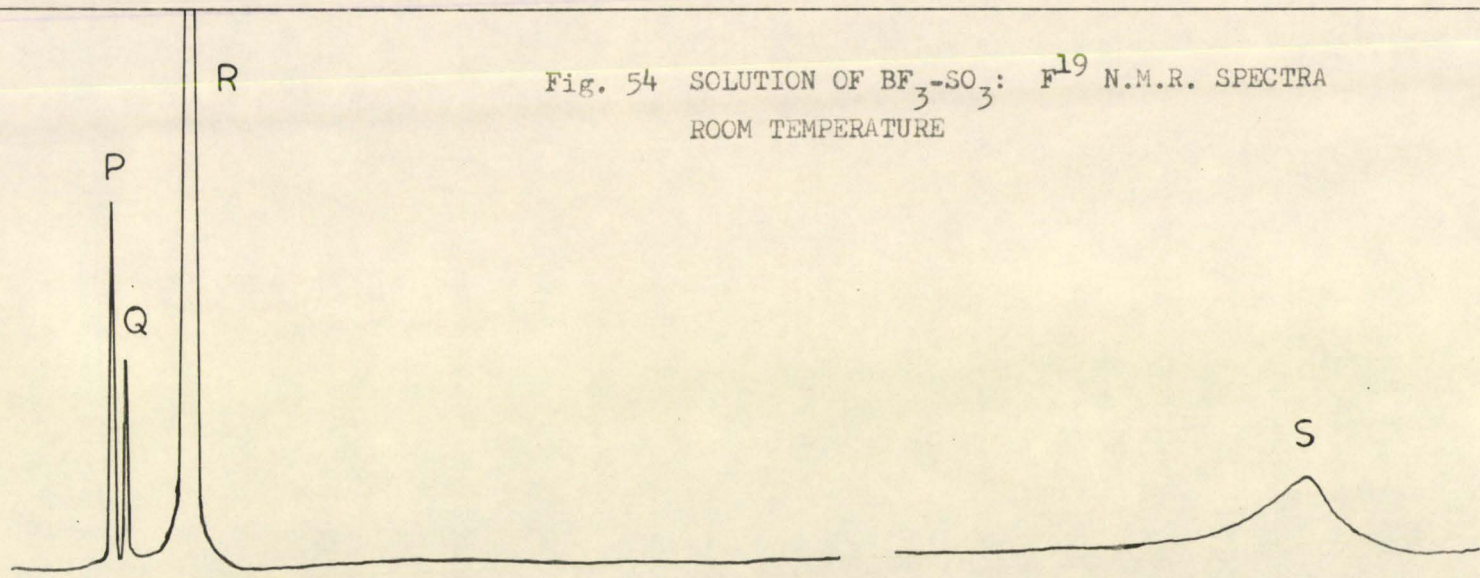
Fig. 55   SOLUTION OF BF_3-SO_3: F^{19} N.M.R. SPECTRA,
HIGH FIELD REGION

(a)
-70°C
V
W

(b)
-66°C
W

9,500   10,000   10,500

C/S
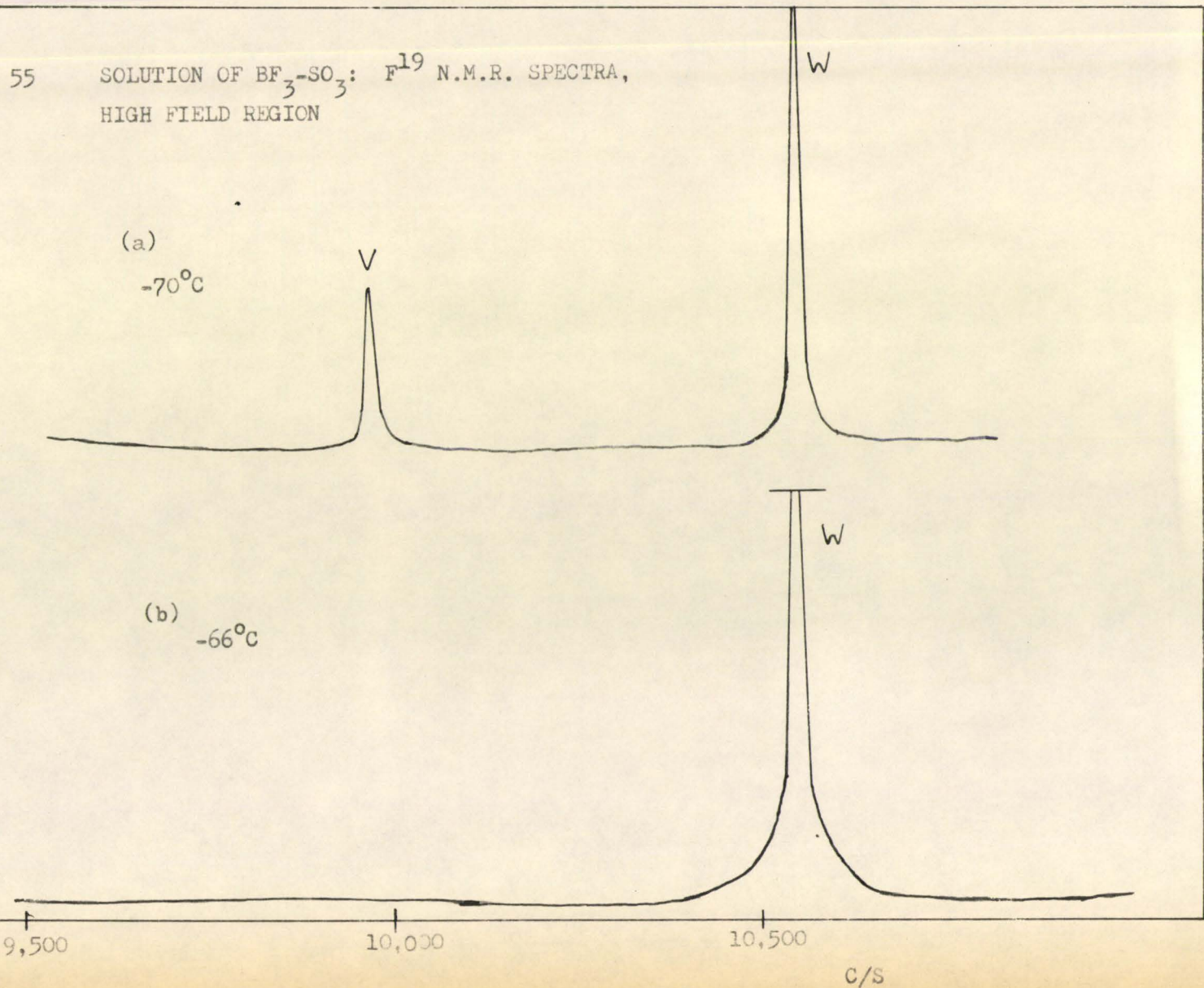
(b) THE REACTION IN LIQUID SULPHUR DIOXIDE

Attempts were made to isolate a compound from the reaction of boron trifluoride with sulphur trioxide, by carrying out the reaction in an inert solvent.

Sulphur trioxide (approximately 100 ml.) was condensed into the vessel shown in Fig. 56 by attaching a cylinder of SO_2 to the apparatus at A, and immersing the vessel in a dry-ice methanol bath. This bath was then replaced by a sodium chloride-ice bath ($-16^{\circ}C$) and SO_3 was distilled through B onto the SO_2. Boron trifluoride was bubbled through the solution for 50 minutes, stopcock C being open to the air through a tube of anhydrous calcium chloride during this stage of the procedure. The cold bath was removed and excess SO_2 was allowed to evaporate at room temperature. A white, extremely hygroscopic solid remained. A portion of the product was transferred in a dry box to a weighing bottle. The contents of the bottle were then added to water, and a known concentration was prepared in a volumetric flask. Aliquots were analyzed for sulphur and boron.

Sulphur was determined by precipitation as barium sulphate, by the method described in Chapter II (b). The results for four analyses are given in Table XXIV. The variation in the results is presumably due to incomplete hydrolysis in some instances. It is evident from the results, however, that the compound contains between 31% and 32% sulphur; this analysis suggests that it has the formula $BF_3 \cdot 3SO_3$ (see Table XXV).

The analysis for boron was done by the determination of the boric acid content of an aqueous solution. Strong acids in an aqueous solution of the compound were titrated with standard sodium hydroxide solution. The

end point was determined by means of a pH meter. The boric acid content was then determined by adding mannitol to the solution, and titrating the strong acid formed,with standard sodium hydroxide solution. The results of four determinations are given in Table XXIV, column (a). The results are low for the composition $BF_3 \cdot 3SO_3$.

Since it is possible that the compound does not completely hydrolyze to give boric acid in water, an attempt was made to ensure complete hydrolysis. The procedure used was similar to that described by Booth and Martin[73] for the determination of total acid in commercial fluoroboric acid. Calcium chloride (approximately 0.2 g.) was added to an aqueous solution of the compound (0.1204 g. of compound) and the acid present was titrated to a methyl red end point. The solution was then heated to boiling and digested (10 minutes at $90^{\circ}C$). The hot solution was titrated again to an approximate end point, heated again to just boiling, and digested further. This process was repeated until no further acid was produced. Mannitol was then added to the cold solution and the boric acid was determined by titrating to a phenolphthalein end point. The results of two determinations are given in Table XXIV,column (b).

A higher value for the percentage of boron was obtained by the second procedure described. This result is in agreement with the suggestion that hydrolysis of the compound was not complete in the first procedure described. Nevertheless, the percentage of boron obtained by the second procedure is still below that expected for the compound $BF_3 \cdot 3SO_3$. Since boric acid is volatile in steam, it is possible that some boric acid was lost during the long digestion period of the analysis procedure. This digestion should have been carried out under reflux.

Freezing-point measurements were made on solutions of this compound and the results are given in Table XXVI and Fig. 57. Concentrations were calculated by assuming the compound has the composition $BF_3 \cdot 3SO_3$. In Fig. 57 the dotted line is the theoretical curve for $\nu = 3$. From the freezing-point results it appears that the compound dissociates in solutions to give slightly more than 3 particles. The formation of 3 particles is consistent with the following mode of ionization.

$$BF_3 \cdot 3SO_3 + 3HSO_3F \rightleftharpoons HS_2O_6F + FB(SO_3F)_3^- + H_2SO_3F^+$$
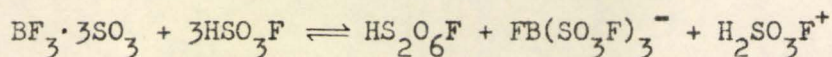
We recall that, when the reaction between BF_3 and SO_3 is carried out in fluorosulphuric acid, a compound, $BF_3 \cdot 3SO_3$, is formed which dissociates in fluorosulphuric acid at $-90^{\circ}C$, in an identical manner. It is possible that the two compounds are identical.

The reaction between BF_3 and SO_3 was studied in solution in sulphuryl chloride. In this case the solvent was removed by heating to $100^{\circ}C$ under vacuum. A white hygroscopic solid, which had the analyses 26.1% S and 6.5% B, was obtained. Presumably, the same compound as that produced with SO_2 as solvent was obtained initially, but when the solution was heated to $100^{\circ}C$ to remove the solvent, the compound decomposed giving polysulphuryl fluorides and leaving a residue containing less sulphur. This suggestion is in agreement with the smaller percentage of sulphur found in this instance. Also, the n.m.r. spectra of the recovered SO_2Cl_2 showed a peak that could be reasonably assigned to a polysulphuryl fluoride. However, this was not confirmed by the addition of a small amount of pure $S_2O_5F_2$ or $S_3O_8F_2$ to the sample.

Table XXIV

THE REACTION OF BF_3 WITH SO_3 : SULPHUR

AND BORON ANALYSES ON THE PRODUCT

%S	%B	
	(a)	(b)
30·8	2·27	2·79
31·7	2·32	2·68
30·8	2·21	
31·9	2·30	

Table XXV

THEORETICAL % BORON AND % SULPHUR

FOR THE COMPLEXES $BF_3 \cdot xSO_3$

Complex	%S	%B
$BF_3 \cdot SO_3$	21·7	7·32
$BF_3 \cdot 2SO_3$	28·1	4·75
$BF_3 \cdot 3SO_3$	31·2	3·51
$BF_3 \cdot 4SO_3$	33·1	2·79

Table XXVI

SOLUTIONS OF THE COMPOUND "$BF_3 \cdot 3SO_3$" :

FREEZING-POINT DEPRESSIONS

W_{HSO_3F} = 156·61 g.

T_o = -88·995°C

W	m^S	ΔT
2·1421	0·001286	0·017
5·9265	0·003647	0·046
11·9015	0·007070	0·085
15·8885	0·009281	0·111
19·6959	0·011198	0·130

Fig. 56   APPARATUS USED FOR STUDYING THE REACTION, IN LIQUID
          SO_2, OF BF_3 WITH SO_3

100 ml.
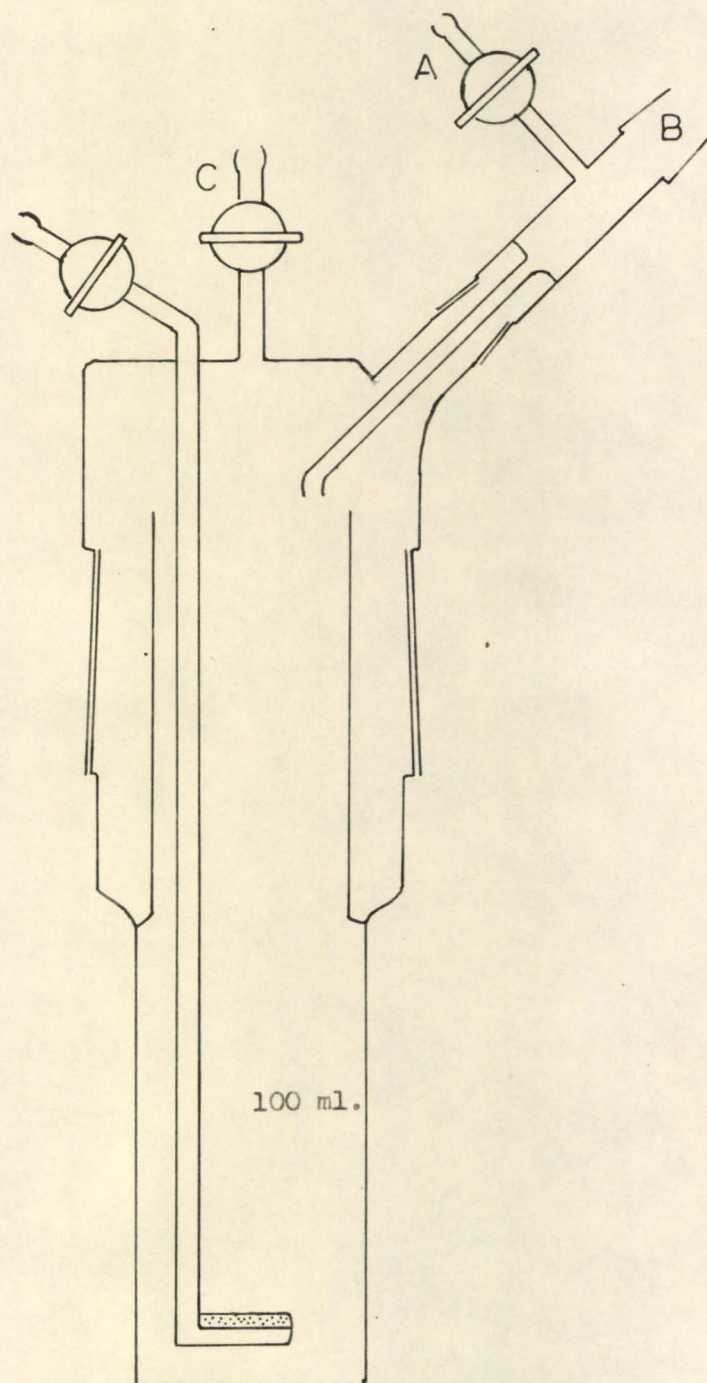
Fig. 57 SOLUTIONS OF THE COMPOUND "$BF_3 \cdot 3SO_3$": FREEZING-POINT DEPRESSIONS
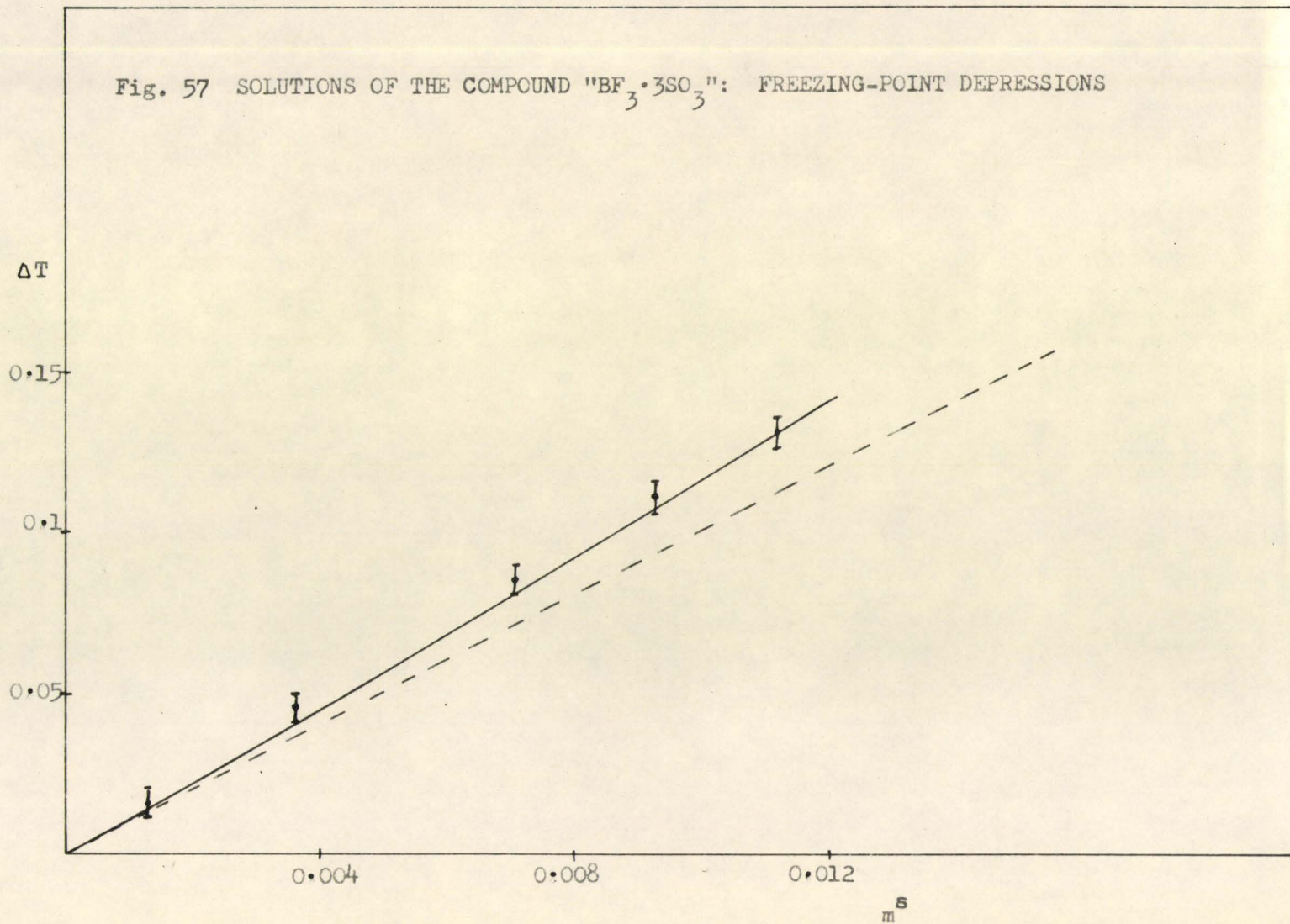
CHAPTER VIII

SOLUTIONS OF ARSENIC TRIFLUORIDE AND "$2AsF_3 \cdot 3SO_3$"

(a) CONDUCTIVITY MEASUREMENTS ON SOLUTIONS OF ARSENIC TRIFLUORIDE

In continuing the general investigation of the behaviour of
fluorides of Group V in fluorosulphuric acid, solutions of arsenic tri-
fluoride were studied. Conductivity results are given in Table XXVII and
Fig. 58. In experiment 2, conductivities were measured 15 to 20 minutes
after each addition of AsF_3, to allow for temperature equilibrium. How-
ever, the conductivity in each case was drifting slightly when recorded.
In experiment 4, a concentrated solution of AsF_3 in fluorosulphuric acid
was allowed to stand for four days. Conductivity measurements were made
by adding small amounts of this solution to the fluorosulphuric acid in
the cell. Again, readings were taken 20 minutes after each addition; how-
ever, in this experiment, also, the conductivity drifted slightly. Addition
of a crystal of KSO_3F to a solution of AsF_3 increased its conductivity,
indicating that this solute behaves as a base in fluorosulphuric acid.
The results of experiments 2 and 4 are shown in Fig. 58, as curves A and
B respectively. Presumably AsF_3 is behaving as a very weak base, according
to 8·1

$$AsF_3 + HSO_3F \rightleftharpoons HAsF_3^+ + SO_3F^- . \qquad 8·1$$
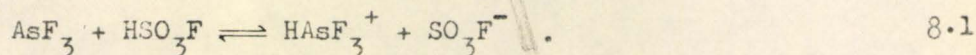
In Fig. 58, the conductivity curve for AsF_3 is compared to the curve for
the strong base KSO_3F and the weak base SbF_3 [42]. The fact that a
solution which had been allowed to stand for several days had a conduc-
tivity which was larger than that of the freshly prepared solution, could

157

. possibly be explained by the formation of a covalent fluorosulphate accord-

ing to 8·2.

$$AsF_3 + HSO_3F \rightleftharpoons AsF_2(SO_3F) + HF \qquad\qquad 8·2$$
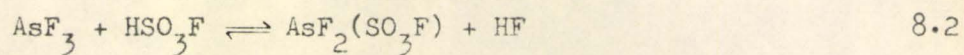
The resulting increase in conductivity could be attributed to the basic

behaviour of the HF produced (see Chapter VII (a)).

Table XXVII

SOLUTIONS OF AsF_3 : CONDUCTIVITY AT $25^{\circ}C$

$\mathcal{K}_0$ (expt. 2) = 1.097×10^{-4} ohm^{-1} cm.$^{-1}$

$\mathcal{K}_0$ (expt. 4) = 1.213×10^{-4} ohm^{-1} cm.$^{-1}$

Expt.	W_{AsF_3}	W_{HSO_3F}	m^s	$10^4\mathcal{K}$
2	0.09715	132.48	0.005559	1.1251
	0.1978	132.56	0.01131	1.1794
	0.3118	132.66	0.01782	1.3172
	0.4366	132.76	0.02493	1.5191
	0.57153	132.88	0.032606	1.7087
	0.75996	133.03	0.043308	2.0373
	0.94734	133.19	0.053921	2.4191
	1.1572	133.37	0.065777	2.8207
	1.4338	133.60	0.081358	3.4654
	1.6550	133.78	0.093784	3.8091
	3.6765	135.47	0.20574	7.8281
	5.86740	137.29	0.32399	12.7485
4	0.08129	138.408	0.004452	1.4037
	0.29655	138.640	0.01622	2.3424
	0.39663	138.748	0.02167	2.8083
	0.77562	139.157	0.04225	3.8257
	2.7600	141.301	0.14808	7.7302
	4.1182	142.768	0.21867	10.7507
	5.0075	143.729	0.26412	13.2486

Fig. 58 SOLUTIONS OF AsF_3 AND OF "$2AsF_3 \cdot 3SO_3$": CONDUCTIVITY AT 25°C
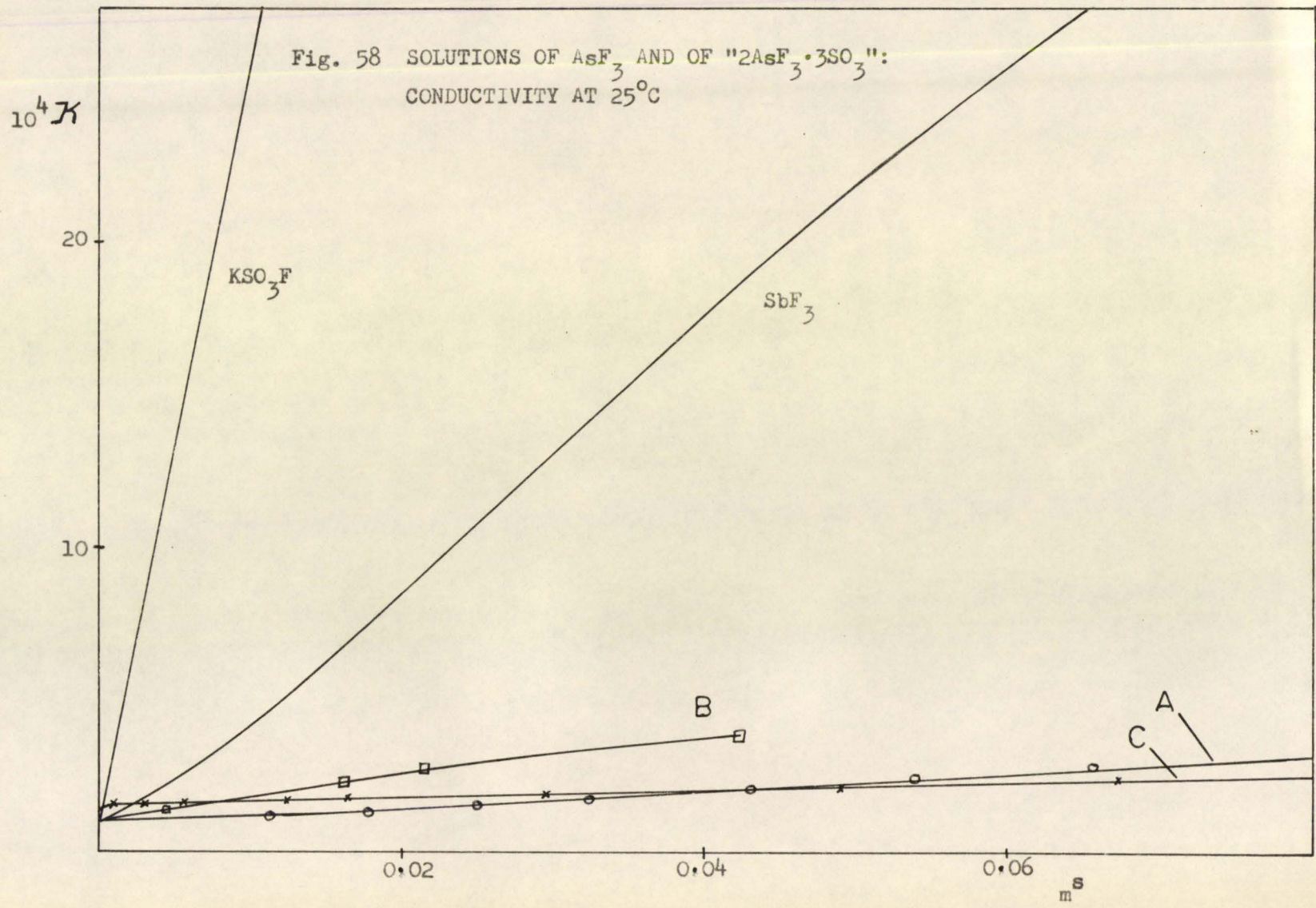
(b)   THE SUPPOSED COMPOUND "$2AsF_3 \cdot 3SO_3$"

Engelbrecht, Aignesberger and Hayek[74] describe the preparation

of a compound $2AsF_3 \cdot 3SO_3$ (b.p. $140^{\circ}C$) by the reaction of arsenic tri-

fluoride with sulphur trioxide. In this work a solution of SO_3 in excess

AsF_3 was refluxed gently for one hour and then distilled in a dry atmos-

phere. The fraction boiling between $135^{\circ}C$ and $142^{\circ}C$ was collected. Con-

ductivity results are given in Table XXVIII and Fig. 58 (curve C), and

cryoscopic results are given in Table XXIX and Fig. 59.

The conductivity results show that the compound is an extremely

weak electrolyte. The increase in conductivity produced by the addition

of a small amount of KSO_3F indicates that the compound ionizes as a base.

However, the freezing-point measurements indicate the presence of two

particles (the dotted line in Fig. 59 is the theoretical curve for $\nu = 2$).

Chan and Gillespie[75] have good evidence from n.m.r. studies

that the supposed compound "$2AsF_3 \cdot 3SO_3$" is actually a constant boiling

mixture of approximately equal amounts of the two compounds $AsF(SO_3F)_2$ and

$AsF_2(SO_3F)$. This theory is supported by the conductimetric and cryoscopic

results given above since, if either of these compounds is a weak base, or

if both are weak bases, the solutions would be very weakly conducting and

cryoscopy would indicate the presence of two particles.

Table XXVIII

SOLUTIONS OF "2AsF$_3$·3SO$_3$" : CONDUCTIVITY AT 25$^?$C

$$\mathcal{K}_o = 1\ 459 \times 10^{-4}\ ohm^{-1}\ cm.^{-1}$$

W$_{solute}$	W$_{HSO_3F}$	m^s	$10^4\mathcal{K}$
0·06446	130·28	0·0009817	1·5769
0·1905	130·50	0·0028958	1·5969
0·3804	130·94	0·005764	1·6240
0·8273	131·90	0·012444	1·6739
1·1013	133·19	0·016406	1·7476
2·0306	135·55	0·029722	1·89127
3·4460	139·56	0·04899	2·1153
4·9347	145·30	0·06738	2·3764
6·9706	153·42	0·09014	2·7146

Table XXIX

SOLUTIONS OF "2AsF$_3$·3SO$_3$" : FREEZING-POINT DEPRESSIONS

$$T_o = -89.008^o C$$

W$_{solute}$	W$_{SO_3F}$	m^s	ΔT
1·8199	165·34	0·02184	0·144
3·3890	166·47	0·04039	0·306
5·1974	167·78	0·06146	0·473
6·8675	168·99	0·08063	0·631
9·5302	170·91	0·1106	0·877

Fig. 59   SOLUTIONS OF "$2AsF_3 \cdot 3SO_3$":
          FREEZING-POINT DEPRESSIONS

163
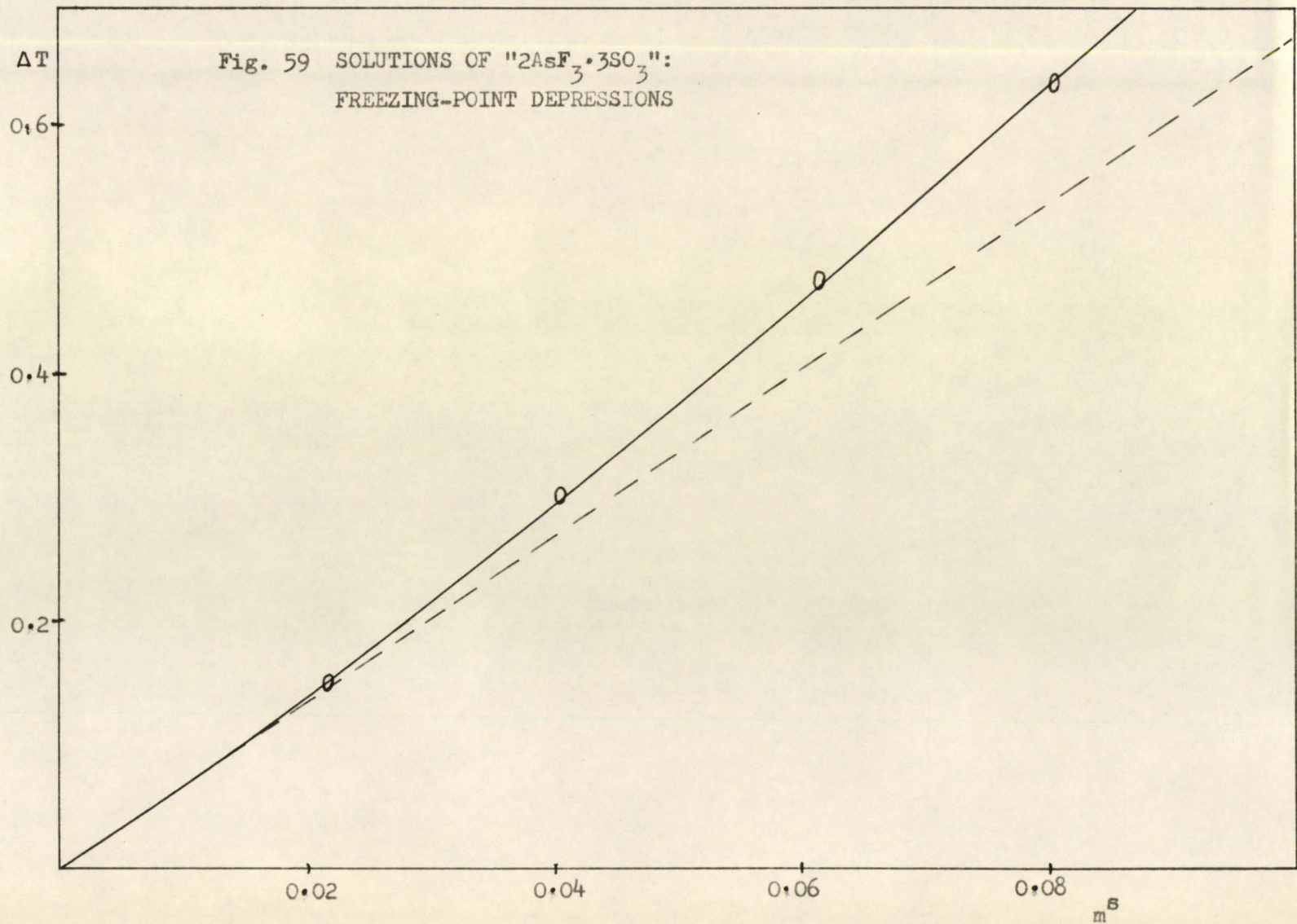
CHAPTER IX

IONIC MOBILITIES IN FLUOROSULPHURIC ACID

(a) INTRODUCTION

Barr[42] found that fluorosulphuric acid has a specific conductance of 1.085×10^{-4} ohm^{-1} cm.$^{-1}$. He concluded that this conductivity is due to the ions produced in autoprotolysis.

$$2HSO_3F \rightleftharpoons H_2SO_3F^+ + SO_3F^-$$
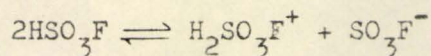
From transport number measurements on potassium fluorosulphate solutions, he was able to show that the fluorosulphate ion conducts the major part of the current (89%). Using this transport number result and conductivity data on KSO_3F solutions, Barr estimated the mobility of the fluorosulphate ion to be 142, compared to 18 for the potassium ion. This high mobility of the fluorosulphate ion suggests that it conducts by a proton-transfer process, in addition to the normal diffusion process of electrical conduction. Autoprotolysis ions of other protonic solvents, such as water and sulphuric acid, are known to conduct by this mechanism.[78]

One of the purposes of the present work was to obtain confirmatory evidence for abnormal conduction by the fluorosulphate ion, and to determine whether the fluorosulphuric acidium ion, $H_2SO_3F^+$, also has an abnormally high mobility.

(b) THE FLUOROSULPHATE ION

The transport number of barium ion in fluorosulphuric acid was
determined by the Hittorf method, using the apparatus and procedure des-
cribed in Chapter III (c). The results of two experiments are given in
Table XXX. During the removal of the excess fluorosulphuric acid a small,
but measureable, amount of barium fluorosulphate was lost due to "bumping".
In order to interpret the results the following considerations were made.

Firstly, it was assumed that there was no back diffusion of Ba^{2+}
from either A or C into the central compartment (Fig. 15). The cell was
tested for diffusion of this type in the following manner. The central
compartment was filled with a solution of $0 \cdot 38$ g. $KMnO_4$ in 50 ml. of water
and the other compartments were filled with water. Initially there was a
sharp boundary, in the connecting arms, between the deep purple colour of
the central compartment and the colourless water of the two outside com-
partments. The cell was placed in the thermostat and after two and one
half hours the boundary had moved less than $1 \cdot 0$ cm. Thus, mixing of the
three compartments by diffusion must be very small.

Secondly, the approximation was made that any loss of $Ba(SO_3F)_2$,
during its recovery by removal of HSO_3F under vacuum, was the same for
both the anode and cathode compartments. Thus the amount of Ba^{2+} trans-
ported to the cathode compartment equals the amount transported from the
anode compartment and is given by W_o, where.

$$W_o = \frac{1}{2} \left[\begin{array}{c} \text{increase in } Ba(SO_3F)_2 \\ \text{content in cathode} \\ \text{compartment} \end{array} + \begin{array}{c} \text{decrease in } Ba(SO_3F)_2 \\ \text{content in anode} \\ \text{compartment} \end{array} \right]$$

165

The error involved in using this approximation is considered to be the largest possible error in the experiment and is estimated as follows. If individual samples each lose the same amount of $Ba(SO_3F)_2$ during the recovery procedure, duplicate analyses of samples from the same compartment should yield the same amount of $Ba(SO_3F)_2$. The largest difference found in the analyses of samples taken from the same compartment was taken as the possible error involved in making the above approximation.

The transport number is obtained from the relation,

$$t_+ = \frac{2\,W_o}{M \times n}$$

where t_+ is the transport number of Ba^{2+};

W_o is the weight of $Ba(SO_3F)_2$ gained or lost (g.);

M is the molecular weight of $Ba(SO_3F)_2$;

n is the number of Faradays passed.

Of the two analyses from the same compartment, the analysis which gave the larger value for the amount of $Ba(SO_3F)_2$ was used in the calculation of t_+. Assuming that the largest error in the experiment was due to mechanical loss of $Ba(SO_3F)_2$, the analysis yielding the larger value of $Ba(SO_3F)_2$ content was probably closer to the actual value.

The mobility of the fluorosulphate ion was determined from transport number measurements and conductivity measurements, on solutions of $Ba(SO_3F)_2$. Since solutions for conductivities were prepared by weight it was necessary to measure densities in order to convert from molal units to molar units. Density measurements were made by the method used by Barr[42] for determining the densities of solutions of alkali metal fluorosulphates and nitro-compounds. A 10 ml. specific gravity bottle was cali-

brated with distilled water (previously boiled to remove CO_2). The bottle, filled with solution, was immersed, to a point just below the stopper, for twenty minutes in a $25 \pm 0.005^\circ C$ water thermostat. Excess solution was removed with filter paper from the capillary stopper. The bottle was then cooled in an ice-water bath, washed with acetone, dried in a stream of dry air, and weighed. The results are shown in Fig. 60 and Table XXXI.

Conductivity results on $Ba(SO_3F)_2$ solutions are given in Table XXXII and Fig. 61. The results of experiment 140, at high concentration, deviate from those of experiment 119. This is probably because the $Ba(SO_3F)_2$ used in experiment 140 was slightly impure. The salt used in that experiment had been stored for six months and had been handled several times, while the $Ba(SO_3F)_2$ used in experiment 119 was freshly prepared.

Barr[42] determined the equivalent conductivity at infinite dilution, Λ_o, for KSO_3F solutions, from a plot of equivalent conductivity, Λ, versus $\sqrt{I}$ (where I is the ionic strength). The value he obtained for Λ_o was 160. Using this value, and the transport number of 0.11 for K^+, he found the mobility of SO_3F^-, λ_o^-, to be 142. In the present work the value for λ_o^- was determined, by a similar procedure, from the results on solutions of $Ba(SO_3F)_2$.

It was suggested in Chapter IV that, at moderate concentrations, $Ba(SO_3F)_2$ may not be completely ionized. The following discussion is concerned with solutions in which the salt concentration is less than 0.03 m. It will be assumed that in such dilute solutions barium fluorosulphate is completely ionized.

Interpolated values of $\mathcal{K}$ at round values of m^s are given in Table XXXIII. The values of molarity, c, were calculated using the density-molality

curve in Fig. 60. The equivalent conductivities, Λ, were calculated from the expression,

$$\Lambda = \frac{\mathcal{K} \times 1000}{2 \times c}$$

where c is the concentration in moles per litre; **thus, for** $Ba(SO_3F)_2$, 2c is the concentration in equivalents per litre (normality). The units of equivalent conductivity are, therefore, $cm.^2\ ohm^{-1}\ (g.\ equiv.)^{-1}$. For convenience no units are given with the values of Λ, Λ_o, and λ_o presented in this work; the above units are implied in each case. The ionic strength, I, is defined by the expression,

$$I = \frac{c}{2}\ (\nu_1 z_1^{\ 2} + \nu_2 z_2^{\ 2})$$

where ν_1 and ν_2 are the numbers of moles of cations and anions respectively, formed from one mole of electrolyte, and z_1 and z_2 are the valencies of the cations and anions respectively. Therefore, I = 3c for barium fluoro-sulphate.

Fig. 62 is a plot of Λ versus $\sqrt{I}$ for $Ba(SO_3F)_2$. The graph is linear for concentrations down to 0·005 m. Below this concentration the specific conductance due to $Ba(SO_3F)_2$ becomes comparable in magnitude to the conductivity due to the autoprotolysis ions and, also, to any impurities in the solution. This probably results in the high values for Λ which occur in this region. Barr[42] found the same effect in the case of the alkali metal fluorosulphates.

Λ_o, found by extrapolating the linear portion of the Λ versus $\sqrt{I}$ curve to infinite dilution, is 149. This value can be divided into two contributions, one from Ba^{2+}, and the other from SO_3F^-.

$$\Lambda_o = \lambda_o Ba^{2+} + \lambda_o SO_3F^-$$

The λ_o's refer to ionic mobilities at infinite dilution. It is assumed that the transport numbers do not change much with concentrations. Therefore, assuming that the transport number for Ba^{2+} at infinite dilution is the same as the value determined by experiment at finite concentrations (0.075 ± 0.02), the values for λ_o were calculated.

$$\lambda_o \, Ba^{2+} = 11 \pm 3.0$$

$$\lambda_o \, SO_3F^- = 138 \pm 3.0$$

This value for $\lambda_o SO_3F^-$ is in good agreement with the value of 142 ± 4.0 obtained by Barr[42].

The Debye-Hückel-Onsager limiting law (9.1) describes, for dilute solutions, the variation of the equivalent conductivity of an electrolyte with concentration[76].

$$\Lambda = \Lambda_o - A \sqrt{I} \qquad\qquad 9.1$$

where,

$$A = \frac{2.801 \times 10^6 \, |z_1 z_2| \, q \Lambda_o}{(\varepsilon T)^{3/2} (1 + \sqrt{q})} + \frac{41.25 \, (|z_1| + |z_2|)}{\eta \, (\varepsilon T)^{1/2}}$$

and

$$q = \frac{|z_1 z_2|}{(|z_1| + |z_2|)(|z_2| t_1^o + |z_1| t_2^o)}$$

The symbols t_1^o and t_2^o refer to the transport numbers, at infinite dilution, of cations and anions respectively. A modified form of this equation (9.2) has been found to fit experimental data at higher concentrations[76].

$$\Lambda = \Lambda_o - A \, \frac{\sqrt{I}}{1 + \kappa a}$$

where $\kappa a = \left(\frac{8\pi N e^2}{1000 \varepsilon kT}\right)^{1/2} a \sqrt{I}$ \qquad\qquad 9.2

The symbol, a, refers to the mean diameter of anion and cation (cm.).

Using equation 9.2, theoretical equivalent conductivity curves, for different values of $\overset{o}{a}$ (the mean diameter of anion and cation in Angstrom units), were obtained for both KSO_3F and $Ba(SO_3F)_2$. These curves are shown as the dotted lines in Figs. 62 and 63. To calculate these curves the following values were used:

$$\varepsilon = 80$$
$$\Lambda_o \text{ for } Ba(SO_3F)_2 = 149$$
$$\Lambda_o \text{ for } KSO_3F = 160$$
$$\eta = 1.56 \text{ cp. (reference 42)}$$

The value for ε was taken as 80 by assuming that the dielectric constant (at $25^\circ C$) of fluorosulphuric acid is approximately the same as that of water.

It may be seen, in Figs. 62 and 63, that the theoretical curves predict a much smaller decrease in the equivalent conductivities with concentration than is actually observed. In fact, no agreement with the experimental curves can be obtained with positive values of $\overset{o}{a}$. It is possible that the value of $\varepsilon = 80$ is in considerable error. However, to increase the slope of the theoretical curves, so that they agree with the experimental curves, it would be necessary to use a value for ε that is very much less than 80. It does not seem reasonable to suggest that the dielectric constant of fluorosulphuric acid is much less than that of water. It seems more probable that the reason for lack of agreement is that equation 9.2, which describes the behaviour of electrolytes which conduct by diffusion alone, does not apply to solutions containing ions which conduct by a proton-transfer mechanism. Similar lack of agreement between experiment and theory has been found for solutions of metal hydrogen sulphates in sulphuric acid.[77]

Table XXX

SOLUTIONS OF $Ba(SO_3F)_2$: TRANSPORT NUMBER MEASUREMENTS

	Expt. 108	Expt. 118
Initial concentration of $Ba(SO_3F)_2$ (m)	0·09903	0·06352
Current (ma.)	19·3	19·3
Period of electrolysis (sec.)	9,000	10,800
Anode Compartment		
initial $W_{Ba(SO_3F)_2}$	2·742	1·451
final $W_{Ba(SO_3F)_2}$ (2 samples)	2·683, 2·681	1·407 1·409
Cathode Compartment		
initial $W_{Ba(SO_3F)_2}$	2·651	1·461
final $W_{Ba(SO_3F)_2}$ (2 samples)	2·636, 2·642	1·468, 1·458
t_+	0.08 ± 0.02	0.07 ± 0.02

$$t_+ = 0.075 \pm 0.02$$

Table XXXI

SOLUTIONS OF $Ba(SO_3F)_2$: DENSITIES AT $25^{\circ}C$

m	d_4^{25}
0.00000	1.7264
0.023606	1.7346
0.030390	1.7371
0.073532	1.7533
0.10973	1.7659
0.12994	1.7707

Table XXXII

SOLUTIONS OF $Ba(SO_3F)_2$: CONDUCTIVITY AT $25^{\circ}C$

W_{HSO_3F} (expt. 119) = 110.94 g.

W_{HSO_3F} (expt. 140) = 121.09 g.

$\mathcal{K}_o$ (expt. 119) = 1.355×10^{-4} ohm^{-1} cm.$^{-1}$

$\mathcal{K}_o$ (expt. 140) = 1.650×10^{-4} ohm^{-1} cm.$^{-1}$

Expt.	W	m	$10^4\mathcal{K}$
119	0.2426	0.00653	29.007
	0.5993	0.01613	66.551
	1.0587	0.02850	110.324
	1.3974	0.03761	140.324
	1.8322	0.04932	176.27
	2.2466	0.06047	212.90
	2.7319	0.07353	244.54
140	0.0488	0.00120	6.825
	0.1785	0.00439	21.324
	0.4727	0.01164	50.296
	0.5807	0.01429	62.219
	0.8558	0.02107	87.882
	1.4429	0.03552	138.50
	2.1077	0.05188	190.52

Table XXXIII

SOLUTIONS OF $Ba(SO_3F)_2$: EQUIVALENT CONDUCTIVITIES AT 25°C

m	c	$\sqrt{I}$	$10^4 K$	Λ
0·002	0·003452	0·09938	9·80	142·0
0·003	0·005177	0·1246	14·3	138·0
0·005	0·008626	0·1609	23·0	133·0
0·010	0·01723	0·2274	44·0	128·0
0·015	0·02583	0·2783	64·0	124·0
0·020	0·03444	0·3139	82·3	119·0
0·025	0·04303	0·3593	100·0	116·2
0·030	0·05159	0·3909	116·5	112·9

Fig. 60   SOLUTIONS OF $Ba(SO_3F)_2$:   DENSITIES AT $25°C$

Fig. 61 SOLUTIONS OF Ba(SO$_3$F)$_2$: CONDUCTIVITY AT 25°C

o Expt. 119
□ Expt. 140

Fig. 62   SOLUTIONS OF Ba(SO₃F)₂:
EQUIVALENT CONDUCTIVITIES AT 25°C

176

Fig. 63 SOLUTIONS OF KSO₃F:
EQUIVALENT CONDUCTIVITIES AT 25°C

(Experimental values, Barr(42))
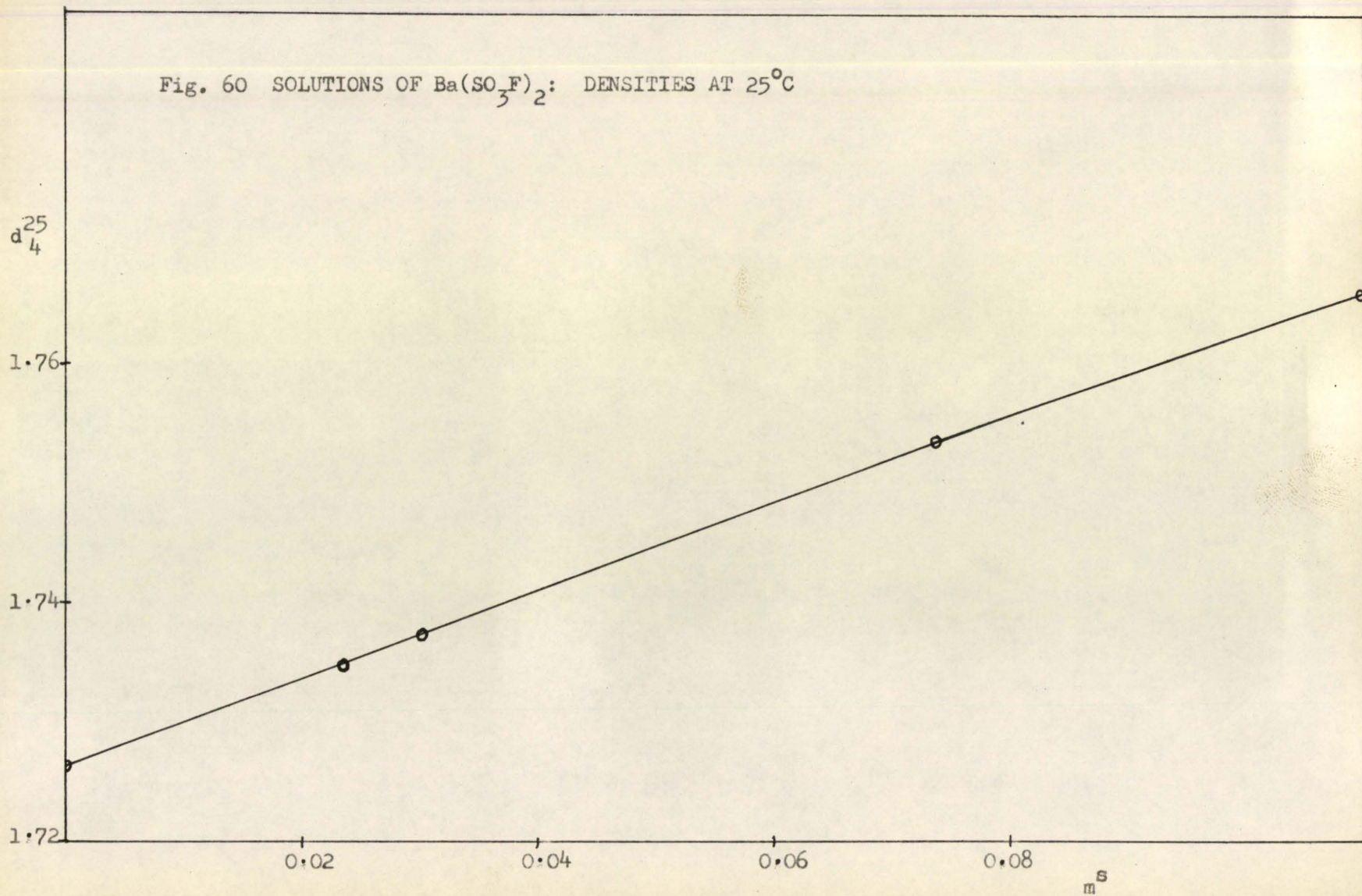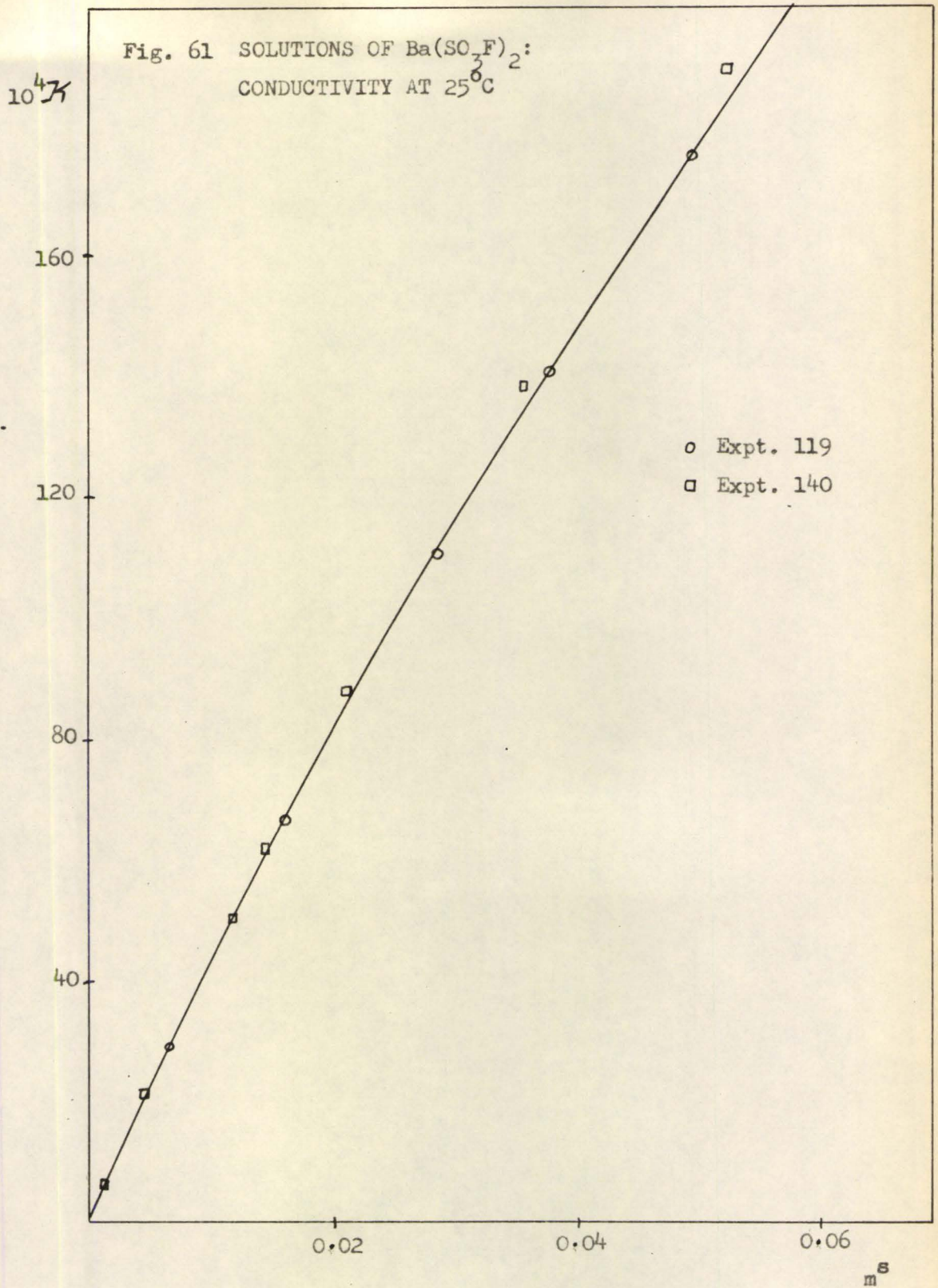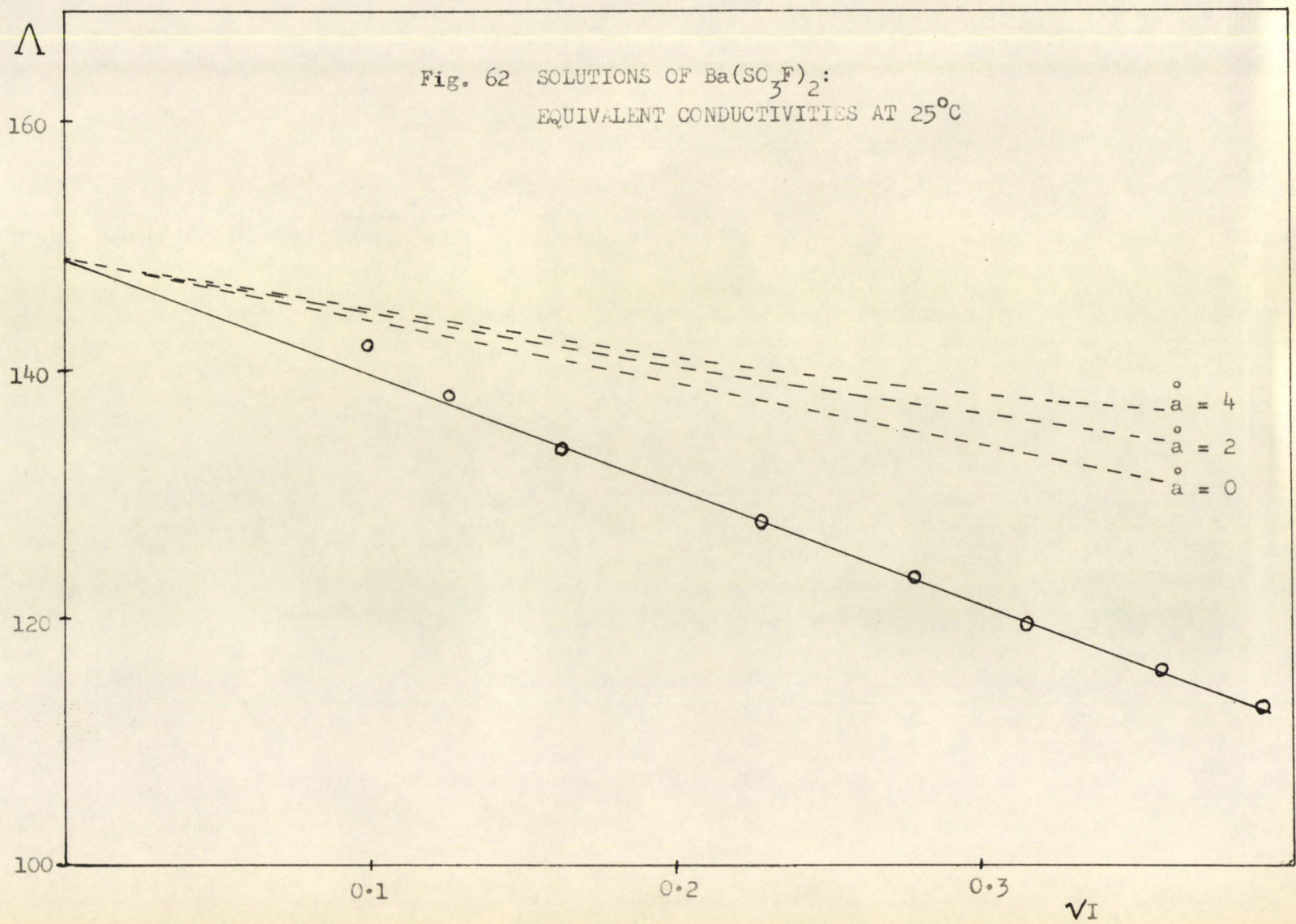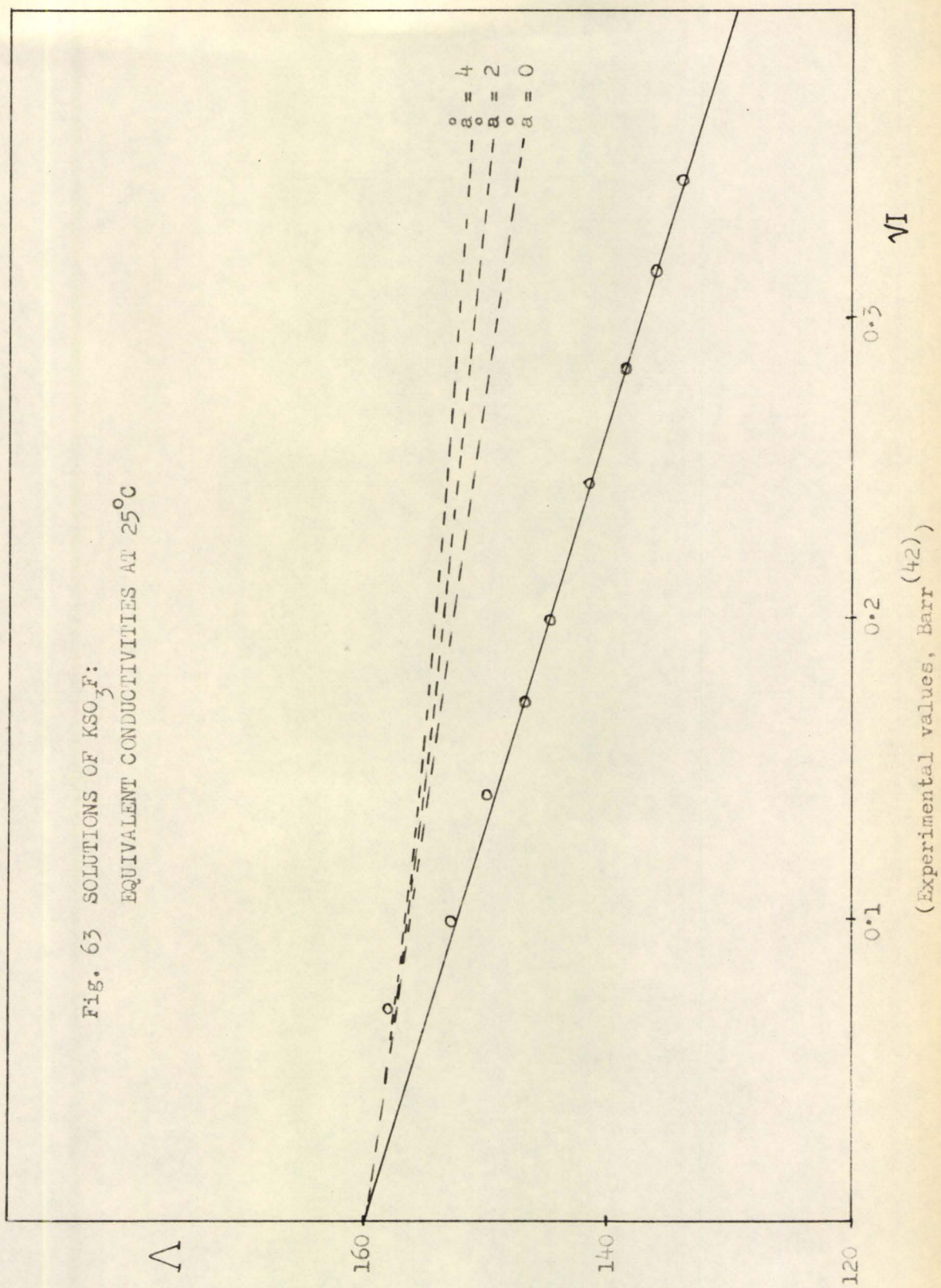
(c) THE FLUOROSULPHURIC ACIDIUM ION

The conductivity-molality curve for the fluorosulphuric acidium ion, $H_2SO_3F^+$, is given in Fig. 23. Table XXXIV contains Λ values for $H_2SO_3F^+$ obtained from this curve at round values of m. The values of c^* in Table XXXIV were obtained by multiplying the concentration, in molal units, by the density of pure fluorosulphuric acid, $1 \cdot 7264$ [42]. The change in density of the solution with concentration is therefore ignored. Such a "pseudo-molarity" usually does not differ significantly from the true molarity, c, particularly for dilute solutions. The maximum error involved is normally of the order of 1%.

Fig. 64 is a graph of Λ versus $\sqrt{c^*}$; the extrapolation of the linear portion of this graph yields the value 190 for $\lambda_o H_2SO_3F^+$. The mobility of the fluorosulphuric acidium ion is even larger than the mobility of the fluorosulphate ion ($\lambda_o SO_3F^- = 140$). Therefore, $H_2SO_3F^+$, like SO_3F^-, very probably conducts by a proton-transfer mechanism.

178

Table XXXIV

THE FLUOROSULPHURIC ACIDIUM ION : EQUIVALENT CONDUCTIVITIES AT 25°C

m	c*	$\sqrt{c^*}$	$10^4 K$	Λ
0·01	0·01726	0·1311	33·0	191·0
0·02	0·03452	0·1857	64·7	187·4
0·03	0·05178	0·2276	96·3	186·0
0·04	0·06904	0·2627	128·0	185·3
0·05	0·08630	0·2938	159·5	184·8
0·06	0·10356	0·3218	191·0	184·4
0·07	0·12082	0·3477	222·0	183·7
0·08	0·13808	0·3716	252·0	182·5
0·09	0·15534	0·3941	282·0	181·5
0·10	0·17260	0·4154	311·0	180·2

Fig. 64 . EQUIVALENT CONDUCTIVITY CURVE FOR $H_2SO_3F^+$ (25°C)
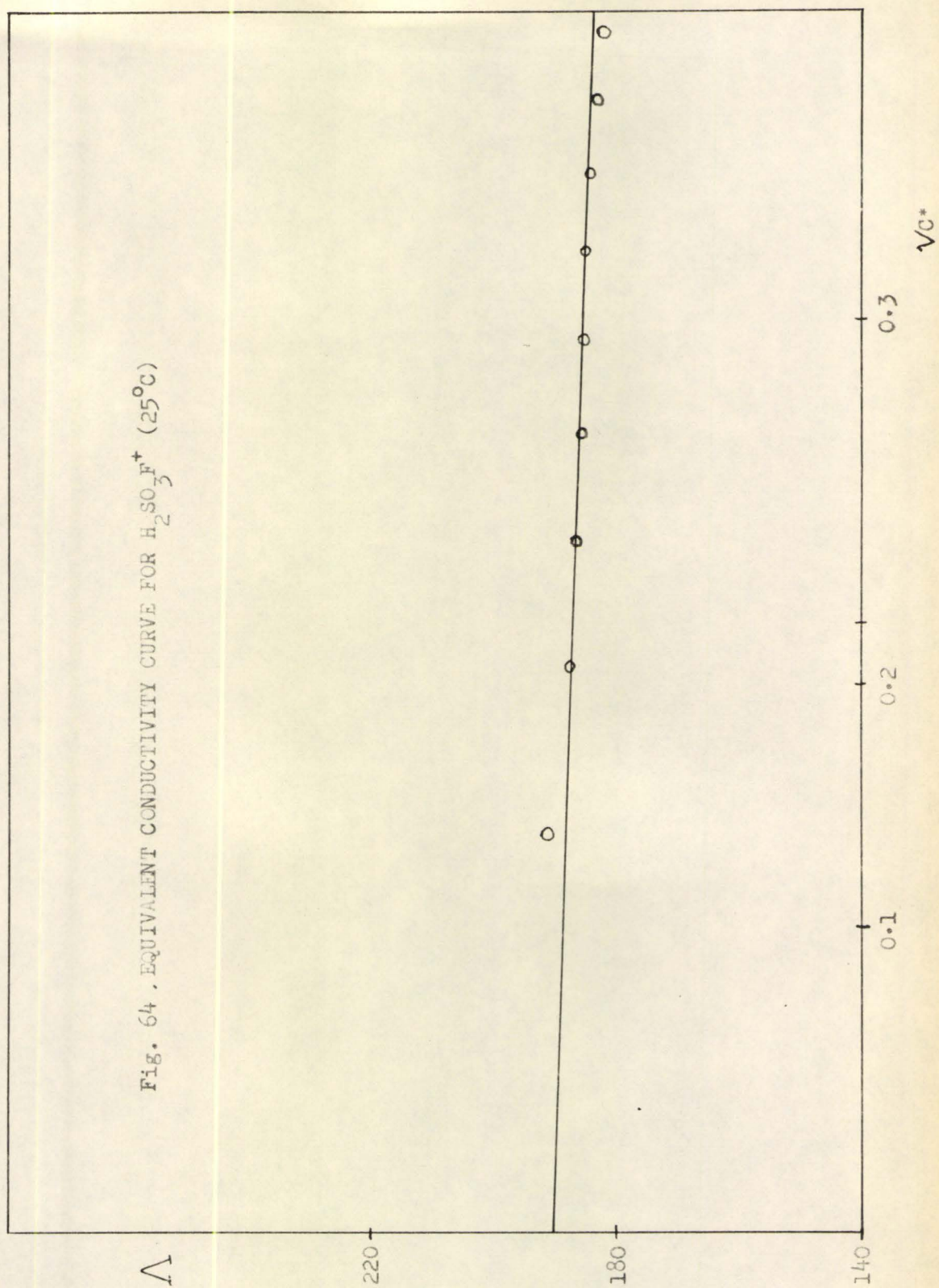
CHAPTER X

SELF-DISSOCIATION REACTIONS OF FLUOROSULPHURIC ACID

(a) AUTOPROTOLYSIS

The conductivity of pure fluorosulphuric acid, at $25^{\circ}C$, is 1.085×10^{-4} ohm^{-1} cm.$^{-1}$. Assuming that this conductivity arises solely from the ions produced in autoprotolysis

$$2HSO_3F \rightleftharpoons H_2SO_3F^+ + SO_3F^- \quad ,$$
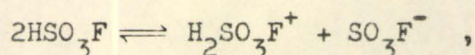
it is possible to calculate K_{ap}. The specific conductance is given by

$$\mathcal{K} = 10^{-3} \quad c \quad (\lambda_o^+ + \lambda_o^-)$$

where λ_o^+ and $_o\lambda^-$ are the mobilities of the fluorosulphuric acidium ion and the fluorosulphate ion respectively. The autoprotolysis constant, K_{ap}, is given by,

$$K_{ap} = c^2 = \mathcal{K}^2 \times 10^6/(\lambda_o^+ + \lambda_o^-)^2$$

Using the value 1.085×10^{-4} ohm^{-1} cm.$^{-1}$ for the specific conductance of pure fluorosulphuric acid, 190 for λ_o^+ and 140 for λ_o^-, the value obtained for K_{ap} (in molar units) is,

$$K_{ap} = 1.08 \times 10^{-7} \text{ mole}^2 \text{ l.}^{-2}$$

In molal units, the value for K_{ap} is,

$$K_{ap} = 3.6 \times 10^{-8} \text{ mole}^2 \text{ kg.}^{-2}$$

This small value for K_{ap}, compared to 2.4×10^{-4} mole^2 kg.$^{-2}$ (at $25^{\circ}C$) for sulphuric acid[78], makes it possible to study dilute solutions in fluorosulphuric acid without making corrections for the presence of autoprotolysis ions, since very low concentrations of electrolytes com-

181

pletely repress the autoprotolysis.

It will be shown in section (b) of this chapter that pure fluoro-sulphuric acid probably contains very small concentrations of ions other than the autoprotolysis ions. If other ions do exist they will make a small contribution to the conductivity of the pure acid and thus the value of K_{ap}, calculated above, will be too large.

(b) SELF-DECOMPOSITION INTO HYDROGEN FLUORIDE AND SULPHUR TRIOXIDE

Fig. 65 and Table XXXV give freezing-point depression data for solutions of water in fluorosulphuric acid. The slope of the freezing-point depression curve for water, above the concentration 0·015 molal, corresponds to the formation of two particles in solution (the dotted line in Fig. 64 is the theoretical curve for $\nu = 2$). Since water is a strong base in sulphuric acid[78] it will, undoubtedly, be a strong base in fluorosulphuric acid, and the simplest explanation of the cryoscopic results would be the ionization,

$$H_2O + HSO_3F \rightleftharpoons H_3O^+ + SO_3F^-$$ 10.1
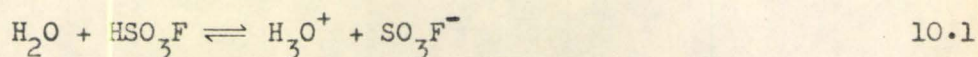
However, Gillespie and Senior[79] found that the conductivities of solutions of water are smaller than would be expected for a strong base. They have interpreted their results as indicating the occurrence of the hydrolysis equilibrium 10·2.

$$H_3O^+ + SO_3F^- \rightleftharpoons HF + H_2SO_4$$ 10·2
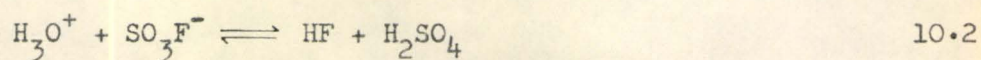
This does not affect the cryoscopic results since, for any value assigned to the equilibrium constant for 10·2, one mole of water produces two moles of particles in solution and a freezing-point curve corresponding to $\nu = 2$ will be obtained. This curve (Fig. 65), however, does not extrapolate to zero concentration for zero ΔT. The initial slope appears to be considerably less than the final slope of $2k_f$.

This could be explained by the presence of free SO_3 and HF in the pure acid, as a consequence of the self-decomposition 10·3.

$$HSO_3F \underset{K_d}{\rightleftharpoons} HF + SO_3$$ 10·3

183
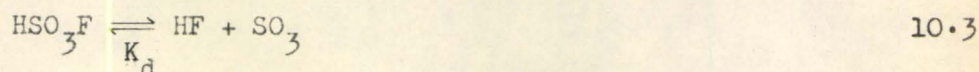
When water is dissolved in HSO_3F it produces HF according to 10·2. This causes a shift of equilibrium 10·3 to the left, resulting in fewer particles than expected in solution, and thus a freezing-point curve with an initial slope less than $2k_f$.

The large scatter in the experimental results makes it difficult to interpret them quantitatively. This scatter arises from the fact that each addition of water was only one drop. Thus, for example, an error as small as 1 mg. in the weight of water added would result in an error of 2% in the concentration.

Table XXXVI and Fig. 66 give cryoscopic results for solutions of potassium fluoride which reacts with fluorosulphuric acid to give KSO_3F and HF. Since the conductivity produced by KF is slightly greater than that produced by KSO_3F (Chapter VII), it may be assumed that HF ionizes as a weak base. Thus a freezing-point curve with a slope slightly larger than that produced by a solute giving three particles in solution would be expected for KF. As can be seen in Fig. 66 the slope of the curve is in fact slightly greater than $3k_f$ (dotted line A), except for an initial flat portion. This smaller initial slope is presumably due to the repression of 10·3 by HF.

Freezing-point results on sulphur trioxide solutions are given in Table XXXVII and Fig. 66. Barr[42] has shown that SO_3 is a non-electrolyte in fluorosulphuric acid. Again, low concentrations of SO_3 show a freezing-point curve with a slope less than k_f, presumably due to repression of 10·3.

It is difficult to interpret these results quantitatively. The freezing point of the pure acid varies over a range of about 0·02 degrees

for different experiments. This is presumably caused by varying amounts of impurities. One impurity which is certain to be present is trace amounts of water. Water will, of course, affect the position of 10.3, and thus the actual amounts of free SO_3 and HF present in the acid probably varies for different experiments. This may be another reason for the scatter in the experimental points in the cryoscopic measurements on solutions of water. Also, there is presumably some decomposition into HF and SO_3 at the boiling point of the acid, and there may be some fractionation in the distillation, resulting in the concentration of variable amounts of SO_3 and HF in the distillate. Woolf (see Chapter I) prepared fluorosulphuric acid by trap to trap distillation under reduced pressure. This could result in a distillate which contains more free HF than that present in the acid used by Barr[42]. Since hydrogen fluoride is a weak base, in the fluorosulphuric acid system, this could explain the high conductivity of Woolf's acid. It would appear, from the curves in Fig. 66, that the concentrations of free SO_3 and HF in fluorosulphuric acid at $-90^\circ C$ are each approximately 0.001 - 0.002 m. Therefore, K_d is approximately 1×10^{-6} to 4×10^{-6} mole^2 kg.$^{-2}$.

In order to interpret freezing-point data, it is not necessary to know K_d accurately, or the concentrations of free SO_3 and HF. Solutes which react to give SO_3 or HF, and thus repress 10.3, may show an initial flat portion in the freezing-point curve. Beyond this portion of the curve it may be assumed that 10.3 is completely repressed, and the freezing-point curve is then determined by the solute alone.

Evidence that the self-decomposition 10.3 occurs at $25^\circ C$ has been obtained by Gillespie and Senior[79], from conductivity measurements on

solutions of water. As in the cryoscopic experiments, there is an initial
flat portion to the conductivity curve due to repression of 10·3. These
workers have also shown that, while iodine is oxidized in solution in
fluorosulphuric acid, it is not oxidized when dissolved in fluorosulphuric
acid which contains excess HF. Presumably the species involved in this
oxidation is free SO_3. Fluorosulphuric acid solutions containing excess
HF will not contain free SO_3, due to repression of 10.3, and hence iodine
is not oxidized.

Hydrogen fluoride is a weak base in fluorosulphuric acid,

$$HF + HSO_3F \rightleftharpoons H_2F^+ + SO_3F^- \qquad\qquad 10.4$$
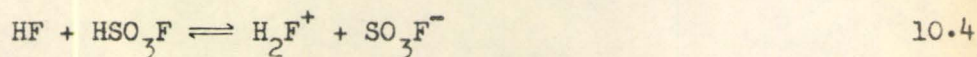
and sulphur trioxide is known to decrease the conductivity of solutions
of bases[42], possibly by the reaction

$$SO_3 + SO_3F^- \rightleftharpoons S_2O_6F^- \qquad\qquad 10.5$$
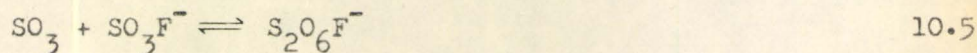
Therefore, it is very probable that ions other than the autoprotolysis
ions are present in pure fluorosulphuric acid.

Table XXXV

SOLUTIONS OF H_2O : FREEZING-POINT DEPRESSIONS

Expt.	T_o	W_{HSO_3F}	W_{H_2O}	m	ΔT
124	-89.015	159.06	0.0499	0.0174	0.070
			0.1084	0.03783	0.205
			0.1607	0.05608	0.327
			0.2147	0.07492	0.446
			0.2794	0.09750	0.586
			0.3348	0.1168	0.698
125	-89.018	172.90	0.0605	0.01942	0.062
			0.1146	0.03679	0.164
			0.1684	0.05406	0.297
			0.2191	0.07034	0.387
			0.2810	0.09021	0.513
126	-89.017	175.57	0.0574	0.01815	0.071
			0.1337	0.04227	0.211
127	-88.991	175.41	0.0516	0.01633	0.055
			0.0980	0.03100	0.145
			0.1494	0.04727	0.236
			0.2077	0.06572	0.352
122	-88.997	148.87	0.0670	0.02498	0.138
			0.1217	0.04538	0.270
			0.1845	0.06879	0.433
			0.2359	0.08796	0.536
			0.2758	0.1028	0.641

Table XXXVI

SOLUTIONS OF KF : FREEZING-POINT DEPRESSIONS

T_o = $-88 \cdot 987^{o}C$

W_{HSO_3F} = $167 \cdot 64$ g.

W_{KF}	m	ΔT
0·0754	0·007742	0·065
0·1647	0·01691	0·157
0·2608	0·02677	0·275
0·3987	0·04093	0·440
0·6283	0·06451	0·703
0·9532	0·08836	1·000

Table XXXVII

SOLUTIONS OF SO_3 : FREEZING-POINT DEPRESSIONS

T_o = $-89 \cdot 015^{o}C$

W_{SO_3}	W_{HSO_3F}	m	ΔT
0·05719	175·45	0·004071	0·009
0·3263	176·10	0·02314	0·070
0·5412	176·62	0·03827	0·121
0·8390	177·34	0·05909	0·200
1·1403	178·07	0·07998	0·288
1·5423	179·04	0·10758	0·391

Fig. 65 SOLUTIONS OF H_2O: FREEZING-POINT DEPRESSIONS

ΔT

0.6

0.4

0.2

0.02   0.04   0.06

$_m{}^s$

△ Expt. 122
○ Expt. 124
□ Expt. 125
● Expt. 126
■ Expt. 127

Fig. 66 SOLUTIONS OF KF AND OF SO₃:
FREEZING-POINT DEPRESSIONS
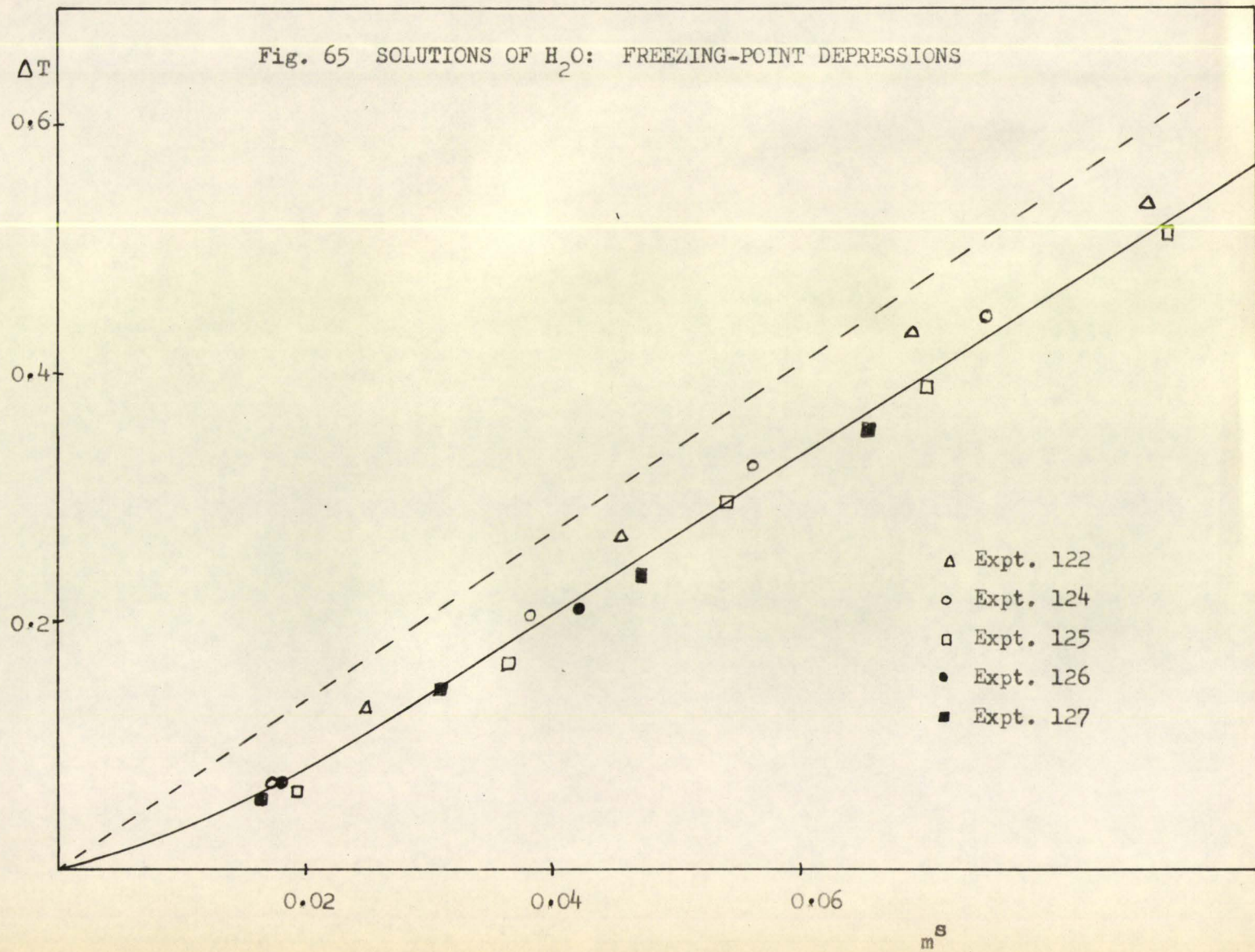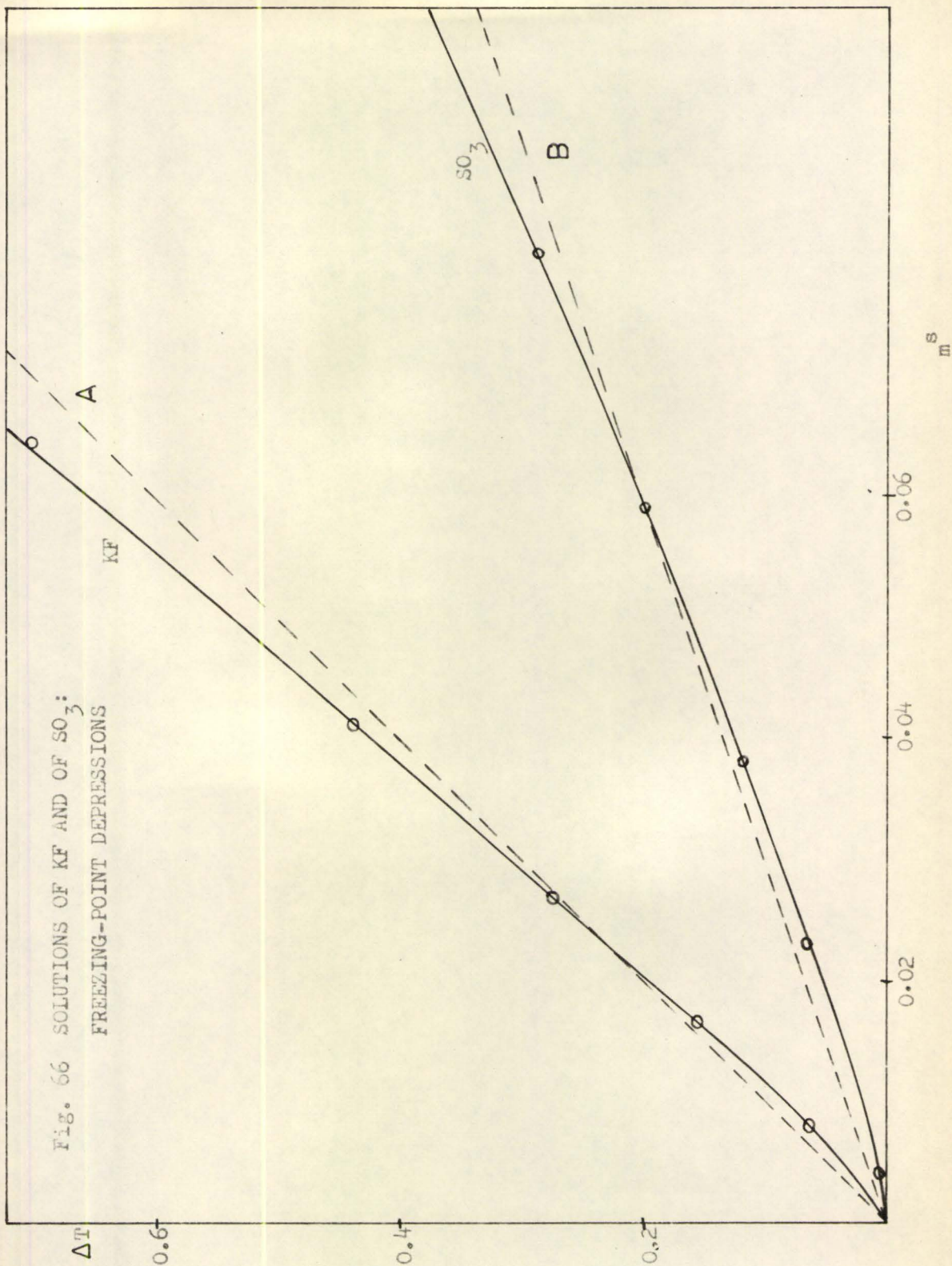
APPENDIX

List of Symbols

a   mean diameter of anion and cation (cm.)

$\overset{o}{a}$ mean diameter of anion and cation ($\overset{o}{A}$)

c   concentration in moles per litre of solution (molarity)

d_4^{25} specific gravity (values are numerically equal to the density in grams per milliliter)

e   electronic charge ($4 \cdot 80223 \times 10^{-10}$ e.s.u.)

ΔH latent heat of fusion (cal.mole^{-1})

H_{app} applied magnetic field strength (gauss)

H_o magnetic field at a particular nucleus (gauss)

I   ionic strength (mole l.$^{-1}$) - defined in chapter IX(b); nuclear spin quantum number (chapter V(d))

J_{12} spin-spin coupling constant, where coupling occurs between nuclei 1 and 2 (c/s)

K   equilibrium constant (in molal units, unless otherwise stated)

k_f cryoscopic constant (mole^{-1} deg. kg.)

k   Boltzmann's constant ($1 \cdot 380257 \times 10^{-16}$ erg deg.$^{-1}$ molecule^{-1})

M   molecular weight (g.)

m_A concentration of A in moles per kg. of solvent (molality)

[A]   concentration of A in moles per kg. of solvent (molality)

m_A^s stoichiometric concentration of A in molal units (meaning the total concentration of A in all its forms in solution)

N   Avogadro number ($6 \cdot 02380 \times 10^{23}$)

n   number of Faradays

R	gas constant ($1 \cdot 98719$ cal. deg.$^{-1}$ mole^{-1})
$r(A/B)$	mole ratio of A to B
T	absolute temperature
T_o	initial freezing point of fluorosulphuric acid (^oC)
ΔT	freezing-point depression (^oC) – the difference between the freezing-point of a solution and T_o
t	transport number
t^o	transport number at infinite dilution
W_A	weight of A (g.)
z	valency of an ion
α	degree of ionization at 25^oC
α'	degree of ionization at -90^oC
ε	dielectric constant
η	viscosity (cp.)
$\mathcal{K}$	specific conductance (ohm^{-1} cm.$^{-1}$)
$\mathcal{K}_o$	initial specific conductance of fluorosulphuric acid (ohm^{-1} cm.$^{-1}$)
Λ	equivalent conductivity of electrolyte (cm.^{2} ohm^{-1} (g. equiv.)$^{-1}$)
Λ_o	equivalent conductivity at infinite dilution (cm.^{2} ohm^{-1} (g. equiv.)$^{-1}$)
λ	ionic equivalent conductivity (cm.^{2} ohm^{-1} (g. equiv.)$^{-1}$)
λ_o	ionic equivalent conductivity at infinite dilution (cm.^{2} ohm^{-1} (g. equiv.)$^{-1}$) – also referred to as the ionic mobility
ν	number of moles of particles produced in solution by one mole of solute
ν_o	radio-frequency radiation (c/s)
$\nu_1 - \nu_2$	chemical shift-separation of n.m.r. signals due to nuclei 1 and 2 (c/s)
$\emptyset$	osmotic coefficient
$\emptyset^{el}$	contribution of electrostatic interionic forces to the osmotic coefficient

REFERENCES

1. T. E. Thorpe and W. Kirman. J. Chem. Soc. 921 (1892).

2. W. Traube. Ber. 46, 2513 (1913).

3. O. Ruff. Ber. 47, 646 (1914).

4. J. Meyer and G. Schramm. Z. anorg. u. allgem.
    Chem. 206, 24 (1932).

5. Standard Oil Development Co. Brit. Patent No.537, 589
    (June 27, 1941); Chem. Abstr. 36, 1328^5 (1942).

6. C. L. Thomas. U. S. Patent No.2,313,103 (March 9, 1943);
    Chem. Abstr. 37, 5076^4 (1943).

7. V. N. Ipatieff and C. B. Linn. U. S. Patent No.2,428,279
    (Sept. 30, 1927); Chem. Abstr. 42, 353 g (1948).

8. C. A. Braidwood. Brit. Patent No.640,485 (July 19, 1950);
    Chem. Abstr. 45, 658c (1951).

9. Dominion Tar and Chemical Co. Ltd., Brit. Patent No.668,283
    (Mar. 12, 1952); Chem. Abstr. 47, 2212d (1953).

10. H. D. Hartough and A. I. Kosak. J. Am. Chem. Soc. 69, 3093 (1947).

11. H. D. Hartough and A. I. Kosak. U. S. Patent No.2,475,564
    (July 5, 1949); Chem. Abstr. 43, 7966f (1949).

12. V. N. Ipatieff and C. B. Linn. U. S. Patent No.2,421,946
    (June 10, 1947); Chem. Abstr. 41, 5296c (1947).

13. J. D. Calfee and F. H. Bratton. U. S. Patent No.2,462,359
    (Feb. 22, 1949); Chem. Abstr. 43, 3834h (1949).

14. A. K. Roebuck and B. L. Evering. U. S. Patent No.2,564,080
    (Aug.14, 1951); Chem. Abstr. 46, 1756b (1952).

15. W. H. C. Rueggeberg and D. J. Torrans. Ind. Eng. Chem. 38,
    211 (1946).

16. C. W. Gates. Can. Patent No.449,652 (July 6, 1948);
    Chem. Abstr. 42, 6983a (1948).

17.   W. Lange and E. Müller. Ber. 63B, 2653 (1930).

18.   W. Hentrich, M. Hardtmann, and A. Ossenbeck. U. S. Patent No.
      1,847,513 (March 1, 1932); Chem. Abstr. 26, 2469 (1932).

19.   G. McCoy, C. E. Inman, and P. G. Harris. U. S. Patent No.
      2,686,202 (Aug. 10, 1954); Chem. Abstr. 49, 12536g (1955).

20.   C. B. Linn. U. S. Patent No.2,428,753 (Oct. 7, 1947);
      Chem. Abstr. 42, 919b (1948).

21.   P. H. Carnell. U. S. Patent No.2,538,293 (Jan. 16, 1951);
      Chem. Abstr. 46, 2290a (1952).

22.   E. A. Coons. U. S. Patent No.2,611,735 (Sept. 23, 1952);
      Chem. Abstr. 47, 2969d (1953).

23.   I. G. Farbenindustrie Akt. - Ges. Brit. Patent No.251,997
      (May 5, 1925); Chem. Abstr. 21, 1553 (1927).

24.   W. Traube and A. Krahmer. Ber. 52B, 1293 (1919).

25.   C. H. Möllering. J. prakt. Chem. 134, 209 (1932).

26.   W. F. Mitchell and J. A. Grant-MacKay. U. S. Patent No.
      2,702,233 (Feb. 15, 1955); Chem. Abstr. 49, 8571g (1955).

27.   DeWalt Secrist Young and J. H. Pearson. U. S. Patent No.
      2,416,133 (Feb. 18, 1947); Chem. Abstr. 41, 2865d (1947).

28.   L. J. Belf. Chem. & Ind. (London), 1296 (1955).

29.   H. Schmidt and H. D. Schmidt. Z. anorg. u. allgem.
      Chem. 279, 289 (1955).

30.   C. B. F. Young and K. R. Hesse. Metal Finishing 45, No.2, 63-7,
      84; No.3, 64-7 (1947).

31.   W. Traube, J. Hoerenz, and F. Wunderlich. Ber. 52B, 1272 (1919).

32.   W. Traube. Ber. 46, 2525 (1913).

33.   H. A. Lehmann and L. Kolditz. Z. anorg. u. allgem. Chem. 272,
      69 (1953).

34.   A. A. Woolf. J. Chem. Soc. 1053 (1950).

35.   A. A. Woolf. J. Chem. Soc. 3678 (1950).

36.   A. A. Woolf. J. Chem. Soc. 433 (1955).

37.   E. Hayek, J. Puschmann, and A. Czaloun. Monatsh. 85, 359 (1954).

38.   W. Traube and E. Brehmer. Ber. 52B, 1284 (1919).

39.   E. Hayek, A. Czaloun, and B. Krismer. Monatsh. 87, 741 (1956).

40.   E. L. Muetterties and D. D. Coffman. J. Am. Chem. Soc. 80, 5914 (1958).

41.   R. J. Gillespie and E. A. Robinson. Can. J. Chem. 40, 644 (1962).

42.   J. Barr. Ph.D. Thesis, University of London, London, England (1959).

43.   H. Siebert. Z. anorg. u. allgem. Chem. 289, 15 (1957).

44.   D. W. A. Sharp. J. Chem. Soc. 3761 (1957).

45.   W. Lange. Ber. 60B, 962 (1927).

46.   E. Wilke-Doerfurt and R. Pfau. Z. Electrochem. 36, 118 (1930).

47.   W. Traube and E. Reubke. Ber. 54, 1618 (1921).

48.   W. Lange. Z. anorg. u. allgem. Chem. 215, 321 (1933).

49.   A. A. Woolf. J. Chem. Soc. 2840 (1954).

50.   F. B. Dudley and G. H. Cady. J. Am. Chem. Soc. 79, 513 (1957).

51.   J. C. D. Brand and W. C. Horning. J. Chem. Soc. 3922 (1952).

52.   C. K. Ingold. Structure and mechanism in organic chemistry. Bell, London. 1953. p.300.

53.   A. I. Vogel. A text-book of quantitative inorganic analysis. 2nd ed. Longmans, Green and Co., New York. 1939. p.401.

54.   A. I. Vogel. A text-book of quantitative inorganic analysis. 2nd ed. Longmans, Green and Co., New York. 1939. p.480.

55.   G. Jones and D. M. Bollinger. J. Am. Chem. Soc. 57, 280 (1935).

56.   J. E. Lind, J. J. Zwolenik, and R. M. Fuoss. J. Am. Chem. Soc. 81, 1557 (1959).

57.   R. J. Gillespie, J. V. Oubridge, and C. Solomons. J. Chem. Soc. 1804 (1957).

58.   B. J. Mair, A. R. Glasgow, and F. D. Rossini. J. Research Natl. Bur. Standards, 26, 591 (1941).

59.   W. J. Taylor and F. D. Rossini. J. Research Natl. Bur. Standards, 32, 197 (1944).

60.   R. J. Gillespie and S. Wasif. J. Chem. Soc. 209 (1953).

61.   W. J. Moore. Physical chemistry. Longmans, Green and Co.,
       London. 1957. p.129.

62.   E. A. Moelwyn-Hughes. Physical chemistry. Pergamon Press,
       New York. 1957. p.736.

63.   R. J. Gillespie and C. Solomons. J. Chem. Soc. 1796 (1957).

64.   S. J. Bass, R. J. Gillespie, and J. V. Oubridge. J. Chem. Soc.
       837 (1960).

65.   R. P. Bell, K. N. Bascombe, and J. C. McCoubrey. J. Chem. Soc.
       1286 (1956).

66.   J. A. Pople, W. G. Schneider, and H. J. Bernstein. High Resolu-
       tion Nuclear Magnetic Resonance. McGraw-Hill, New York. 1957.

67.   J. D. Roberts. Nuclear Magnetic Resonance. McGraw-Hill,
       New York. 1959.

68.   R. J. Gillespie and R. F. M. White. Progress in stereochemistry.
       Vol.3. Butterworths, London. 1962. p.53.

69.   E. Hayek and W. Koller. Monatsh. 82, 942 (1951).

70.   R. J. Gillespie, J. V. Oubridge, and E. A. Robinson. Proc. Chem.
       Soc. 428 (1961).

71.   R. J. Gillespie and E. A. Robinson. Can. J. Chem. 40, 675 (1962).

72.   H. A. Lehmann and L. Kolditz. Z. anorg. u. allgem. Chem. 272,
       73 (1953).

73.   H. S. Booth and D. R. Martin. Boron trifluoride and its deriva-
       tives. John Wiley and Sons, Inc., New York. 1949. p.234.

74.   A. Engelbrecht, A. Aignesberger, and E. Hayek. Monatsh. 86, 470
       (1955).

75.   S. S. Chan and R. J. Gillespie. Unpublished results.

76.   R. A. Robinson and R. H. Stokes. Electrolyte solutions.
       Butterworths, London. 1955. p.138.

77.   R. H. Flowers, R. J. Gillespie, E. A. Robinson, and C. Solomons.
       J. Chem. Soc. 4327 (1960).

78.   R. G. Gillespie. Rev. Pure and Appl. Chem. 9, 1 (1959).

79.   R. J. Gillespie and J. B. Senior. Unpublished results.